# MAPPING OF CATARACT GENES IN THE CANINE GENOME AND MOLECULAR ANALYSIS OF *PAX6* FOR CAUSAL ASSOCIATION WITH CATARACT, ANIRIDIA, AND OTHER OCULAR DISEASES

A Dissertation

Presented to the Faculty of the Graduate School

of Cornell University

In Partial Fulfillment of the Requirements for the Degree of

Doctor of Philosophy

by

Linda Susan Hunter

January 2008

# MAPPING OF CATARACT GENES IN THE CANINE GENOME AND MOLECULAR ANALYSIS OF *PAX6* FOR CAUSAL ASSOCIATION WITH CATARACT, ANIRIDIA, AND OTHER OCULAR DISEASES

Linda Hunter, D.V.M., Ph.D.

Cornell University 2008

Cataracts are the leading cause of blindness and low vision throughout the world. Millions of people suffer as a result of this debilitating disease, and millions of dollars are spent annually on cataract removal surgery, which is the only cure. Genes have been identified which cause cataracts when mutated in man and/or mouse. Understanding the functions of these genes, as well as the mechanisms involved in cataract formation may help us to develop ways to prevent, delay, or cure cataracts. Animal models have contributed significantly to our understanding of normal lens development, as well as abnormal development and cataract formation. With the recent advances in canine genomics, the dog has become a promising model for studying the molecular aspects of ocular diseases. Furthermore, inherited cataracts occur in over 20 breeds of dog.

The chromosomal locations of 21 genes known to cause cataracts in man, and/or mouse were determined in the canine genome using a Radiation-Hybrid mapping technique. This created a tool which could facilitate association and linkage analysis in canine pedigrees with inherited cataracts. Next, the canine homologue of the cataract-associated gene *PAX6* was selected for cloning and characterization, and was found to have remarkable homology with the human gene. Finally, canine *PAX6* was evaluated for mutations causing cataract, aniridia, persistent pupillary membranes,

sclero-cornea, and choroidal hypoplasia. Direct sequence analysis of *PAX6* in affected dogs revealed only single nucleotide polymorphisms and microsatellite changes. However, further pedigree information and analysis is needed to definitively rule out *PAX6*'s involvement in these ocular diseases.

## BIOGRAPHICAL SKETCH

Linda Hunter was born Wednesday September 21, 1966 in the Bronx, New York to Delila Carraway and Harry Hunter. She grew up with her older sister Lisa, in Albany, New York where she attended Saint John's, Saint Ann's, and Sacred Heart Catholic elementary schools. She graduated with Honors from Albany High School in 1984 and was voted "Most Likely to Succeed" by a graduating class of over 600 students. Linda graduated from Cornell University in 1988 with Honors and Distinction, majoring in Animal Science. She immediately entered the New York State College of Veterinary Medicine at Cornell, where she graduated in 1992, fulfilling a life-long dream of becoming a veterinarian. Linda practiced veterinary medicine at small animal clinics in East Greenbush, and Buffalo, New York before joining the Humane Society of Charlotte in Charlotte, North Carolina.

After several years of consideration, Linda decided to return to Cornell University once again to pursue graduate studies in the Field of Veterinary Medicine. She had always loved Ithaca, and was thrilled to be back in the academic environment of her Alma Mater. After rotating through the laboratories of Gustavo Aguirre, Judy Appleton, and Geoffrey Sharp, Linda chose the Aguirre laboratory because of their use of canine models to study inherited eye diseases. She felt that her skills and training as a veterinarian would be an asset in a lab focused on dog models. While studying the molecular aspects of inherited eye diseases in dogs, Linda worked closely with Duska Sidjanin evaluating genes which cause cataracts, in particular the *PAX6* gene which she cloned and characterized.

The years spent working towards the Ph.D. degree went by quickly, but were filled with personal growth, development and transition. Linda was the first person in her family to achieve such a high level of education and hopefully her path will leave a trail for others to follow.

Dedicated To

God

My Grandmother Lila Mae Carraway,

And My Mother Delila Carraway

Your Love, Guidance And Strength

Molded Me Into The Person I Am Today.

# ACKNOWLEDGMENTS

I thank my original thesis advisor Dr. Gustavo Aguirre for welcoming me into his laboratory and allowing me to study molecular biology and the genetics of inherited eye diseases in dogs. I thank Dr. Vicki Meyers-Wallen for assuming the position of my thesis advisor after Dr. Aguirre left Cornell University and joined the faculty at the University of Pennsylvania. I also thank my Committee members Dr. Drew Noden, Dr. Roy Levine, and Dr. James Casey for their time and patience. I thank Dr. Douglas McGregor for his commitment and dedication to increasing the number of veterinarians pursuing graduate studies and research. I am thankful to Dr. Greg Acland, Dr. Duska Sidjanin, Dr. Anna Kukekova, and Dr. James Kijas for their instruction and guidance in the laboratory. I thank Jennifer Johnson and Orly Goldstein for technical support, and Keith Watarmura for support with computer and graphic issues. Finally, I thank my family and friends for their encouragement and emotional support: Delila Carraway, Lisa and John Johnson, Arlene Hudson, Vajezatha Payne, Darlene Hagler, Terri Knox, Constance Everhart, Trina Jones, Lisa Daley and Donald House.

My graduate research was supported by a National Institutes of Health (NIH) Institute Training Fellowship administered by Dr. Douglas McGregor, an NIH National Research Science Award (NRSA grant F32-EY13677), Cornell University Graduate Research Assistantship, The Morris Animal Foundation/Seeing Eye, Inc., the Van Sloan Fund for Canine Genetic Research and the James A. Baker Institute for Animal Health under the leadership of Dr. Douglas Antzcak.

TABLE OF CONTENTS

LIST OF FIGURES

LIST OF TABLES

LIST OF ABBREVIATIONS

**BAC:** bacterial artificial chromosome
**bp:** base pair
**cDNA:** complementary DNA
**CDS:** coding sequence
**CFA:** *Canis familiaris* autosome
**cM:** centiMorgan
**CNS:** central nervous system
**cR:** centiRay
**CTS:** carboxy (COOH)-terminal subdomain
**DNA:** deoxyribonucleic acid
**EST:** expressed sequence tag
**FISH:** flourescence *in situ* hybridization
**GD:** Gos D'atura
**HD:** homeodomain
**HSA:** *homo sapiens* autosome
**Kb:** kilobase
**LOD:** logarithm of odds
**Mb:** megabase
**NTS:** amino (NH2)- terminal subdomain
**OD:** right eye
**OMIM:** online Mendelian inheritance in man
**OS:** left eye
**PAGE:** polyacrylamide gel electrophoresis
**PAX6:** paired-box 6
**PCR:** polymerase chain reaction
**PD:** paired domain
**PPM:** persistent pupillary membrane
**PST:** proline-serine-threonine
**RH:** radiation hybrid
**RNA:** ribonucleic acid
**SCWT:** soft-coated wheaten terrier
**Sey:** small eye
**SNP:** single nucleotide polymorphism
**STS:** sequence tagged site
**TIGR:** The Institute for Genomic Research
**TK:** thymidine kinase
**UCSC:** University of California, Santa Cruz
**UTR:** untranslated region
**WT:** wild-type

# CHAPTER 1

# INTRODUCTION

Approximately half of all human blindness is caused by cataracts, making them the most significant cause of visual impairment worldwide (1). The cure for cataracts is surgical removal of the opacified lens and its replacement with an artificial intra-ocular lens (IOL). Approximately 1.4 million cataract surgeries are performed annually in the United States (2). Both the public health, and economics of our society will greatly benefit from identification of the etiologies and mechanisms of cataract formation.

A cataract is any opacity of the normally transparent ocular lens, or its surrounding capsule. Cataracts may be caused by injury or trauma to the lens or lens capsule, infection (e.g. rubella), systemic disease (e.g. diabetes mellitus), drugs (e.g. steroids), heredity, or age-related changes in the lens. Cataracts are described by their location within the lens, their morphology or physical characteristics, their disease progression, and when in the patient's life they occur. Nuclear cataracts occur in the center, or nucleus of the lens, while cortical cataracts occur in the outer area surrounding the nucleus (Figure 1.1). Capsular cataracts occur in the lens capsule which surrounds the entire lens, and subcapsular opacities occur just under the capsule. Opacities associated with the anterior or posterior lens sutures are referred to as sutural cataracts, and those present at the lens periphery where the zonular fibers connect the lens to the ciliary body, are considered equatorial or zonular. Polar opacities occur at the center (pole) of the anterior or posterior lens surface, while axial opacities go through the central pole of the lens.

In addition to their location, cataracts are described by their morphology, which varies greatly. Punctate cataracts are small opaque specks while pulverulent

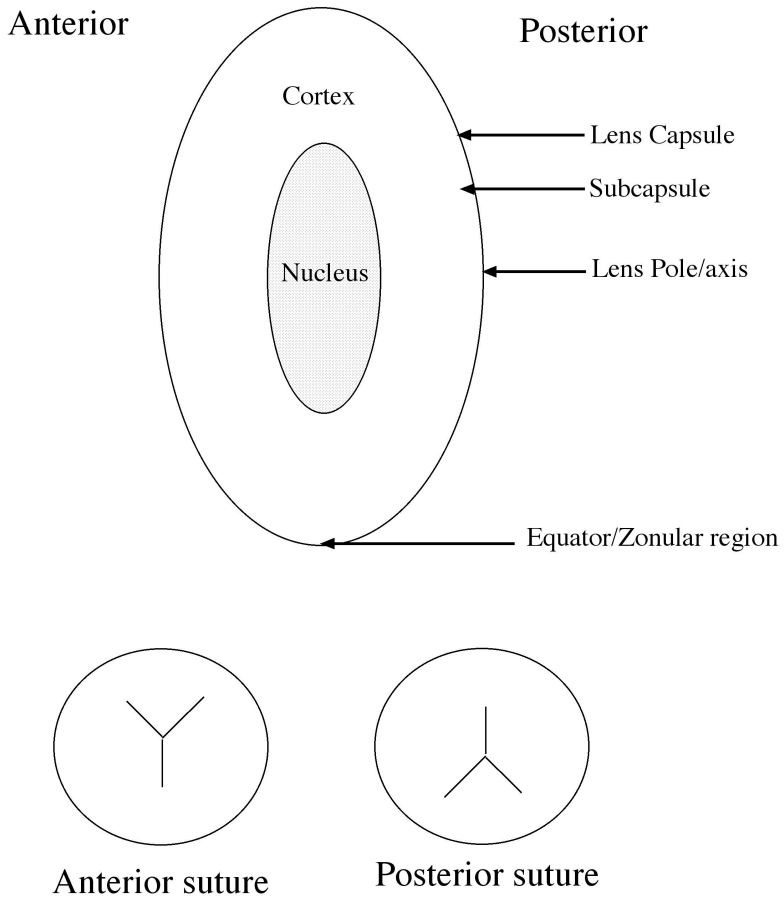


Figure 1.1. Lens diagram. Cataracts occur in different locations within the lens including the central nucleus, outer cortex, or in association with the lens capsule. In addition, lens opacities may be associated with the anterior or posterior Y-sutures. Cataract locations are further described as anterior, posterior, polar or zonular depending on their position within the lens.

cataracts have multiple specks that appear like dust, and can be fine (tiny) or coarse (large) in texture. Cuneiform cataracts look like cones, wedges or spikes, and coraliform cataracts resemble sea coral with finger-like extensions. There are also stellate or star-like opacities as well as other shapes. In addition to morphology, some cataracts reflect different wavelengths of light and appear brunescent (brown) or cerulean (blue) in color.

Along with location in the lens and morphology, cataracts are described by their stage of development. Cataracts can remain stagnant or progress in their maturity. Early or incipient cataracts usually involve less than 15% of the lens and may not affect vision. A cataract may grow from this stage into an immature cataract involving more than 15% of the lens. Immature cataracts usually compromise vision to some degree. Mature cataracts are those which involve the entire lens and cause blindness. These often result in swelling of the lens which may in turn, result in degeneration of the zonular fibers, lens subluxation, or luxation, impingement upon the ciliary body, obstruction of aqueous humor outflow and the development of secondary glaucoma. A hypermature cataract is one in which the cortex of the lens has liquified resulting in a decrease in the total lens size. The liquified cortex may escape into the anterior or posterior ocular chambers causing inflammation and lens-induced uveitis. The final stage of cataract progression is known as the Morgagnian stage in which the integrity of the cortex is so compromised that it can no longer support the solid nucleus, causing it to sink ventrally. All cataracts do not necessarily proceed through all 5 stages of progression. A cataract may arrest in one stage indefinitely or progress to some degree and then remain stagnant.

Cataracts can be present at birth (congenital), or occur at any time throughout life. Cataracts occur most commonly in the elderly and over half of the population aged 80 and older have evidence of cataract formation, or have had cataract surgery

(3). The etiology of age-related cataracts is not fully understood, however, the interaction between an individual's genetic background and exposure to certain environmental risk factors suggests the importance of heredity in the development of senile cataracts. Factors such as UV light exposure (4), alcohol consumption (5), and cigarette smoking (6), are associated with an increased risk of cataract formation, while several nutrients have been associated with a decreased risk of cataract formation (7, 8).

Although age-related cataracts are more common, congenital cataracts are an important disease in children, and represent the most common cause of treatable childhood blindness in the United States and in Europe (9, 10). Approximately 33% of all congenital cataracts are inherited (11), but as more cataract genes are identified, this percentage will likely increase. The study of congenital cataracts has contributed significantly to our understanding of the molecular bases of inherited cataracts because of the early manifestation of the phenotype, and the ease of diagnosis, both of which facilitate molecular genetic studies. Cataracts may be inherited as autosomal dominant (12-14) , autosomal recessive (15-17) or X-linked (18, 19) traits.

The identification of genes involved in cataract formation has advanced our understanding of normal lens biology, and the factors that regulate both lens transparency, and pathology. In addition, the identification of cataract genes and mutations has revealed both genetic and phenotypic heterogeneity. The occurrence of the same cataract phenotypes in patients with mutations in different genes is an example of genetic heterogeneity. For example, in man, pulverulent nuclear cataracts may result from mutations in crystallin genes; CRYBB1 (20), CRYBB2 (21), or CRYGC (22), as well as gap junction proteins; connexin 46 (23), and connexin 50 (24). Alternatively, the occurrence of different cataract phenotypes in patients with mutations in the same gene reveals phenotypic heterogeneity. For example, in man,

mutations in CRYGC can cause either pulverulent nuclear cataracts (22), or lamellar cataracts (25). Molecular genetic studies are needed to increase our understanding of the relationship between cataract phenotypes and their corresponding genetic mutations, which will help to explain the genetic and phenotypic heterogeneity observed. Such heterogeneity however, makes it difficult to perform direct linkage studies in man, and to combine linkage data from different families in order to obtain statistically significant logarithm of odds (LOD) scores. The use of animal models has helped to overcome this difficulty.

***Animal models***

There are many benefits to using animal models in molecular genetic studies. Laboratory animals can be readily examined for phenotypic evaluation, and they can be examined often and over long periods of time to follow disease progression. They can also be housed in regulated environments with controlled exposure to risk factors such as diet and ultraviolet light. The typically shorter life-span and generation interval of animal models also facilitates the observation of disease progression, and allows the generation of large pedigrees which can provide statistically significant data for association and linkage studies. Increased progeny numbers, and planned breedings, also help in determining the mode of inheritance for a particular disease. In addition, animal models provide ready access to blood, and tissue samples necessary for DNA analysis, as well as RNA and protein expression studies. Animal models are also important in determining the efficacy and safety of gene therapy protocols before using them in people.

***Mouse models***

Both normal and pathological development of ocular structures, and the corresponding genes involved, have been attained through the study of mouse embryos (26). The molecular and developmental pathology of mouse cataract models has been instrumental in advancing our knowledge of the mechanisms underlying cataract formation (27). There are over 60 inherited cataracts described in the mouse (11). In addition, there are over 35 cataract loci, from which mutations have been identified in at least 19 genes that cause cataracts as a primary phenotype (28).

Although mouse models have been used extensively to study the genetics of human diseases, they can have some limitations. For example, mutations in the same genes can result in different phenotypes in the mouse versus man. Mutations in *PAX6* cause aniridia in man, a disease characterized by partial to complete absence of the iris (29, 30). However, spontaneous *Pax6* mutations in the mouse result in the "small eye" phenotype, which is characterized by microphthalmia, cataracts and small body size (31, 32). Similarly, mutations in *PITX3* cause cataracts and anterior segment mesenchymal dysgenesis in man (33, 34), but cause aphakia (absence of the lens) in the mouse (35, 36).

Another limitation in mouse models is the lack of certain phenotypes which occur in man. This may result from the lack of naturally occurring mutations in homologous genes, or from the lack of anatomical structures in the mouse which are present in man. For example, mice do not have a macula and therefore cannot be used as direct anatomical models for diseases affecting the macula such as age-related macular degeneration (AMD) and Stargardt's disease, a recessive form of macular degeneration (37) (38). Similarly, mice do not have a fovea and cannot anatomically replicate diseases such as foveal hypoplasia (39, 40). Since only primates have maculas and foveas they would make ideal animal models for these diseases.

In an effort to overcome the lack of naturally occurring mouse mutations, genetic engineering techniques have been used to generate new phenotypes in hope of creating diseases in the mouse that resemble those seen in man. These techniques include the use of radiation, or chemicals like ethylnitrosourea (ENU), to induce mutations, as well as transgenic, and targeted gene knockout techniques. Such genetic engineering projects may generate artificial mutations in mice, but again, the phenotypes seen may not be similar to those in man. Furthermore, transgenic techniques often randomly insert foreign DNA into the mouse genome using non-homologous recombination techniques. The foreign DNA or gene is then subject to the promoters, enhancers, and regulators present at its new location in the mouse genome. This new environment may affect the temporal-spatial expression of the inserted fragment in such a way that it fails to recreate the desired molecular and phenotypic characteristics. Targeted gene knockout techniques also have tremendous variability depending on the strain of mouse used and the corresponding genetic background. Hence, a gene knockout may be lethal in one mouse strain but not in another.

Today, there are a variety of animal models to choose from for molecular studies, including: insects, fish, amphibians, birds, and mammals. Each model has strengths and weaknesses, and the anatomical and physiological properties of one model may be more appropriate than another in studying a particular disease, or a specific aspect of a particular disease. Historically, the mouse model has been used extensively, and as a result, has well developed genetic tools and documented genetic engineering techniques. However, as genetic resources develop for other species, and genomic sequences become available, opportunities will emerge to choose new animal models based on how well their anatomy, physiology, and phenotypes match the

diseases of man. Given this choice, a canine model for human ocular diseases becomes desirable.

***Canine models***

The dog model has many of the same benefits as other animal models including access for phenotypic evaluation, and a short life-span which facilitates the manifestation of age-related phenotypes earlier than would be achieved in man. The short generation interval, along with the use of selective mating, allows production of informative progeny, determination of disease mode of inheritance, and the generation of large pedigrees for association and linkage analysis with increased statistical power. Canine models, as other models, also provide ready access to tissue samples for histopathology, DNA, RNA, and protein analysis. However, dogs have additional advantages in that there are over 300 different dog breeds which exhibit great interbreed phenotypic variation while exhibiting minimal intrabreed differences (41-44). In this way, individual dog breeds function as genetic isolates which often show increased frequency of certain genetic disorders (45). For example, autosomal recessive diseases are seen with increased frequency in genetically isolated breed populations, thus creating unique opportunities for genetic study. The tremendous natural genetic variation of dog breeds also provides a large reservoir of allelic differences which can be used to study genetic diseases and traits (41, 46). Additionally, dogs can be selectively inbred to eliminate heterogeneous genetic background, and selectively outbred to reveal genetic background effects on phenotypic expression (41). Furthermore, the dog is physiologically similar to man, and suffers from many naturally occurring diseases which are biologically, histologically, and clinically similar to their human counterparts (41, 47). These qualities make the dog an ideal model for the study of human diseases. Finally, the

dog also represents a large animal model intermediate between the mouse and man that can be used for in vivo testing of gene therapy techniques.

Progress in canine genetics has created the genetic basis on which to study inherited diseases in dogs, and has made this species a viable option for phenotypic evaluation and gene discovery (48). Resources for molecular studies using canine models include somatic cell (49) and bacterial artificial chromosome (BAC) libraries (50), canine linkage maps (51-53), a cytogenic map characterized by fluorescent in situ hybridization (FISH) (54), canine-rodent somatic cell hybrid lines for radiation hybrid (RH) mapping (55), and RH-maps of the canine genome (56-58). Additional resources include integrated RH/linkage maps (59, 60), and an integrated 4249 marker FISH/RH map of the canine genome (61). Comparative maps of canine and human chromosomes reveal homologous segments between both species allowing comparative genetic studies (54, 62, 63). The creation of Minimal Screening Sets (MSS), consisting of subsets of microsatellite markers dispersed over the entire canine genome, facilitate genome wide scans for candidate genes on chromosomes linked to disease phenotypes (64-66). Finally, the 1.5X (poodle) (67), and 7.5X (boxer) (68) genomic sequences have been tremendous assets in advancing the use of canine models in molecular biology.

Canine genetic resources have already been used successfully to map homologous human disease-associated genes (e.g. *TSC2*- tuberous sclerosis 2*, PKD1*- polycystic kidney disease 1*,* and *CLN3*- ceroid lipofuscinosis neuronal 3) in the dog (CFA6) and show that there is often greater homology between human and dog chromosomes than between human and mouse chromosomes (69). These resources were also instrumental in mapping canine early retinal degeneration (*erd*) to chromosomal segments homologous to HSA12 (70), progressive rod-cone degeneration (*prcd*) to CFA9 (71, 72), and hereditary renal carcinoma to CFA 5 (73).

Linkage analysis and positional cloning led to the identification of a mutation in the canine hypocretin-2 receptor gene in a family of Doberman pinschers with inherited narcolepsy (74). This finding was pivotal in establishing the subsequent identification of hypocretin mutations in human narcolepsy patients (75-77).

Progress in canine genomics has also helped to identify canine models of human ocular diseases. For example, the locus for recessively inherited, human achromatopsia or colorblindness (ACHM3) links to HSA8q21-22 (78, 79) and is caused by mutations in the cyclic nucleotide-gated channel beta-subunit gene (CNGB3) (80). Similarly, naturally occurring, recessively inherited retinal cone degeneration (cd) in Alaskan malamutes and German shorthaired pointers, links to CFA29 in a region homologous to HSA8, and is caused by mutations in the same gene; CNGB3 (81). Cone degeneration in dogs is homologous to achromatopsia in man at both the phenotypic and molecular levels making the dog an excellent model for this disease.

Retinitis pigmentosa (RP) in man is a heterogeneous group of inherited diseases characterized by the loss of photoreceptors and progressive retinal degeneration. RP can have a recessive, dominant or X-linked mode of inheritance. A subset of autosomal dominant forms of RP are caused by mutations in the *rhodopsin* gene which codes for the light absorbing pigment found in rod photoreceptors (82-84). Naturally occurring rhodopsin mutations in English mastiff dogs also result in dominantly inherited retinal degeneration, making these dogs excellent canine models for rhodopsin RP in man (85-87).

Human X-linked retinitis pigmentosa 3 (XLRP3) is caused by mutations in the *retinitis pigmentosa GTPase regulator* (*RPGR*) gene (88). X-linked progressive retinal atrophy (XLPRA) in Siberian huskies was the first X-linked retinal degeneration in animals ever reported and the first canine retinal degeneration disease

assigned to a chromosome (89, 90). Like the human disease, canine XLPRA is also caused by mutations in the *RPGR* gene, creating yet another canine model which is homologous with the human disease phenotypically, genetically, and with regard to mode of inheritance (91).

Autosomal recessive congenital stationary night blindness (csnb) and retinal dystrophy in the briard dog are caused by naturally occurring mutations in the *RPE65* gene (92-94). These diseases are homologous to Leber's congenital amaurosis type 2 (LCA2) and autosomal recessive retinitis pigmentosa in man (respectively), and both of these disorders are also caused by *RPE65* mutations (95-98). The briard has been used successfully as the first large animal model to test gene therapy for LCA (99-101).

***Canine cataracts***

The advances in canine genetics, identification of homologous canine models for human diseases, and the successful use of dogs in translational and gene therapy studies encourages the development of canine models for molecular studies of cataract. Primary or isolated cataracts, which occur without other ophthalmic or systemic diseases, occur in 164 of the approximately 300 recognized dog breeds worldwide (102). Over 20 dog breeds have naturally occurring inherited cataracts, and an additional 40 breeds have a high incidence of breed-related cataracts which are suspected of being inherited (102, 103). Inherited cataracts have been documented in Labrador (104, 105), golden (104, 106, 107), and Chesapeake Bay (108) retrievers, Bishon Frise (109, 110), standard poodles (111, 112), American cocker spaniels (113, 114), German shepherds (115), German Pinschers (116), Rottweilers (117), Tibetan terriers (118), Afghan hounds (119), dachshunds (120), Leonbergers (121), and Entlebucher mountain dogs (122-124).

Congenital, inherited cataracts have been described in the miniature schnauzer (125-129), Welsh springer spaniel (130), cocker spaniels (131), West Highland white terrier (132), old English sheepdog (133), chow chow (134), Norwegian buhund (135), akita (136), and English cocker spaniel breeds (137). Recently, cataract-associated mutations in the *heat shock factor 4* (*HSF4*) gene were identified in Staffordshire bull terriers, Boston terriers, and Australian shepherds, making these 3 breeds the first with cataracts described at the molecular level (138).

***Normal lens development***

To begin to understand how, when, and why cataracts develop, one must first understand normal lens development. In the early embryo, the prosencephalon evaginates to form the optic vesicle day 9.5 in the mouse (139), day 15-17 in the dog (140, 141), and day 24 (Carnegie stage 11) in man (142). This optic vesicle induces the overlying surface ectoderm to thicken and form the lens placode which will invaginate and pinch off to form the lens vesicle, day 10-12 in the mouse (139), day 25 in the dog (140, 141), and day 33 (Carnegie stage 13) in man (142). Initially, the lens vesicle is a hollow sphere surrounded by a single layer of epithelial cells. However, the posterior cells of the vesicle are induced by the developing retina to elongate and form primary lens fibers. The elongating primary lens fibers fill the cavity of the lens vesicle, and produce crystallin proteins which fill the cells as they lose their nuclei and organelles (26). These primary lens fiber cells form the nucleus of the lens. Secondary lens fibers originate from the germinal epithelium of the anterior lens vesicle. These anterior epithelial cells divide and produce new cells which migrate toward the lens vesicle equator, where they elongate and form secondary lens fibers. Like primary lens fibers, the secondary fibers lose their nuclei, and organelles, but unlike primary fibers, they are produced throughout life and

continue to elongate and pack around the core of primary lens fibers repeatedly (Figure 1.2).

The function of the lens is to refract light rays, and to focus them on to the retina. To accomplish this task, the lens must be transparent. The normal transparency of the lens is dependent upon many factors. 1) The structural proteins of the lens including the intermediate filaments which are part of the cytoskeleton, as well as cell matrix proteins must be organized in a precise network which allows light to pass through. Also, the soluble crystallin proteins which comprise over 90% of the proteins in the lens, are essential for normal lens development and transparency. 2) Lens membrane proteins form intercellular junctions, and channels between cells which are critical for maintaining ionic homeostasis, necessary for lens clarity. 3) Finally, transcription factors are critical for regulating the temporal-spatial gene expression necessary for normal lens morphogenesis. Because lens transparency is dependent upon structural proteins, membrane proteins, and transcription factors, the genes which encode these proteins are key candidate genes for cataract phenotypes.

### *1. Lens structural proteins*

#### *a. Intermediate filaments*

The cytoskeleton of lens cells, like other cells, is made up of microtubules, actin filaments, and intermediate filaments, which determine cell size, shape, and motility, and which organize and support the cytoplasm. During lens fiber cell differentiation, however, crystallins are produced, and the cytoskeleton is altered as the cell loses its nucleus and membranous organelles, and drastically elongates (143, 144). The type III intermediate filament, vimentin, is expressed in lens epithelial cells, and in early, differentiating lens fiber cells, but it is lost in mature lens fiber cells (145). However, beaded filament structural protein 1 (BFSP1, filensin, CP115) and

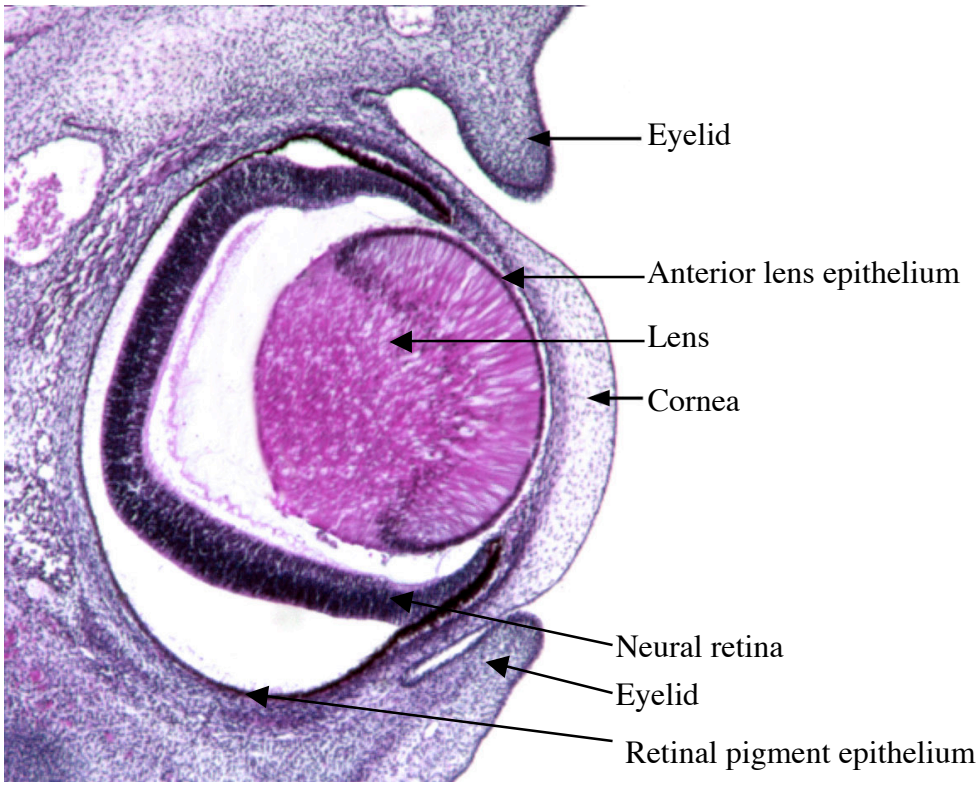


Figure 1.2. Developing canine eye from an approximately 30 day-old fetus, with structures labeled.

BFSP2 (phakinin, CP49) are lens-specific intermediate filaments (146), which are not expressed in lens epithelial cells, but are expressed in the plasma membrane of young differentiating fiber cells, and in the cytoplasm of older, more mature fiber cells which have lost their nuclei (145). These two intermediate filaments heterodimerize, and form a special beaded filament structure in the lens (147). Alpha crystallins may also be required for the assembly of beaded filament (148), and their function as molecular chaperones may in turn, be facilitated by their incorporation in this cytoskeletal structure (149). BFSP1 and 2, and their assembly into beaded filament, are not required for normal lens development, but are required to maintain lens clarity (150, 151).

Mutations in *BFSP1* (152),and *BFSP2* (153-155) cause non-congenital cataract in man. Similarly, a progressive increase in light scatter, and decrease in lens optical clarity, are observed in *Bfsp1* (150), and *Bfsp2* (151, 156) knockout mice. In addition, the organization of the lens fiber cell plasma membrane is altered in *Bfsp2* knockout mice, which suggests that the plasma membrane and its interaction with the cytoskeleton, play a role in lens clarity (156). Furthermore, strains of mice have been identified with naturally occurring *Bfsp2* mutations, and these mice also show increased light scatter which progresses with age (157-159).

***b. Cell matrix glycoprotein***

Another structural protein of the lens is secreted protein, acidic, cysteine-rich (SPARC), also known as osteonectin. SPARC is a calcium-binding, glycoprotein that interacts with collagen, and other extra-cellular matrix proteins, and regulates cell-matrix interactions (160-162). It also determines the production and deposition of the basement membrane protein laminin-1, in lens epithelial cells (163, 164). In addition, SPARC regulates cellular adhesions (163, 164) (160, 162), as well as cell shape and

morphology (161, 162, 165, 166). SPARC is important in maintaining lens cell osmotic homeostasis by regulating cell size, shape, and water content (165). It is required for normal differentiation and elongation of lens fiber cells, and normal lens function (167, 168).

SPARC is widely expressed in both embryonic and adult tissues including the lens, and is important for cellular proliferation and turnover (166, 169). In the human eye, SPARC is expressed in lens epithelial cells, and lens capsule, but not in the differentiated lens fiber cells of the nucleus or cortex (170, 171). In addition, SPARC is expressed in the aqueous humor, vitreous, cornea, ciliary epithelium, and retina (170). Similarly, in rodent eyes, Sparc is expressed in lens epithelial cells, lens capsule epithelia, cornea, sclera, ciliary body, choroid and retina (163, 172). The expression of *SPARC* is increased in human senile cataract (171, 173), and mice with targeted disruption of the *Sparc* gene appear normal at birth but developed lens vacuoles, cataract, and ruptured lens capsule (167, 168, 174). This suggests that *SPARC* is not required for the initial development of a normal lens, but is required for maintenance of lens clarity, and lens capsule integrity.

***c. Soluble structural proteins: crystallins***

Crystallins are divided into three main classes based on their molecular weight. These including alpha, beta, and gamma crystallins, which together, make up 90% of the soluble protein of the lens (175). Crystallin proteins form dimers, trimers, or oligomers with themselves and other crystallins, which are important in maintaining both crystallin stability and solubility, which in turn are necessary for lens transparency (175-177). As well, crystallins contribute to lens transparency through their unique spatial order and arrangement in the lens, as well as their refractive index gradient (175). The formation of cataracts is associated with the unfolding of

crystallins and formation of insoluble aggregates that often associate with membrane proteins (175). Primary and secondary lens fiber cells synthesize crystallin proteins that fill the cell and contribute to the loss of cell nuclei and organelles (26). Since the lens fiber cells are continuously added to the lens, but never lost, the crystallins must be stable enough to last throughout life. The expression of crystallin genes in the lens is regulated by transcription factors including Maf (178-180) Prox1 and Six3 (181), Pax6 (178, 182, 183) and, Sox 1 (184).

Alpha crystallins are important for normal lens development, and are the first crystallins to be expressed during lens development, in the lens vesicle and lens epithelial cells (175). Alpha crystallins function as small heat shock proteins, and molecular chaperones which stabilize lens proteins and prevent protein aggregation (185). The formation of protein aggregates in the lens is thought to contribute to the loss of lens clarity. Alpha crystallins also interact with other crystallins, as well as with the cytoskeleton and beaded filament, and these interactions are thought to be crucial for their normal function as heat shock proteins and molecular chaperones (186). There are two types of alpha crystallins; acidic alpha crystallin (CRYAA), and basic alpha crystallin (CRYAB). Mutations in alpha crystallins cause cataracts in man (13, 15, 187-191), and mouse (192, 193).

Beta and gamma crystallins are both part of a superfamily of proteins which contain four Greek key motifs. However, beta crystallins form dimers, while the gamma crystallins form monomers, and are particularly stable in dehydrated environments (175). The Greek key motifs are important in calcium binding, and in interactions with other proteins (194, 195). Thus, mutations which disrupt the Greek key motif may interfere with calcium binding and disturb normal lens ionic homeostasis, which in turn, could alter lens transparency. Likewise, disruption of the Greek key motifs may interfere with the ability of beta, and gamma crystallins to bind

or interact with other proteins, to form monomers, dimers and other aggregates important in maintaining lens clarity. Beta, and gamma crystallins are expressed in the lens fiber cells during development and are required for normal differentiation and elongation of the lens fiber cells (179, 180, 186).

Beta crystallins are divided into two groups; CRYBA and CRYBB. There are four CRYBA crystallin genes (*CRYBA1, CRYBA2, CRYBA3, CRYBA4*), and three CRYBB crystallin genes (*CRYBB1, CRYBB2, CRYBB3*). Mutations in the beta crystallins cause cataracts in man (196) (20, 21, 197, 198) and in mouse (199-201). There are at least seven gamma crystallins in mammals including *CRYGA, B, C, D, E, F,* and *S*, where *CRYGE*, and *F* are pseudogenes (202). Mutations in gamma crystallins cause cataract in man (25, 203-205), and mouse (206-210).

***2. Membrane proteins***

Because the lens is avascular and does not contain blood vessels, the transport system created by membrane proteins is critical for supplying nutrients throughout the lens, especially to the centrally located lens fiber cells. This transport system must also remove waste products. Membrane proteins are also critical for maintaining the osmotic homeostasis within the lens fiber and epithelial cells. Abnormalities in osmotic gradients in the lens can alter the solubility of proteins, causing them to aggregate and precipitate, resulting in refractive index changes, light scatter, and cataract.

The connexin family of transmembrane proteins form gap junctions between cells which allow passage of ions and small molecules. These intercellular channels are composed of six connexin units arranged in a hexamer to form a pore in the cell membrane which unites with that of an adjacent cell (211). Connexins are expressed in the developing blastomere, and throughout life, and are important for maintaining

ionic gradients within the cell (211). Connexins can open and close in response to pH and ionic gradients across cells, and are important for maintaining osmotic homeostasis which is necessary for normal lens clarity. While there are at least 20 different connexins in man, only *Connexins 43*, *46*, and *50* are expressed in the lens (212). These connexins are expressed during development in the embryonic lens vesicle, and later in the lens epithelial and fiber cells, and are important in the development and elongation of lens fibers (213, 214). *Connexin 46* (*Cx46*) and *Connexin 50 (Cx50*) knockout mice show loss of solubility and abnormal precipitation of crystallins, and the development of nuclear cataract (215, 216). Mutations in *CX50*, also known as gap junction protein alpha 8 (*GJA8*), cause cataract in man (24, 217-221), and mouse (222-225). And mutations in *CX46* (*GJA3*) cause cataract in man (23, 226-231).

Lens membrane proteins form transport channels between cells important in regulating and maintaining osmotic homeostasis. These channels transport water, ions, and molecules between communicating cells. Major intrinsic protein of lens fiber 26 (MIP26), also known as lens instrinsic membrane protein1 (LIM1), or aquaporin 0 (AQP0), is the most abundant membrane protein in the lens, and is a member of the aquaporin family of water transport proteins (232) (233). This membrane protein allows transport of water molecules between cells, and helps to maintain normal ionic homeostasis in lens cells (232, 233). In turn, the function of the MIP26 water channel is regulated by calcium and hydrogen ions in the cell (234). *MIP26* is expressed during embryogenesis in the differentiating primary lens fiber cells, and continues to be expressed in adult secondary lens fibers (235, 236). Mutations in *MIP26* cause cataract in man (236, 237), and mouse (238-240).

Lens intrinsic membrane protein 2 (LIM2), also called membrane protein 19 (MP19), is the second most abundant lens membrane protein. It is expressed during

embryogenesis (241) and plays a role in the development of lens fiber cells, forming intercellular channels between lens fiber and epithelial cells (186). Mutant *Lim2* proteins fail to localize to cell membranes in mice with cataracts (242), suggesting that the presence of *Lim2* in the membrane is necessary for normal lens transparency. *LIM2* mutations cause cataract in man (16), and mouse (243-245).

***3. Transcription factors***

Transcription factors bind to specific DNA sequences and can promote or inhibit gene expression. When transcription factors bind to gene promoters they initiate gene transcription, while binding to gene enhancers, or silencers, can increase or decrease transcription respectively. In addition to binding to target DNA sequences, transcription factors can bind to, and interact with other transcription factors. They regulate the temporal, and spatial expression of genes and are important in lens development, growth, and maintenance. As a result, abnormalities in transcription factors which are involved in eye and lens morphogenesis can affect the time and location of the expression of critical genes during lens development, growth and maintenance, and adversely affect lens transparency. Mutations in a number of transcription factors are associated with cataracts in man and mouse.

The transcription factors; CEH10 homeodomain-containing homolog (CHX10), eyes absent 1 (EYA1), forkhead box E3 (FOXE3), and paired box 6 (PAX6) are all expressed during embryogenesis, and are important regulators for ocular development. *CHX10* is expressed in the progenitor cells of the fetal retina, and in the inner nuclear layer of the adult retina (246). Although *CHX10* is only expressed in the retina, mutations in *CHX10* cause microphthalmia, cataracts and iris abnormalities (246). This suggests that the developing retina is correlated to the development of the rest of the eye.

*EYA1* is expressed in the developing CNS, and eye, including the lens placode, corneal ectoderm, iris, ciliary body, retinal pigment epithelium (RPE), and optic nerve (247). Expression of *Eya1* in the lens placode requires *Pax6* (247). EYA1 functions as both a transcription factor (248) as well as a protein-tyrosine phosphatase enzyme (249). The transcription factor EYA1 binds to and interacts with other transcription factors including SIX1 and SIX2 (250). Mutations in *EYA1* cause congenital cataracts and anterior segment abnormalities in man (251).

*FOXE3* is a member of the forkhead box (FOX) family of genes. It is expressed in the developing eye, in the lens placode, lens vesicle, and undifferentiated anterior lens epithelial cells (252). FOXE3 is a transcription factor which regulates lens development, and in particular the closing of the lens vesicle and its pinching off from the surface ectoderm (252). Also, within the lens epithelium, FOXE3 regulates cell proliferation and differentiation (252). Mutations in *FOXE3* cause anterior segment dysgenesis and cataract (253), and aphakia (254) in man, and dysgenetic lens in mouse, characterized by cataract and fusion of the lens and cornea (252).

Paired box 6 (PAX6*)* is one of nine transcription factors in the PAX family (255). It has both homeo, and paired domains which bind to DNA target sequences. This transcription factor is the master control gene for eye development and is essential for normal eye formation. It is required for the differentiation of the surface ectoderm into lens placode (256), and targeted expression of *Pax6* produces ectopic eyes in *Xenopus* (257) and *Drosophila* (258). PAX6 regulates a plethora of genes both directly and indirectly (259, 260), including the crystallin genes (261, 262), and other transcription factors including *MAF* (263), the *EYA* genes (1, 2, & 3) (247), and itself (256, 264). *PAX6* is expressed in the central nervous system (CNS), eye, nose, and pancreas in mouse (139, 256, 265, 266), and in man (29, 267). Mutations in *PAX6* are dominant to semidominant, and homozygous lethal, causing cataract, and

micropthalmia (*small eye*) in the mouse (31, 265, 268), and aniridia, foveal hypoplasia, cataract, and corneal abnormalities in man (29, 30, 269-273).

The transcription factors heat shock factor 4 (HSF4), paired-like homeodomain transcription factor 3 (PITX3), & sex-determining region Y (SRY) box 1 (SOX1), are also expressed during embryogenesis, and play critical roles in lens development. HSF4 is a member of the heat shock factor family of transcription factors which regulate the transcription of heat shock proteins and molecular chaperones in response to heat shock or other stresses. HSF4 binds to the heat shock response element, and represses transcription of heat shock response genes (274). In man, HSF4 is expressed in brain, heart, muscle and pancreas (274). In mouse, Hsf4 is expressed in the developing and adult lens anterior epithelium, and fiber cells and regulates the differentiation of secondary lens fibers (275). Hsf4 also regulates expression of gamma crystallins in the developing and adult lens (276), and *Hsf4* null mice maintain lens fiber cell nuclei and organelles, causing lens opacity (275). Mutations in *HSF4* cause cataract in man (277, 278), mouse (279) and in dogs (138).

PITX3 is a transcription factor in the pituitary homeobox (PTX) family. It is important in eye, brain, and pituitary development, and is involved in the regulation of *Foxe3* (280). In the developing lens, *Pitx3* is expressed in the lens placode (281, 282), and throughout the lens vesicle, including the anterior lens epithelium and lens equator (283). Mutations in *PITX3* cause cataract (34, 284-286), and anterior segment mesenchymal dysgenesis (ASMD) in man (33), and aphakia in mouse (35, 36).

The SOX family of transcription factors, like SRY protein, contains a high mobility group (HMG) DNA-binding domain. A member of this family, SOX1, is expressed in the developing nervous system, as well as the lens fiber cells and the anterior lens epithelium of the developing lens (184, 287). SOX1 regulates expression of crystallin genes (184, 288, 289), and is required for normal lens development and

elongation of the lens fiber cells (184). *Sox1* null mice have cataracts and microphthalmia (184).

The musculoaponeurotic fibrosarcoma homologue (*MAF*) family of genes encode basic leucine-zipper (b-ZIP) transcription factors which bind as homo, and heterodimers to DNA targets, and function as regulators of cell differentiation (290). During embryogenesis, *Maf* is expressed in the lens placode, lens vesicle, lens fiber cells, epithelial cells and optic nerve (180, 291). However, in the adult mouse, *Maf* expression is restricted to the secondary lens fibers (180). During lens development, Maf is required for normal differentiation, and elongation of lens fiber cells, and for crystallin gene expression (179, 180, 291). As a result, targeted mutations of the *Maf* gene in mice result in abnormal lens development with lens fibers that fail to elongate normally, and that contain decreased expression of crystallin genes (179, 180, 291). Mutations in *MAF* cause cataract in man (292-294) and mouse (295, 296).

The transcription factor homologue of Drosophila Sine oculis homeo box 5 (*SIX5*) is a member of the sine oculis family of homeobox genes. SIX5 interacts with *EYA1* to activate gene transcription (297), and also plays a role in maintaining ionic homeostasis in the lens, which is necessary for lens transparency (298, 299). *SIX5* is expressed in the lens epithelium, cornea, ciliary body, and retina in man (300), and in mouse (298, 299). Mutations in *Six5* cause cataracts in mice (298, 301).

***Radiation hybrid mapping***

Transcription factors, membrane proteins, and structural proteins in the lens are all critical for normal lens development and function, and the genes which encode these proteins are candidates for cataract formation in dogs. In order to study these genes in dogs their locations in the canine genome should first be identified. Radiation hybrid mapping is a technique used to locate genes and markers on

chromosomes. This technique requires the creation of a radiation hybrid panel of cells created by fusing cells from two species. Canine-hamster radiation hybrid cell lines have been made by irradiating thymidine kinase positive (TK+) canine fibroblast cells to fragment their chromosomes, and then fusing these cells with TK-negative hamster cells (55). To select fused cells containing canine DNA, only those cells which are TK(+ ) are chosen for inclusion in a radiation hybrid panel. Each hybrid cell contains a random complement of canine chromosome fragments, and hamster DNA. Enough canine-hamster radiation hybrid cells are then selected for a panel to represent the entire canine genome.

Canine-specific PCR primers designed for genes or markers of interest, can then be used to amplify DNA from each radiation hybrid cell line in the panel. Only those cell lines containing the chromosomal fragment on which the gene or marker is located will produce a positive PCR reaction. The resulting pattern of positive and negative PCR reactions from each cell line can then be analyzed statistically using software such as MULTIMAP (302). Such analysis reveals the predicted location of genes and markers in relation to one another, or in relation to a set of established markers when information from previously determined markers is combined with current data.

A canine-hamster RH3000 panel (containing canine fibroblast cells irradiated with 3000 rads of radiation) is available commercially (Research Genetics, Inc., Huntsville, AL), and consists of 92 cell lines, and an RH5000 panel (created using 5000 rads of radiation) containing 126 cell lines is available to the academic community (55, 56). The location of genes on canine chromosomes can be determined using these radiation hybrid panels. Establishing the location of cataract genes in the canine genome in relation to established markers creates a tool for

association and linkage testing in pedigrees segregating cataract phenotypes, and also facilitates the development of the dog as a model for molecular studies.

***PAX6***

Although the *Paired box 6* (*PAX6)* gene is associated with cataracts in both man (271, 303), and mouse (304), mutations in *PAX6* are also the primary cause of human aniridia (270, 305). Aniridia is an ocular condition characterized by the complete, or nearly complete absence of the iris. Normally, the iris is composed of three layers. 1) The anterior epithelial layer of the iris, derived from ectoderm, is visible when looking at the eye and determines the eye color. This layer crosses the iridocorneal angle and is continuous with the posterior epithelium of the cornea. 2) The stromal layer, which lies beneath the anterior epithelia, is derived from mesenchyme, and is composed of connective tissue and muscle. The sphincter muscle located at the pupillary circumference of the iris causes pupil constriction, while the dilator muscle composed of radial fibers spanning from the outer ciliary portion of the iris to the inner pupillary portion, causes pupil dilation. 3) The posterior pigmented epithelium, or innermost layer, lies posterior to the stromal layer of the iris. It is an extension of the retinal pigment epithelium (RPE) and therefore is derived from ectoderm.

All three layers of the iris are partially or completely missing in patients with aniridia. The mechanism of the pathogenesis of aniridia is not known but there are at least three theories: 1) aniridia results from abnormal migration and/or proliferation of mesenchymal cells, 2) aniridia results from abnormalities at the tip of the optic cup which derives from neuroectoderm, or 3) aniridia is a result of abnormal remodeling, and regression of iris tissue which involves inappropriate apoptosis (306). In man, aniridia is often accompanied by other ocular abnormalities such as cataract, corneal

opacification, foveal hypoplasia, nystagmus and glaucoma (OMIM#106210). Aniridia has also been described in the Catalan sheepdog breed in Spain (307). Affected dogs have classic aniridia phenotype with practically complete absence of the iris, and, like man, some dogs also have cataract, corneal opacity, and glaucoma. Because the vast majority of human aniridia cases are caused by mutations in *PAX6* (270, 305), this gene is also a prime candidate for canine aniridia.

***PAX6 Expression***

In the mouse, *Pax6* expression is first detected at embryonic day 8 (E-8), in the surface ectoderm, prosencephalon, rhombencephalon (hindbrain), and spinal cord (139, 256). In the developing eye, *Pax6* is expressed in the optic sulcus at day 8.5, optic vesicle at day 9.5, and in the optic cup, surface ectoderm, lens placode, and lens vesicle, between days 10-12 (139, 256). *Pax6* expression is maintained in the surface ectoderm as it develops into the anterior corneal epithelium, and conjunctiva, and in the lens vesicle as it forms the lens (139, 256, 308). The surface ectoderm thickens to form the lens placode, which invaginates and pinches off to form the lens vesicle which will form the lens, while the remaining surface ectoderm gives rise to the cornea, conjunctiva, and eye lids. *Pax6* expression is crucial for the induction of the lens placode from the surface ectoderm (256, 309). As well, *Pax6* is expressed in the optic stalk (day 12.5) as it forms a trough for optic nerve elongation, and in the inner and outer layers of the optic cup (day 10.5) as they form the developing neural retina, and pigmented retinal epithelium, respectively (139, 256). In chick embryos, *Pax6* is expressed at the distal tip of the optic cup, and in the developing iris smooth muscle and epithelium (310)

Similarly, in man *PAX6* expression is first detected between day 22-23 in the neural tube, and later in the forebrain, hindbrain, somites, and spinal cord (267). In 6

week-old human embryos, *PAX6* is expressed in the surface ectoderm, lens vesicle, the inner and outer layers of the optic cup and the optic stalk (311). By 8-22 weeks, expression is present in the developing cornea, conjunctiva, and lens, as well as the developing retina, and ciliary epithelia (29, 311). The inner layer of the optic cup develops into the neural retina while the outer layer develops into the retinal pigment epithelium (RPE). At the distal tip of the optic cup, the outer layer of pigmented epithelium will form the ciliary body, the posterior layer of the iris, and the sphincter and dilator muscles within the stromal layer of the iris. Also, the connective tissue of the iris stromal layer derives from neural crest cells and mesoderm, while the blood vessels originate from the hyaloid vasculature which originated from angiogenic mesenchyme (141). After 21 weeks, *PAX6* expression in the retina is restricted to the inner nuclear, and ganglion cell layers (311). In the adult human eye, *PAX6* continues to be expressed in the cornea, and lens (312), and in the inner nuclear, and ganglion cell layers of the retina (313).

To date, no studies have been done to determine *PAX6* expression in canine embryos, or in adult dogs. However, if the expression of *PAX6* in the dog is similar to that of the mouse and man, then it should occur in the same developing structures, including the CNS, eye, nose, and pancreas. Likewise, within the developing canine eye, *PAX6* expression would occur within the same developing ocular structures as man and mouse, but at their unique time of development in the dog. Thus, *PAX6* expression in the canine optic vesicle and lens placode would occur at days 15-17, expression in the optic cup, at day 19, in the lens vesicle at days 19-25, and in the differentiating retina, at days 25-33 (140, 141). Although this is purely speculative, the consistency in *Pax6* expression patterns across species supports these assumptions (314).

***PAX6 mutations cause a variety of ocular phenotypes***

Mutations in *PAX6* cause a wide variety of ocular phenotypes in addition to cataracts and aniridia. These include: corneal dystrophy, keratitis, iris coloboma, ectopic pupil, foveal hypoplasia, and optic nerve dystrophy (OMIM# 607108). In addition, mutations in *PAX6* have also been associated with Peter's anomaly (315), nystagmus (40), and microphthalmia (303). Furthermore, *PAX6* is expressed in multiple structures of the eye during development including the surface ectoderm, lens placode, lens vesicle, optic cup, optic stalk, retina, cornea, conjunctiva, and the ciliary body and iris (29, 267, 311-313). The wide variety of phenotypes associated with *PAX6* mutations, the number of ocular structures involved, and the pervasive expression of *PAX6* during eye morphogenesis, make this gene a candidate for a wide variety of ocular diseases.

***Siberian huskies with cataract***

Naturally occurring hereditary cataracts have been documented in over 20 breeds of dog (102, 103, 138). Siberian huskies are predisposed to developing cataracts (103), and have an increased prevalence of primary cataracts when compared with other dog breeds in North America (102). Hereditary cataracts in Siberian huskies are typically posterior cortical, and can be present at birth (congenital), or develop very early, typically being diagnosed by 1.5 years of age (102). These cataracts may be unilateral or bilateral, and may remain static or progress to a total cataract. The mode of inheritance is unknown. The association of *PAX6* with cataracts in man (40, 271, 303, 316) and in mouse (31, 304), and its expression in the embryonic surface ectoderm, lens placode, lens vesicle, and lens (29, 139, 256, 311), make *PAX6* a prime candidate for cataracts in Siberian huskies.

***Basenjis with persistent pupillary membranes***

During prenatal development, a vascular structure called the tunica vasculosa lentis (TVL) provides the anterior and posterior blood supply of the embryonic lens. This structure is developed in man by 9 weeks of gestation, and is formed from the hyaloid vasculature derived from embryonic mesoderm (317). The anterior part of the TVL lies posterior to the iris and is continuous with the pupillary membrane, which is supplied by the major arterial circle, and the posterior ciliary arteries (317). The pupillary membrane regresses 10-12 days postnatally in the mouse (318), while in man this membrane begins to regress late in gestation, and may continue to regress after birth (317). Similarly, in dogs, the hyaloid blood vessels begin to regress prenatally in late gestation (day 45), while the pupillary membranes continue to regress postnatally until around day 14 (103). The presence of the pupillary membrane, beyond this period, is considered abnormal. The precise mechanism responsible for the normal attenuation and regression of the pupillary membrane vasculature is unclear, but involves apoptosis and macrophage-mediated phagocytosis of endothelial cells (319).

Strands of PPM originate at the iris collarette; the junction between the inner pupillary, and outer ciliary zones of the iris. From the iris collarette, strands may cross the pupil and connect back to the iris, or connect from iris to cornea, or iris to lens. If the strands connect iris to iris there is usually little consequence, and vision is not affected. However, iris to cornea and iris to lens strands can result in areas of opacity at the attachment site, leading to corneal or lens opacities respectively. In some cases, PPM may have one connection to the iris and one end floating free within the aqueous humor of the anterior chamber. In more severe cases, the pupil is obstructed and deprivation amblyopia may result. Such cases require surgical intervention to remove the obstructing membrane over the pupil and allow light to pass through to the retina.

Inherited, congenital PPM occurs in Basenji dogs (103, 320-324). The mode of inheritance for this disease is not clear, but Basenjis often have strands which connect the iris collarette to the cornea and cause corneal opacities which may affect normal vision. In man, PPM can occur in association with aniridia (325, 326). Patients with *PAX6* mutations have also been observed with PPM in conjuction with circumpupillary aplasia (partial aniridia), and nystagmus (327). These patients may also have cataract, corneal dystrophy, foveal hypoplasia, and hypoplastic optic nerve heads. Another patient with a *PAX6* mutation had PPM with nystagmus, cataract, optic nerve hypoplasia, and iris ectropion (a condition where the pigmented epithelium of the posterior iris protrudes into the anterior iris) (328). In addition, some *PAX6* mutations are associated with persistent hyperplastic primary vitreous (PHPV) in man (329). This supports a relationship between *PAX6* and phenotypes involving intra-ocular vascular structures. The association of PPM with aniridia phenotypes, the association of aniridia with *PAX6* mutations, and the identification of patients with *PAX6* mutations which have PPM, as well as those with PHPV, supports the selection of this gene for evaluation in dogs with PPM.

***Soft-coated wheaten terriers with persistent pupillary membrane, sclero-cornea, and choroidal hypoplasia***

Soft-coated wheaten terriers (SCWTs) have been observed with congenital ocular abnormalities including lens luxation/subluxation, cataract, microphthalmia, PPM, corneal edema, sclero-cornea, and choroidal hypoplasia (330). Similarly, SCWTs with a recessively inherited, ocular syndrome consisting of PPM, sclero-cornea, and choroidal hypoplasia were observed by a veterinary ophthalmologist in our laboratory. Some of these dogs also had cataracts, and/or microcornea; however, lens luxation/subluxation, microphthalmia, and corneal edema were not observed.

*PAX6* was evaluated in SCWTs with PPM, sclero-cornea, and choroidal hypoplasia because mutations in *PAX6* have been associated with these abnormalities.

Persistent pupillary membranes and their association with *PAX6* were described above. Sclero-cornea is a condition where the limbic border is obscured by an invasion of scleral tissue into the cornea. The sclera is the white, fibrous, outer covering of the eye, composed of elastin and collagen fibers. The connective tissue of the sclera develops from neural crest (141). The cornea is the transparent, avascular covering over the iris, pupil, and aqueous humor of the anterior eye chamber. The refraction of light rays as they pass through the cornea is important for normal vision. An elevated density of sensory nerve fibers in the cornea make it extremely sensitive to stimuli, while the lack of blood vessels gives the cornea immune privilege. The line of demarcation between the transparent cornea and the fibrous sclera is referred to as the limbus. When the white sclera invades the clear cornea, obscuring the normal limbus, sclero-cornea results, and vision is adversely affected. *PAX6* is expressed in both the developing (29, 311), and adult (312) cornea. In man, mutations in *PAX6* can cause corneal dystrophy, corneal opacity, pannus and autosomal dominant keratitis (OMIM#106210). In addition, a missense mutation in the *PAX6* paired domain results in sclero-cornea with microphthalmia (331) (332). Because *PAX6* mutations cause corneal diseases as well as sclero-cornea, this gene is a candidate for sclero-cornea in SCWTs.

The uvea is the pigmented vascular structure of the eye, composed of the iris, the ciliary body and the choroid. The choroid is located between the outer sclera, and the inner retina and is continuous with the ciliary body and iris. The choroid is composed of pigmented cells called melanocytes which derive from neural crest cells, as well as blood vessels which derive from angiogenic mesoderm, and connective tissue derived from both neural crest and mesoderm (141). The lack of development

of the choroid layer of the eye, characterized by areas of depigmentation (paleness), is referred to as choroidal hypoplasia. Since the choroid is derived from both neural crest and mesodermal cells, abnormalities in either could contribute to the development of choroidal hypoplasia. Mutations in *PAX6* are associated with abnormal development of the uvea including the iris, and ciliary body (305), as well as the choroid (329). As a result, *PAX6* is a candidate gene for choroidal hypoplasia in SCWTs.

***Conclusion***

Cataracts are a major cause of visual impairment throughout the world. Molecular studies using animal models can help us to identify genes associated with cataract formation. The objective of my research has been to develop the dog as an animal model for the study of molecular aspects of cataractogenesis. To facilitate the development and use of canine models to study cataracts, 21 cataract candidate genes were mapped to canine chromosomes in relation to microsatellite, and gene markers (chapter 2). This created a resource which could be used to test for association and linkage of these cataract candidate genes with cataract phenotypes in canine pedigrees. The cataract candidate gene *PAX6* was then chosen as the first gene for further evaluation. This gene was cloned, and characterized, and compared with the homologous human and mouse genes (Chapter 3). Because of its close association with human aniridia, the canine *PAX6* gene was also evaluated for association with aniridia in a family of Catalan sheepdogs. In addition, *PAX6* was examined for mutations associated with cataracts, persistent pupillary membranes, sclero-cornea, and choroidal hypoplasia in three different canine breeds (Chapter 4).
This research has helped to develop the dog as a viable animal model for molecular studies of cataract, and other inherited ocular diseases which occur in man

REFERENCES

1. Resnikoff S, Pascolini D, Etya'ale D, Kocur I, Pararajasegaram R, Pokharel GP, Mariotti SP. Global data on visual impairment in the year 2002. Bull World Health Organ 2004;82(11):844-51. Epub 2004 Dec 14.

2. NEI/NIH. Mission and Challenges for Vision Research Report. In: National Eye Institute; 2006. (http://www.nei.nih.gov/resources/strategicplans/neiplan/frm_mission.asp)

3. NEI/NIH. Vision Problems in the U.S.:Prevalence of adult vision impairment and age-related eye diseases in America. Report. Bethesda, Maryland: National Eye Institute; 2002. Report No.: Publication No. EY-47. (http://catalog.nei.nih.gov/productcart/pc/viewPrd.asp?idcategory=25&idproduct=47)

4. West S. Ocular ultraviolet B exposure and lens opacities: a review. J Epidemiol 1999;9(6 Suppl):S97-101.

5. Manson JE, Christen WG, Seddon JM, Glynn RJ, Hennekens CH. A prospective study of alcohol consumption and risk of cataract. Am J Prev Med 1994;10(3):156-61.

6. Klein BE, Klein R, Linton KL, Franke T. Cigarette smoking and lens opacities: the Beaver Dam Eye Study. Am J Prev Med 1993;9(1):27-30.

7. Mares-Perlman JA, Brady WE, Klein BE, Klein R, Haus GJ, Palta M, Ritter LL, Shoff SM. Diet and nuclear lens opacities. Am J Epidemiol 1995;141(4):322-34.

8. Mares-Perlman JA, Lyle BJ, Klein R, Fisher AI, Brady WE, VandenLangenberg GM, Trabulsi JN, Palta M. Vitamin supplement use and incident cataracts in a population-based study. Arch Ophthalmol 2000;118(11):1556-63.

9. Evans CA. 1995 Presidential Address. Public health: vision and reality. Am J Public Health 1996;86(4):476-9.

10. Evans J, Rooney C, Ashwood F, Dattani N, Wormald R. Blindness and Partial Sight in England and Wales: April 1990 - March 1991. Health Trends 1996;28:5-12.

11. Weigong H, Shibo L. Congenital cataracts: gene mapping. Human Genetics 2000;106(1):1-13.

12. Bateman JB, Spence MA, Marazita ML, Sparkes RS. Genetic linkage analysis of autosomal dominant congenital cataracts. Am J Ophthalmol 1986;101(2):218-225.

13. Litt M, Kramer P, LaMorticella DM, Murphey W, Lovrien EW, Weleber RG. Autosomal dominant congenital cataract associated with a missense mutation in the human alpha crystallin gene CRYAA. Hum Mol Genet 1998;7(3):471-474.

14. Ionides A, Francis P, Berry V, Mackay D, Bhattacharya S, Shiels A, Moore A. Clinical and genetic heterogeneity in autosomal dominant cataract. Br J Ophthalmol 1999;83(7):802-808.

15. Pras E, Frydman M, Levy-Nissenbaum E, Bakhan T, Raz J, Assia EI, Goldman B, Pras E. A nonsense mutation (W9X) in CRYAA causes autosomal recessive cataract in an inbred Jewish Persian family. Invest Ophthalmol Vis Sci 2000;41(11):3511-3515.

16. Pras E, Levy-Nissenbaum E, Bakhan T, Lahat H, Assia E, Geffen-Carmi N, Frydman M, Goldman B. A missense mutation in the LIM2 gene is associated with autosomal recessive presenile cataract in an inbred Iraqi Jewish family. Am J Hum Genet 2002;70(5):1363-7. Epub 2002 Mar 26.

17. Riazuddin SA, Yasmeen A, Yao W, Sergeev YV, Zhang Q, Zulfiqar F, Riaz A, Riazuddin S, Hejtmancik JF. Mutations in betaB3-crystallin associated with autosomal recessive cataract in two Pakistani families. Invest Ophthalmol Vis Sci 2005;46(6):2100-2106.

18. Stambolian D, Lewis RA, Buetow K, Bond A, Nussbaum R. Nance-Horan syndrome: localization within the region Xp21.1-Xp22.3 by linkage analysis. Am J Hum Genet 1990;47(1):13-19.

19. Francis PJ, Berry V, Hardcastle AJ, Maher ER, Moore AT, Bhattacharya SS. A locus for isolated cataract on human Xp. J Med Genet 2002;39(2):105-109.

20. Mackay DS, Boskovska OB, Knopf HL, Lampi KJ, Shiels A. A nonsense mutation in CRYBB1 associated with autosomal dominant cataract linked to human chromosome 22q. American Journal of Human Genetics 2002;5:1216-1221.

21. Gill D, Klose R, Munier FL, McFadden M, Priston M, Billingsley G, Ducrey N, Schorderet DF, Heon E. Genetic heterogeneity of the Coppock-like cataract: a mutation in CRYBB2 on chromosome 22q11.2. Invest Ophthalmol Vis Sci 2000;41(1):159-65.

22. Ren Z, Li A, Shastry BS, Padma T, Ayyagari R, Scott MH, Parks MM, Kaiser-Kupfer MI, Hejtmancik JF. A 5-base insertion in the gammaC-crystallin gene is associated with autosomal dominant variable zonular pulverulent cataract. Hum Genet 2000;106(5):531-7.

23. Mackay D, Ionides A, Kibar Z, Rouleau G, Berry V, Moore A, Shiels A, Bhattacharya S. Connexin46 mutations in autosomal dominant congenital cataract. Am J Hum Genet 1999;64(5):1357-64.

24. Berry V, Mackay D, Khaliq S, Francis PJ, Hameed A, Anwar K, Mehdi SQ, Newbold RJ, Ionides A, Shiels A, Moore T, Bhattacharya SS. Connexin 50 mutation in a family with congenital "zonular nuclear" pulverulent cataract of Pakistani origin. Hum Genet 1999;105(1-2):168-70.

25. Santhiya ST, Shyam Manohar M, Rawlley D, Vijayalakshmi P, Namperumalsamy P, Gopinath PM, Loster J, Graw J. Novel mutations in the gamma-crystallin genes cause autosomal dominant congenital cataracts. J Med Genet 2002;39(5):352-8.

26. Gilbert SF. Chapter 12: The central nervous system and the epidermis. In: Developmental Biology. 6 ed. Sunderland, MA: Sinauer Associates, Inc; 2000. p. 399-403.

27. Francis PJ, Berry V, Moore AT, Bhattacharya S. Lens biology: development and human cataractogenesis. Trends Genet 1999;15(5):191-6.

28. MGI. Mouse Genome Informatics & Database (MGD). In: The Jackson Laboratory, Bar Harbor, Maine; 2007. (http://www.informatics.jax.org/)

29. Ton CC, Hirvonen H, Miwa H, Weil MM, Monaghan P, Jordan T, van Heyningen V, Hastie ND, Meijers-Heijboer H, Drechsler M, et al. Positional cloning and characterization of a paired box- and homeobox-containing gene from the aniridia region. Cell 1991;67(6):1059-74.

30. Glaser T, Walton DS, Maas RL. Genomic structure, evolutionary conservation and aniridia mutations in the human PAX6 gene. Nat Genet. 1992;2(3):232-239.

31. Hill RE, Favor J, Hogan BL, Ton CC, Saunders GF, Hanson IM, Prosser J, Jordan T, Hastie ND, van Heyningen V. Mouse small eye results from mutations in a paired-like homeobox-containing gene. Nature 1991;354(6354):522-5.

32. Hogan BL, Hirst EM, Horsburgh G, Hetherington CM. Small eye (Sey): a mouse model for the genetic analysis of craniofacial abnormalities. Development 1988;103(Supplement):115-119.

33. Semina EV, Ferrell RE, Mintz-Hittner HA, Bitoun P, Alward WL, Reiter RS, Funkhauser C, Daack-Hirsch S, Murray JC. A novel homeobox gene PITX3 is mutated in families with autosomal-dominant cataracts and ASMD. Nat Genet 1998;19(2):167-70.

34. Berry V, Yang Z, Addison PK, Francis PJ, Ionides A, Karan G, Jiang L, Lin W, Hu J, Yang R, Moore A, Zhang K, Bhattacharya SS. Recurrent 17 bp duplication in PITX3 is primarily associated with posterior polar cataract (CPP4). J Med Genet 2004;41(8):e109.

35. Semina EV, Murray JC, Reiter R, Hrstka RF, Graw J. Deletion in the promoter region and altered expression of Pitx3 homeobox gene in aphakia mice. Hum Mol Genet. 2000;9(11):1575-1585.

36. Rieger DK, Reichenberger E, McLean W, Sidow A, Olsen BR. A double-deletion mutation in the Pitx3 gene causes arrested lens development in aphakia mice. Genomics 2001;72(1):61-72.

37. Weng J, Mata NL, Azarian SM, Tzekov RT, Birch DG, Travis GH. Insights into the function of Rim protein in photoreceptors and etiology of Stargardt's disease from the phenotype in abcr knockout mice. Cell 1999;98(1):13-23.

38. Karan G, Lillo C, Yang Z, Cameron DJ, Locke KG, Zhao Y, Thirumalaichary S, Li C, Birch DG, Vollmer-Snarr HR, Williams DS, Zhang K. Lipofuscin accumulation, abnormal electrophysiology, and photoreceptor degeneration in mutant ELOVL4 transgenic mice: a model for macular degeneration. Proc Natl Acad Sci U S A. 2005;102(11):4164-4169.

39. Azuma N, Nishina S, Yanagisawa H, Okuyama T, Yamada M. PAX6 missense mutation in isolated foveal hypoplasia. Nature Genetics 1996;13(2):141-142.

40. Hanson I, Churchill A, Love J, Axton R, Moore T, Clarke M, Meire F, van Heyningen V. Missense mutations in the most ancient residues of the PAX6 paired domain underlie a spectrum of human congenital eye malformations. Hum Mol Genet 1999;8(2):165-72.

41. Ostrander EA, Galibert F, Patterson DF. Canine genetics comes of age. Trends in Genetics 2000;16:117-124.

42. Parker HG, Kim LV, Sutter NB, Carlson S, Lorentzen TD, Malek TB, Johnson GS, DeFrance HB, Ostrander EA, Kruglyak L. Genetic Structure of the Purebred Domestic Dog. Science 2004;304(5674):1160-1164.

43. Sutter NB, Ostrander EA, Guyon R, Lorentzen TD, Hitte C, Kim L, Cadieu E, Parker HG, Quignon P, Lowe JK, Renier C, Gelfenbeyn B, Vignaux F, DeFrance HB, Gloux S, Mahairas GG, Andre C, Galibert F, Everts RE, Versteeg SA, Groot PC, Rothuizen J, van Oost BA, Tiret L, Kessler JL, Bentolila S, Faure S, Bach JM, Weissenbach J, Panthier JJ, Mellersh CS, Richman M, Priat C, Jouquand S, Werner P, DeRose S, Patterson DF, Neff MW, Broman KW, Ray K, Acland GM, Aguirre GD, Ziegle JS, Rine J. Dog star rising: the canine genetic system. Nat Rev Genet 2004;5(12):900-910.

44. Ostrander EA, Wayne RK. The canine genome. Genome Res 2005;15(12):1706-1716.

45. Peltonen L. Positional cloning of disease genes: advantages of genetic isolates. Hum Hered 2000;50(1):66-75.

46. Ostrander EA, Giniger E. Semper fidelis: what man's best friend can teach us about human biology and disease. American Journal of Human Genetics 1997;61(3):475-480.

47. Starkey MP, Scase TJ, Mellersh CS, Murphy S. Dogs really are man's best friend--canine genomics has applications in veterinary and human medicine! Briefings in functional genomics and proteomics 2005;4(2):112-128.

48. Ostrander EA, Kruglyak L. Unleashing the canine genome. Genome Res 2000;10(9):1271-4.

49. Langston AA, Mellersh CS, Neal CL, Ray K, Acland GM, Gibbs M, Aguirre GD, Fournier RE, Ostrander EA. Construction of a panel of canine-rodent hybrid cell lines for use in partitioning of the canine genome. Genomics 1997;46(3):317-25.

50. Li R, Mignot E, Faraco J, Kadotani H, Cantanese J, Zhao B, Lin X, Hinton L, Ostrander EA, Patterson DF, de Jong PJ. Construction and characterization of an eightfold redundant dog genomic bacterial artificial chromosome library. Genomics. 1999;58(1):9-17.

51. Mellersh CS, Langston AA, Acland GM, Fleming MA, Ray K, Wiegand NA, Francisco LV, Gibbs M, Aguirre GD, Ostrander EA. A linkage map of the canine genome. Genomics 1997;46(3):326-36.

52. Neff MW, Broman KW, Mellersh CS, Ray K, Acland GM, Aguirre GD, Ziegle JS, Ostrander EA, Rine J. A second-generation genetic linkage map of the domestic dog, Canis familiaris. Genetics 1999;151(2):803-20.

53. Werner P, Mellersh CS, Raducha MG, DeRose S, Acland GM, Prociuk U, Wiegand N, Aguirre GD, Henthorn PS, Patterson DF, Ostrander EA, Breen M, Langford CF, Carter NP, Holmes NG, Dickens HF, Thomas R, Suter N, Ryder EJ, Pope M, Binns MM. Anchoring of canine linkage groups with chromosome-specific markers. Mamm Genome 1999;10(8):814-23.

54. Breen M, Thomas R, Binns MM, Carter NP, Langford CF. Reciprocal chromosome painting reveals detailed regions of conserved synteny between the karyotypes of the domestic dog (Canis familiaris) and human. Genomics 1999;61(2):145-55.

55. Vignaux F, Hitte C, Priat C, Chuat JC, Andre C, Galibert F. Construction and optimization of a dog whole-genome radiation hybrid panel. Mamm Genome 1999;10(9):888-94.

56. Priat C, Hitte C, Vignaux F, Renier C, Jiang Z, Jouquand S, Cheron A, Andre C, Galibert F. A whole-genome radiation hybrid map of the dog genome. Genomics 1998;54(3):361-78.

57. Guyon R, Lorentzen TD, Hitte C, Kim L, Cadieu E, Parker HG, Quignon P, Lowe JK, Renier C, Gelfenbeyn B, Vignaux F, DeFrance HB, Gloux S, Mahairas GG, Andre C, Galibert F, Ostrander EA. A 1-Mb resolution radiation hybrid map of the canine genome. Proc Natl Acad Sci U S A 2003;100(9):5296-301. Epub 2003 Apr 16.

58. Hitte C, Madeoy J, Kirkness EF, Priat C, Lorentzen TD, Senger F, Thomas D, Derrien T, Ramirez C, Scott C, Evanno G, Pullar B, Cadieu E, Oza V, Lourgant K, Jaffe DB, Tacher S, Dreano S, Berkova N, Andre C, Deloukas P, Fraser C, Lindblad-Toh K, Ostrander EA, Galibert F. Facilitating genome navigation: survey sequencing and dense radiation-hybrid gene mapping. Nat Rev Genet 2005;6(8):643-8.

59. Mellersh CS, Hitte C, Richman M, Vignaux F, Priat C, Jouquand S, Werner P, Andre C, DeRose S, Patterson DF, Ostrander EA, Galibert F. An integrated linkage-radiation hybrid map of the canine genome. Mamm Genome 2000;11(2):120-30.

60. Breen M, Jouquand S, Renier C, Mellersh CS, Hitte C, Holmes NG, Cheron A, Suter N, Vignaux F, Bristow AE, Priat C, McCann E, Andre C, Boundy S, Gitsham P, Thomas R, Bridge WL, Spriggs HF, Ryder EJ, Curson A, Sampson J, Ostrander EA, Binns MM, Galibert F. Chromosome-specific single-locus FISH probes allow anchorage of an 1800-marker integrated radiation-hybrid/linkage map of the domestic dog genome to all chromosomes. Genome Res 2001;11(10):1784-95.

61. Breen M, Hitte C, Lorentzen TD, Thomas R, Cadieu E, Sabacan L, Scott A, Evanno G, Parker HG, Kirkness EF, Hudson R, Guyon R, Mahairas GG, Gelfenbeyn B, Fraser CM, Andre C, Galibert F, Ostrander EA. An integrated 4249 marker FISH/RH map of the canine genome. BMC Genomics 2004;5(1):65.

62. Yang F, O'Brien PC, Milne BS, Graphodatsky AS, Solanky N, Trifonov V, Rens W, Sargan D, Ferguson-Smith MA. A complete comparative chromosome map for the dog, red fox, and human and its integration with canine genetic maps. Genomics 1999;62(2):189-202.

63. Sargan DR, Yang F, Squire M, Milne BS, O'Brien PC, Ferguson-Smith MA. Use of flow-sorted canine chromosomes in the assignment of canine linkage, radiation hybrid, and syntenic groups to chromosomes: refinement and verification of the comparative chromosome map for dog and human. Genomics 2000;69(2):182-95.

64. Richman M, Mellersh CS, Andre C, Galibert F, Ostrander EA. Characterization of a minimal screening set of 172 microsatellite markers for genome-wide screens of the canine genome. Journal of biochemical and biophysical methods 2001;47(1-2):137-149.

65. Cargill EJ, Clark LA, Steiner JM, Murphy K, E. Multiplexing of canine microsatellite markers for whole-genome screens. Genomics 2002;80(3):250-253.

66. Clark LA, Tsai KL, Steiner JM, Williams DA, Guerra T, Ostrander EA, Galibert F, Murphy KE. Chromosome-specific microsatellite multiplex sets for linkage studies in the domestic dog. Genomics 2004;84(3):550-554.

67. Kirkness EF, Bafna V, Halpern AL, Levy S, Remington K, Rusch DB, Delcher AL, Pop M, Wang W, Fraser CM, Venter JC. The dog genome: survey sequencing and comparative analysis. Science 2003;301(5641):1898-903.

68. Lindblad-Toh K, Wade CM, Mikkelsen TS, Karlsson EK, Jaffe DB, Kamal M, Clamp M, Chang JL, Kulbokas EJ, 3rd, Zody MC, Mauceli E, Xie X, Breen M, Wayne RK, Ostrander EA, Ponting CP, Galibert F, Smith DR, DeJong PJ, Kirkness E, Alvarez P, Biagi T, Brockman W, Butler J, Chin CW, Cook A, Cuff J, Daly MJ, DeCaprio D, Gnerre S, Grabherr M, Kellis M, Kleber M, Bardeleben C, Goodstadt L, Heger A, Hitte C, Kim L, Koepfli KP, Parker HG, Pollinger JP, Searle SM, Sutter NB, Thomas R, Webber C, Baldwin J, Abebe A, Abouelleil A, Aftuck L, Ait-Zahra M, Aldredge T, Allen N, An P, Anderson S, Antoine C, Arachchi H, Aslam A, Ayotte L, Bachantsang P, Barry A, Bayul T, Benamara M, Berlin A, Bessette D, Blitshteyn B, Bloom T, Blye J, Boguslavskiy L, Bonnet C, Boukhgalter B, Brown A, Cahill P, Calixte N, Camarata J, Cheshatsang Y, Chu J, Citroen M, Collymore A, Cooke P, Dawoe T, Daza R, Decktor K, DeGray S, Dhargay N, Dooley K, Dorje P, Dorjee K, Dorris L, Duffey N, Dupes A, Egbiremolen O, Elong R, Falk J, Farina A, Faro S, Ferguson D, Ferreira P, Fisher S, FitzGerald M, Foley K, Foley C, Franke A, Friedrich D, Gage D, Garber M, Gearin G, Giannoukos G, Goode T, Goyette A, Graham J, Grandbois E, Gyaltsen K, Hafez N, Hagopian D, Hagos B, Hall J, Healy C, Hegarty R, Honan T, Horn A, Houde N, Hughes L, Hunnicutt L, Husby M, Jester B, Jones C, Kamat A, Kanga B, Kells C, Khazanovich D, Kieu AC, Kisner P, Kumar M, Lance K, Landers T, Lara M, Lee W, Leger JP, Lennon N, Leuper L, LeVine S, Liu J, Liu X, Lokyitsang Y, Lokyitsang T, Lui A, Macdonald J, Major J, Marabella R, Maru K, Matthews C, McDonough S, Mehta T, Meldrim J, Melnikov A, Meneus L, Mihalev

A, Mihova T, Miller K, Mittelman R, Mlenga V, Mulrain L, Munson G, Navidi A, Naylor J, Nguyen T, Nguyen N, Nguyen C, Nicol R, Norbu N, Norbu C, Novod N, Nyima T, Olandt P, O'Neill B, O'Neill K, Osman S, Oyono L, Patti C, Perrin D, Phunkhang P, Pierre F, Priest M, Rachupka A, Raghuraman S, Rameau R, Ray V, Raymond C, Rege F, Rise C, Rogers J, Rogov P, Sahalie J, Settipalli S, Sharpe T, Shea T, Sheehan M, Sherpa N, Shi J, Shih D, Sloan J, Smith C, Sparrow T, Stalker J, Stange-Thomann N, Stavropoulos S, Stone C, Stone S, Sykes S, Tchuinga P, Tenzing P, Tesfaye S, Thoulutsang D, Thoulutsang Y, Topham K, Topping I, Tsamla T, Vassiliev H, Venkataraman V, Vo A, Wangchuk T, Wangdi T, Weiand M, Wilkinson J, Wilson A, Yadav S, Yang S, Yang X, Young G, Yu Q, Zainoun J, Zembek L, Zimmer A, Lander ES. Genome sequence, comparative analysis and haplotype structure of the domestic dog. Nature. 2005;438(7069):803-19.

69. Jonasdottir TJ, Mellersh CS, Moe L, Vignaux F, Ostrander EA, Lingaas F. Chromosomal assignment of canine TSC2, PKD1 and CLN3 genes by radiation hybrid- and linkage analyses. Anim Genet 2000;31(2):123-6.

70. Acland GM, Ray K, Mellersh CS, Langston AA, Rine J, Ostrander EA, Aguirre GD. A novel retinal degeneration locus identified by linkage and comparative mapping of canine early retinal degeneration. Genomics 1999;59(2):134-42.

71. Acland GM, Ray K, Mellersh CS, Gu W, Langston AA, Rine J, Ostrander EA, Aguirre GD. Linkage analysis and comparative mapping of canine progressive rod-cone degeneration (prcd) establishes potential locus homology with retinitis pigmentosa (RP17) in humans. Proc Natl Acad Sci U S A 1998;95(6):3048-53.

72. Sidjanin DJ, Miller B, Kijas J, McElwee J, Pillardy J, Malek J, Pai G, Feldblyum T, Fraser C, Acland G, Aguirre G. Radiation hybrid map, physical map, and low-pass genomic sequence of the canine prcd region on CFA9 and comparative mapping with the syntenic region on human chromosome 17. Genomics 2003;81(2):138-48.

73. Jonasdottir TJ, Mellersh CS, Moe L, Heggebo R, Gamlem H, Ostrander EA, Lingaas F. Genetic mapping of a naturally occurring hereditary renal cancer syndrome in dogs. Proc Natl Acad Sci U S A 2000;97(8):4132-7.

74. Lin L, Faraco J, Li R, Kadotani H, Rogers W, Lin X, Qiu X, de Jong PJ, Nishino S, Mignot E. The sleep disorder canine narcolepsy is caused by a mutation in the Hypocretin (Orexin) receptor 2 gene. Cell 1999;98:365-376.

75. Siegel JM. Narcolepsy: a key role for hypocretins (orexins). Cell 1999;98(4):409-412.

76. Nishino S, Ripley B, Overeem S, Lammers GJ, Mignot E. Hypocretin (orexin) deficiency in human narcolepsy. The Lancet 2000;355(9197):39-40.

77. Peyron C, Faraco J, Rogers W, Ripley B, Overeem S, Charnay Y, Nevsimalova S, M. A, Reynolds D, Albin R, Li R, Hungs M, Pedrazzoli M, Padigaru M, Kucherlapati M, Fan J, Maki R, Lammers GJ, Bouras C, Kucherlapati R, Nishino S, Mignot E. A mutation in a case of early onset narcolepsy and a generalized absence of hypocretin peptides in human narcoleptic brains. Nature Genetics 2000;6(9):991-997.

78. Milunsky A, Huang XL, Milunsky J, DeStefano A, Baldwin CT. A locus for autosomal recessive achromatopsia on human chromosome 8q. Clinical Genetics 1999;56(1):82-85.

79. Winick JD, Blundell ML, Galke BL, Salam AA, Leal SM, Karayiorgou M. Homozygosity mapping of the Achromatopsia locus in the Pingelapese. American Journal of Human Genetics 1999;64(6):1679-1685.

80. Kohl S, Baumann B, Broghammer M, Jagle H, Sieving P, Kellner U, Spegal R, Anastasi M, Zrenner E, Sharpe LT, Wissinger B. Mutations in the CNGB3 gene encoding the beta-subunit of the cone photoreceptor cGMP-gated channel are responsible for achromatopsia (ACHM3) linked to chromosome 8q21. Human Molecular Genetics 2000;9(14):2107-2116.

81. Sidjanin DJ, Lowe JK, McElwee JL, Milne BS, Phippen TM, Sargan DR, Aguirre GD, Acland GM, Ostrander EA. Canine CNGB3 mutations establish cone degeneration as orthologous to the human achromatopsia locus ACHM3. Hum Mol Genet 2002;11(16):1823-33.

82. Dryja TP, McGee TL, Reichel E, Hahn LB, Cowley GS, Yandell DW, Sandberg MA, Berson EL. A point mutation of the rhodopsin gene in one form of retinitis pigmentosa. Nature 1990;343(6256):364-366.

83. Berson EL, Rosner B, Sandberg MA, Dryja TP. Ocular findings in patients with autosomal dominant retinitis pigmentosa and a rhodopsin gene defect (Pro-23-His). Arch Ophthalmol 1991;109(1):92-101.

84. Cideciyan AV, Hood DC, Huang Y, Banin E, Li ZY, Stone EM, Milam AH, Jacobson SG. Disease sequence from mutant rhodopsin allele to rod and cone photoreceptor degeneration in man. Proc Natl Acad Sci U S A 1998;95(12):7103-7108.

85. Kijas JW, Cideciyan AV, Aleman TS, Pianta MJ, Pearce-Kelling SE, Miller BJ, Jacobson SG, Aguirre GD, Acland GM. Naturally occurring rhodopsin mutation in the dog causes retinal dysfunction and degeneration mimicking human dominant retinitis pigmentosa. Proc Natl Acad Sci U S A 2002;99(9):6328-33. Epub 2002 Apr 23.

86. Kijas JW, Miller BJ, Pearce-Kelling SE, Aguirre GD, Acland GM. Canine models of ocular disease: outcross breedings define a dominant disorder present in the English mastiff and bull mastiff dog breeds. Journal of heredity 2003;94(1):27-30.

87. Cideciyan AV, Jacobson SG, Aleman TS, Gu D, Pearce-Kelling SE, Sumaroka A, Acland GM, Aguirre GD. In vivo dynamics of retinal injury and repair in the rhodopsin mutant dog model of human retinitis pigmentosa. Proc Natl Acad Sci U S A 2005;102(14):5233-5238.

88. Meindl A, Dry K, Herrmann K, Manson F, Ciccodicola A, Edgar A, Carvalho MR, Achatz H, Hellebrand H, Lennon A, Migliaccio C, Porter K, Zrenner E, Bird A, Jay M, Lorenz B, Wittwer B, D'Urso M, Meitinger T, Wright A. A gene (RPGR) with homology to the RCC1 guanine nucleotide exchange factor is mutated in X-linked retinitis pigmentosa (RP3). Nat Genet 1996;13(1):35-42.

89. Acland GM, Blanton SH, Hershfield B, Aguiree GD. XLPRA: a canine retinal degeneration inherited as an X-linked trait. American Journal of Medical Genetics 1994;52(1):27-33.

90. Zeiss CJ, Acland GM, Aguirre GD. Retinal pathology of canine X-linked progressive retinal atrophy, the locus homologue of RP3. Invest Ophthalmol Vis Sci 1999;40(13):3292-3304.

91. Zhang Q, Acland GM, Wu WX, Johnson JL, Pearce-Kelling S, Tulloch B, Vervoort R, Wright AF, Aguirre GD. Different RPGR exon ORF15 mutations in Canids provide insights into photoreceptor cell degeneration. Hum Mol Genet 2002;11(9):993-1003.

92. Narfstrom K, Wrigstad A, Nilsson SE. The Briard dog: a new animal model of congenital stationary night blindness. British Journal of Ophthalmology 1989;73(9):750-756.

93. Aguirre GD, Baldwin V, Pearce-Kelling S, Narfstrom K, Ray K, Acland GM. Congenital stationary night blindness in the dog: common mutation in the RPE65 gene indicates founder effect. Mol Vis 1998;4(23).

94. Veske A, Nilsson SE, Narfstrom K, Gal A. Retinal dystrophy of Swedish briard/briard-beagle dogs is due to a 4-bp deletion in RPE65. Genomics 1999;57(1):57-61.

95. Marlhens F, Bareil C, Griffoin JM, Zrenner E, Amalric P, Eliaou C, Liu SY, Harris E, Redmond TM, Arnaud B, Claustres M, Hamel CP. Mutations in RPE65 cause Leber's congenital amaurosis. Nat Genet 1997;17(2):139-141.

96. Gu SM, Thompson DA, Srikumari CR, Lorenz B, Finckh U, Nicoletti A, Murthy KR, Rathmann M, Kumaramanickavel G, Denton MJ, Gal A. Mutations in RPE65 cause autosomal recessive childhood-onset severe retinal dystrophy. Nat Genet 1997;17(2):194-197.

97. Morimura H, Fishman GA, Grover SA, Fulton AB, Berson EL, Dryja TP. Mutations in the RPE65 gene in patients with autosomal recessive retinitis pigmentosa or leber congenital amaurosis. Proc Natl Acad Sci U S A 1998;95(6):3088-3093.

98. Thompson DA, Gyurus P, Fleischer LL, Bingham EL, McHenry CL, Apfelstedt-Sylla E, Zrenner E, Lorenz B, Richards JE, Jacobson SG, Sieving PA, Gal A. Genetics and phenotypes of RPE65 mutations in inherited retinal degeneration. Invest Ophthalmol Vis Sci 2000;41(13):4293-4299.

99. Acland GM, Aguirre GD, Ray J, Zhang Q, Aleman TS, Cideciyan AV, Pearce-Kelling SE, Anand V, Zeng Y, Maguire AM, Jacobson SG, Hauswirth WW, Bennett J. Gene therapy restores vision in a canine model of childhood blindness. Nat Genet 2001;28(1):92-5.

100. Narfstrom K, Katz ML, Bragadottir R, Seeliger M, Boulanger A, Redmond TM, Caro L, Lai CM, Rakoczy PE. Functional and structural recovery of the retina after gene therapy in the RPE65 null mutation dog. Invest Ophthalmol Vis Sci 2003;44(4):1663-1672.

101. Acland GM, Aguirre GD, Bennett J, Aleman TS, Cideciyan AV, Bennicelli J, Dejneka NS, Pearce-Kelling SE, Maguire AM, Palczewski K, Hauswirth WW, Jacobson SG. Long-term restoration of rod and cone vision by single dose rAAV-mediated gene transfer to the retina in a canine model of childhood blindness. Molecular Therapy 2005;12(6):1072-1082.

102. Gelatt KN, Mackay EO. Prevalence of primary breed-related cataracts in the dog in North America. Vet Ophthalmol 2005;8(2):101-11.

103. Gelatt KN. Chapter 10: Diseases and surgery of the canine lens. In: Katz S, editor. Essentials of Veterinary Ophthalmology. 1 ed. Baltimore, Maryland: Lippincott Williams and Wilkins; 2000. p. 227-252.

104. Curtis R, Barnett KC. A survey of cataracts in golden and labrador retrievers. Journal of Small Animal Practice 1989;30:277-286.

105. Sidjanin DJ, McElwee J, Miller B, Aguirre GD. Cloning of canine galactokinase (GALK1) and evaluation as a candidate gene for hereditary cataracts in Labrador retrievers. Anim Genet 2005;36(3):265-266.

106. Rubin LF. Cataract in Golden Retrievers. Journal of the American Veterinary Medical Association 1974;165(5):457-458.

107. Gelatt KN. Cataracts in the Golden Retriever dog. Veterinary Medicine/Small Animal Clinician 1972;67(10):1113-1115.

108. Gelatt KN, Whitley RD, Lavach JD, Barrie KP, Williams LW. Cataracts in Chesapeake Bay Retrievers. Journal of the American Veterinary Medical Association 1979;175(11):1176-1178.

109. Gelatt KN, Wallace MR, Andrew SE, MacKay EO, Samuelson DA. Cataracts in the Bichon Frise. Vet Ophthalmol 2003;6(1):3-9.

110. Wallace MR, MacKay EO, Gelatt KN, Andrew SE. Inheritance of cataract in the Bichon Frise. Vet Ophthalmol 2005;8(3):203-5.

111. Rubin LF, Flowers RD. Inherited cataract in a family of standard poodles. Journal of the American Veterinary Medical Association 1972;161(2):207-208.

112. Barnett KC, Startup FG. Hereditary cataract in the standard poodle. Veterinary Research 1985;117(1):15-16.

113. Van Buskirk R. The lens epithelium of American cocker spaniels with inherited and non-inherited lens cataracts. Research Veterinary Science 1977;22(2):237-242.

114. Yakely W. A study of heritability of cataracts in the American Cocker Spaniel. Journal of the American Veterinary Medical Association 1978;172:814-817.

115. Barnett K. Hereditary cataract in the German shepherd. Journal of Small Animal Practice 1986;27:387-395.

116. Leppanen M, Martenson J, Maki K. Results of ophthalmologic screening examinations of German Pinschers in Finland--a retrospective study. Vet Ophthalmol 2001;4(3):165-169.

117. Bjerkas E, Bergsjo T. Hereditary cataract in the Rottweiler dog. Progress in Veterinary and Comparative Ophthalmology 1991;1:7-10.

118. Ketteritzsch K, Hamann H, Brahm R, Grussendor H, Rosenhagen CU, Distl O. Genetic analysis of presumed inherited eye diseases in Tibetan Terriers. The Veterinary Journal 2004;168(2):151-159.

119. Roberts SR, Helper LC. Cataracts in Afghan hounds. Journal of the American Veterinary Medical Association 1972;160(4):427-432.

120. Muller C, Wohlke A, Distl O. Evaluation of three canine gamma-crystallins (CRYGB, CRYGC, and CRYGS) as candidates for hereditary cataracts in the dachshund. Mol Vis 2007;13:125-132.

121. Heinrich CL, Lakhani KH, Featherstone HJ, Barnett KC. Cataract in the UK Leonberger population. Vet Ophthalmol 2006;9(5):350-356.

122. Spiess BM. [Inherited eye diseases in the Entlebucher mountain dog]. Schweiz Arch Tierheilkd. 1994;136(3):105-110.

123. Heitmann M, Hamann H, Brahm R, Grussendorf H, Rosenhagen CU, Distl O. Analysis of prevalence of presumed inherited eye diseases in Entlebucher Mountain Dogs. Vet Ophthalmol 2005;8(3):145-151.

124. Muller C, Wohlke A, Distl O. Evaluation of canine gamma-crystallin C (CRYGC) with hereditary cataracts in Entlebucher mountain dogs. Anim Genet 2006;37(4):422-423.

125. Rubin LF, Koch SA, Huber RJ. Hereditary cataracts in miniature schnauzers. Journal of the American Veterinary Medical Association 1969;154(11):1456-1458.

126. Gelatt KN, Samuelson DA, Bauer JE, Das ND, Wolf ED, Barrie KP, Andresen TL. Inheritance of congenital cataracts and microphthalmia in the Miniature Schnauzer. American Journal of Veterinary Research 1983;44(6):1130-1132.

127. Gelatt KN, Samuelson DA, Barrie KP, Das ND, Wol fED, Bauer JE, Andresen TL. Biometry and clinical characteristics of congenital cataracts and microphthalmia in the Miniature Schnauzer. Journal of the American Veterinary Medical Association 1983;183(1):99-102.

128. Zhang RL, Samuelson DA, Zhang ZG, Reddy VN, Shastry BS. Analysis of eye lens-specific genes in congenital hereditary cataracts and microphthalmia of the miniature schnauzer dog. Invest Ophthalmol Vis Sci 1991;32(9):2662-2665.

129. Shastry BS, Reddy VN. Studies on congenital hereditary cataract and microphthalmia of the miniature schnauzer dog. Biochemical and Biophysical Research Communications 1994;203(3):1663-1667.

130. Barnett KC. Hereditary cataract in the Welsh Springer spaniel. The Journal of Small Animal Practice 1980;21(11):621-625.

131. Olesen HP, Jensen OA, Norn MS. Congenital hereditary cataract in Cocker Spaniels. Journal of Small Animal Practice 1974;15(12):741-750.

132. Narfstrom K. Cataract in the West Highland white terrier. The Journal of Small Animal Practice 1981;22(7):467-471.

133. Koch SA. Cataracts in interrelated old English Sheepdogs. Journal of the American Veterinary Medical Association 1972;160(3):299-301.

134. Collins BK, Collier LL, Johnson GS, Shibuya H, Moore CP, da Silva Curiel JM. Familial cataracts and concurrent ocular anomalies in chow chows. Journal of the American Veterinary Medical Association 1992;200(10):1485-1491.

135. Bjerkas E, Haaland MB. Pulverulent nuclear cataract in the Norwegian buhund. Journal of Small Animal Practice 1995;36(11):471-474.

136. Laratta LJ, Riis RC, Kern TJ, Koch SA. Multiple congenital ocular defects in the Akita dog. The Cornell Veterinarian 1985;75(3):381-392.

137. Davidson MG. Congenital cataracts in English cocker spaniels. Veterinary Research 1988;122(23):568.

138. Mellersh CS, Pettitt L, Forman OP, Vaudin M, Barnett KC. Identification of mutations in HSF4 in dogs of three different breeds with hereditary cataracts. Vet Ophthalmol 2006;9(5):369-378.

139. Walther C, Gruss P. Pax-6, a murine paired box gene, is expressed in the developing CNS. Development 1991;113(4):1435-49.

140. Aguirre G, Rubin LF, Bistner SI. Development of the canine eye. American Journal of Veterinary Research 1972;33(12):2399-2414.

141. Noden DM, de Lahunta A. Chapter 6: Central nervous system and eye. In: The Embryology of Domestic Animals; Developmental Mechanisms and Malformations. Baltimore, Maryland: Williams and Wilkins; 1985. p. 92-119.

142. O'Rahilly R, Muller F. Developmental stages in human embryos. Publication 637 ed. Davis, California: Carnegie Institute of Washington; 1987.

143. Quinlan RA, Sandilands A, Procter JE, Prescott AR, Hutcheson AM, Dahm R, Gribbon C, Wallace P, Carter JM. The eye lens cytoskeleton. Eye 1999;13(Pt 3b):409-416.

144. Bassnett S. Lens organelle degradation. Experimental Eye Research 2002;74(1):1-6.

145. Sandilands A, Prescott AR, Carter JM, Hutcheson AM, Quinlan RA, Richards J, FitzGerald PG. Vimentin and CP49/filensin form distinct networks in the lens which are independently modulated during lens fibre cell differentiation. Journal of Cell Science 1995;108(4):1397-1406.

146. DePianto DJ, Hess JF, Blankenship TN, FitzGerald PG. Isolation and characterization of the human CP49 gene promoter. Invest Ophthalmol Vis Sci 2003;44(1):235-243.

147. Hess JF, Casselman JT, Kong AP, FitzGerald PG. Primary sequence, secondary structure, gene structure, and assembly properties suggests that the lens-specific cytoskeletal protein filensin represents a novel class of intermediate filament protein. Experimental Eye Research 1998;66(5):625-644.

148. Carter JM, Hutcheson AM, Quinlan RA. In vitro studies on the assembly properties of the lens proteins CP49, CP115: coassembly with alpha-crystallin but not with vimentin. Experimental Eye Research 1995;60(2):181-192.

149. Graw J. Congenital hereditary cataracts. Int Journal of Developmental Biology 2004;48(8-9):1031-1044.

150. Alizadeh A, Clark J, Seeberger T, Hess J, Blankenship T, FitzGerald PG. Targeted deletion of the lens fiber cell-specific intermediate filament protein filensin. Invest Ophthalmol Vis Sci 2003;44(12):5252-5258.

151. Alizadeh A, Clark JI, Seeberger T, Hess J, Blankenship T, Spicer A, FitzGerald PG. Targeted genomic deletion of the lens-specific intermediate filament protein CP49. Invest Ophthalmol Vis Sci 2002;43(12):3722-3727.

152. Ramachandran RD, Perumalsamy V, Hejtmancik JF. Autosomal recessive juvenile onset cataract associated with mutation in BFSP1. Hum Genet 2007;121(3-4):475-482.

153. Zhang L, Gao L, Li Z, Qin W, Gao W, Cui X, Feng G, Fu S, He L, Liu P. Progressive sutural cataract associated with a BFSP2 mutation in a Chinese family. Mol Vis 2006;12:1626-1631.

154. Conley YP, Erturk D, Keverline A, Mah TS, Keravala A, Barnes LR, Bruchis A, Hess JF, FitzGerald PG, Weeks DE, Ferrell RE, Gorin MB. A juvenile-onset, progressive cataract locus on chromosome 3q21-q22 is associated with a missense mutation in the beaded filament structural protein-2. Am J Hum Genet 2000;66(4):1426-31. Epub 2000 Mar 22.

155. Jakobs PM, Hess JF, FitzGerald PG, Kramer P, Weleber RG, Litt M. Autosomal-dominant congenital cataract associated with a deletion mutation in the human beaded filament protein gene BFSP2. Am J Hum Genet 2000;66(4):1432-6. Epub 2000 Mar 16.

156. Sandilands A, Prescott AR, Wegener A, Zoltoski RK, Hutcheson AM, Masaki S, Kuszak JR, Quinlan RA. Knockout of the intermediate filament protein CP49 destabilises the lens fibre cell cytoskeleton and decreases lens optical quality, but does not induce cataract. Experimental Eye Research 2003;76(3):385-391.

157. Simirskii VN, Lee RS, Wawrousek EF, Duncan MK. Inbred FVB/N mice are mutant at the cp49/Bfsp2 locus and lack beaded filament proteins in the lens. Invest Ophthalmol Vis Sci 2006;47(11):4931-4934.

158. Sandilands A, Wang X, Hutcheson AM, James J, Prescott AR, Wegener A, Pekny M, Gong X, Quinlan RA. Bfsp2 mutation found in mouse 129 strains causes the loss of CP49' and induces vimentin-dependent changes in the lens fibre cell cytoskeleton. Experimental Eye Research 2004;78(4):875-889.

159. Alizadeh A, Clark J, Seeberger T, Hess J, Blankenship T, FitzGerald PG. Characterization of a mutation in the lens-specific CP49 in the 129 strain of mouse. Invest Ophthalmol Vis Sci 2004;45(3):884-891.

160. Brekken RA, Sage EH. SPARC, a matricellular protein: at the crossroads of cell-matrix communication. Matrix Biology 2001;19(8):816-827.

161. Norose K, Lo WK, Clark JI, Sage EH, Howe CC. Lenses of SPARC-null mice exhibit an abnormal cell surface-basement membrane interface. Experimental Eye Research 2000;71(3):295-307.

162. Lane TF, Sage EH. The biology of SPARC, a protein that modulates cell-matrix interactions. FASEB Journal 1994;8(2):163-173.

163. Weaver MS, Sage EH, Yan Q. Absence of SPARC in lens epithelial cells results in altered adhesion and extracellular matrix production in vitro. Journal of Cell Biochemistry 2006;97(2):423-432.

164. Yan Q, Perdue N, Blake D, Sage EH. Absence of SPARC in murine lens epithelium leads to increased deposition of laminin-1 in lens capsule. Invest Ophthalmol Vis Sci 2005;46(12):4652-4660.

165. Yan Q, Clark JI, Wight TN, Sage EH. Alterations in the lens capsule contribute to cataractogenesis in SPARC-null mice. Journal of Cell Science 2002;115(13):2747-2756.

166. Yan Q, Blake D, Clark JI, Sage EH. Expression of the matricellular protein SPARC in murine lens: SPARC is necessary for the structural integrity of the capsular basement membrane. Journal of Histochemistry and Cytochemistry 2003;51(4):503-511.

167. Bassuk JA, Birkebak T, Rothmier JD, Clark JM, Bradshaw A, Muchowski PJ, Howe CC, Clark JI, Sage EH. Disruption of the Sparc locus in mice alters the differentiation of lenticular epithelial cells and leads to cataract formation. Experimental Eye Research 1999;68(3):321-331.

168. Norose K, Clark JI, Syed NA, Basu A, Heber-Katz E, Sage EH, Howe CC. SPARC deficiency leads to early-onset cataractogenesis. Invest Ophthalmol Vis Sci 1998;39(13):2674-2680.

169. Sage H, Vernon RB, Decker J, Funk S, Iruela-Arispe ML. Distribution of the calcium-binding protein SPARC in tissues of embryonic and adult mice. Journal of Histochemistry and Cytochemistry 1989;37(6):819-829.

170. Yan Q, Clark JI, Sage EH. Expression and characterization of SPARC in human lens and in the aqueous and vitreous humors. Experimental Eye Research 2000;71(1):81-90.

171. Kantorow M, Huang Q, Yang XJ, Sage EH, Magabo KS, Miller KM, Horwitz J. Increased expression of osteonectin/SPARC mRNA and protein in age-

related human cataracts and spatial expression in the normal human lens. Mol Vis 2000;6:24-29.

172. Gilbert RE, Cox AJ, Kelly DJ, Wilkinson-Berka JL, Sage EH, Jerums G, Cooper ME. Localization of secreted protein acidic and rich in cysteine (SPARC) expression in the rat eye. Connective Tissue Research 1999;40(4):295-303.

173. Kantorow M, Horwitz J, Carper D. Up-regulation of osteonectin/SPARC in age-related cataractous human lens epithelia. Mol Vis 1998;4:17.

174. Gilmour DT, Lyon GJ, Carlton MB, Sanes JR, Cunningham JM, Anderson JR, Hogan BL, Evans MJ, Colledge WH. Mice deficient for the secreted glycoprotein SPARC/osteonectin/BM40 develop normally but show severe age-onset cataract formation and disruption of the lens. Embo J 1998;17(7):1860-70.

175. Cartier M, Tsui L-C, Ball SP, Lubsen NH. Crystallin Genes and Cataract. In: Wright AF, Jay B, editors. Molecular Genetics of Inherited Eye Disorders. Chur, Switzerland: Harwood Academic Publishers; 1994. p. 413-443.

176. Bateman OA, Sarra R, van Genesen ST, Kappe G, Lubsen NH, Slingsby C. The stability of human acidic beta-crystallin oligomers and hetero-oligomers. Experimental Eye Research 2003;77(4):409-422.

177. Sergeev YV, Wingfield PT, Hejtmancik JF. Monomer-dimer equilibrium of normal and modified beta A3-crystallins: experimental determination and molecular modeling. Biochemistry 2000;39(51):15799-15806.

178. Yang Y, Cvekl A. Tissue-specific regulation of the mouse alphaA-crystallin gene in lens via recruitment of Pax6 and c-Maf to its promoter. Journal of Molecular Biology 2005;351(3):453-469.

179. Kim JI, Li T, Ho IC, Grusby MJ, Glimcher LH. Requirement for the c-Maf transcription factor in crystallin gene regulation and lens development. Proc Natl Acad Sci U S A 1999;96(7):3781-5.

180. Kawauchi S, Takahashi S, Nakajima O, Ogino H, Morita M, Nishizawa M, Yasuda K, Yamamoto M. Regulation of lens fiber cell differentiation by

transcription factor c-Maf. Journal of Biological Chemistry 1999;274(27):19254-19260.

181. Lengler J, Krausz E, Tomarev S, Prescott A, Quinlan RA, Graw J. Antagonistic action of Six3 and Prox1 at the gamma-crystallin promoter. Nucleic Acids Research 2001;29(2):515-526.

182. Cvekl A, Sax CM, Bresnick EH, Piatigorsky J. A complex array of positive and negative elements regulates the chicken alpha A-crystallin gene: involvement of Pax-6, USF, CREB and/or CREM, and AP-1 proteins. Molecular And Cellular Biology 1994;14(11):7363-7376.

183. Yang Y, Chauhan BK, Cveklova K, Cvekl A. Transcriptional regulation of mouse alphaB- and gammaF-crystallin genes in lens: opposite promoter-specific interactions between Pax6 and large Maf transcription factors. Journal of Molecular Biology 2004;344(2):351-368.

184. Nishiguchi S, Wood H, Kondoh H, Lovell-Badge R, Episkopou V. Sox1 directly regulates the gamma-crystallin genes and is essential for lens development in mice. Genes Dev 1998;12(6):776-81.

185. Horwitz J. The function of alpha-crystallin in vision. Semin Cell Dev Biol 2000;11(1):53-60.

186. He W, Li S. Congenital cataracts: gene mapping. Hum Genet 2000;106(1):1-13.

187. Beby F, Commeaux C, Bozon M, Denis P, Edery P, Morle L. New phenotype associated with an Arg116Cys mutation in the CRYAA gene: nuclear cataract, iris coloboma, and microphthalmia. Arch Ophthalmol 2007;125(2):213-216.

188. Santhiya ST, Soker T, Klopp N, Illig T, Prakash MV, Selvaraj B, Gopinath PM, Graw J. Identification of a novel, putative cataract-causing allele in CRYAA (G98R) in an Indian family. Mol Vis 2006;12:768-773.

189. Vanita V, Singh JR, Hejtmancik JF, Nuernberg P, Hennies HC, Singh D, Sperling K. A novel fan-shaped cataract-microcornea syndrome caused by a mutation of CRYAA in an Indian family. Mol Vis 2006;12:518-522.

190. Liu M, Ke T, Wang Z, Yang Q, Chang W, Jiang F, Tang Z, Li H, Ren X, Wang X, Wang T, Li Q, Yang J, Liu J, Wang QK. Identification of a CRYAB mutation associated with autosomal dominant posterior polar cataract in a Chinese family. Invest Ophthalmol Vis Sci 2006;47(8):3461-3466.

191. Berry V, Francis P, Reddy MA, Collyer D, Vithana E, MacKay I, Dawson G, Carey AH, Moore A, Bhattacharya SS, Quinlan RA. Alpha-B crystallin gene (CRYAB) mutation causes dominant congenital posterior polar cataract in humans. American Journal of Human Genetics 2001;69(5):1141-1145.

192. Graw J, Loster J, Soewarto D, Fuchs H, Meyer B, Reis A, Wolf E, Balling R, Hrabe de Angelis M. Characterization of a new, dominant V124E mutation in the mouse alphaA-crystallin-encoding gene. Invest Ophthalmol Vis Sci 2001;42(12):2909-2915.

193. Chang B, Hawes NL, Roderick TH, Smith RS, Heckenlively JR, Horwitz J, Davisson MT. Identification of a missense mutation in the alphaA-crystallin gene of the lop18 mouse. Mol Vis 1999;5:21.

194. Salim A, Zaidi ZH. Homology models of human gamma-crystallins: structural study of the extensive charge network in gamma-crystallins. Biochemical and Biophysical Research Communications 2003;300(3):624-630.

195. Rajini B, Shridas P, Sundari CS, Muralidhar D, Chandani S, Thomas F, Sharma Y. Calcium binding properties of gamma-crystallin: calcium ion binds at the Greek key beta gamma-crystallin fold. J Biol Chem 2001;276(42):38464-38471.

196. Billingsley G, Santhiya ST, Paterson A, D,, Ogata K, Wodak S, Hosseini S, M,, Manisastry S, M,, Vijayalakshmi P, Gopinath PM, Graw J, Heon E. CRYBA4, a novel human cataract gene, is also involved in microphthalmia. American Journal of Human Genetics 2006;79(4):702-709.

197. Yao K, Tang X, Shentu X, Wang K, Rao H, Xia K. Progressive polymorphic congenital cataract caused by a CRYBB2 mutation in a Chinese family. Mol Vis 2005;11:758-63.

198. Litt M, Carrero-Valenzuela R, LaMorticella DM, Schultz DW, Mitchell TN, Kramer P, Maumenee IH. Autosomal dominant cerulean cataract is associated with a chain termination mutation in the human beta-crystallin gene CRYBB2. Hum Mol Genet 1997;6(5):665-8.

199. Graw J, Jung M, Loster J, Klopp N, Soewarto D, Fella C, Fuchs H, Reis A, Wolf E, Balling R, Hrabe de Angelis M. Mutation in the betaA3/A1-crystallin encoding gene Cryba1 causes a dominant cataract in the mouse. Genomics 1999;62(1):67-73.

200. Kannabiran C, Rogan PK, Olmos L, Basti S, Rao GN, Kaiser-Kupfer M, Hejtmancik JF. Autosomal dominant zonular cataract with sutural opacities is associated with a splice mutation in the betaA3/A1-crystallin gene. Mol Vis 1998;4:21.

201. Graw J, Loster J, Soewarto D, Fuchs H, Reis A, Wolf E, Balling R, Hrabe de Angelis M. Aey2, a new mutation in the betaB2-crystallin-encoding gene of the mouse. Invest Ophthalmol Vis Sci 2001;42(7):1574-80.

202. Brakenhoff RH, Henskens HA, van Rossum MW, Lubsen NH, Schoenmakers JG. Activation of the gamma E-crystallin pseudogene in the human hereditary Coppock-like cataract. Human Molecular Genetics 1994;3(2):279-283.

203. Heon E, Priston M, Schorderet DF, Billingsley GD, Girard PO, Lubsen N, Munier FL. The gamma-crystallins and human cataracts: a puzzle made clearer. Am J Hum Genet 1999;65(5):1261-7.

204. Mackay DS, Andley UP, Shiels A. A missense mutation in the gammaD crystallin gene (CRYGD) associated with autosomal dominant "coral-like" cataract linked to chromosome 2q. Mol Vis 2004;10:155-62.

205. Sun H, Ma Z, Li Y, Liu B, Li Z, Ding X, Gao Y, Ma W, Tang X, Li X, Shen Y. Gamma-S crystallin gene (CRYGS) mutation causes dominant progressive cortical cataract in humans. J Med Genet 2005;42(9):706-10.

206. Graw J, Neuhauser-Klaus A, Klopp N, Selby PB, Loster J, Favor J. Genetic and allelic heterogeneity of Cryg mutations in eight distinct forms of dominant cataract in the mouse. Invest Ophthalmol Vis Sci 2004;45(4):1202-13.

207. Graw J, Loster J, Soewarto D, Fuchs H, Reis A, Wolf E, Balling R, Hrabe de Angelis M. V76D mutation in a conserved gD-crystallin region leads to dominant cataracts in mice. Mamm Genome 2002;13(8):452-5.

208. Bu L, Yan S, Jin M, Jin Y, Yu C, Xiao S, Xie Q, Hu L, Xie Y, Solitang Y, Liu J, Zhao G, Kong X. The gamma S-crystallin gene is mutated in autosomal recessive cataract in mouse. Genomics 2002a;80(1):38-44.

209. Klopp N, Loster J, Graw J. Characterization of a 1-bp deletion in the gammaE-crystallin gene leading to a nuclear and zonular cataract in the mouse. Invest Ophthalmol Vis Sci 2001;42(1):183-187.

210. Klopp N, Favor J, Loster J, Lutz RB, Neuhauser-Klaus A, Prescott A, Pretsch W, Quinlan RA, Sandilands A, Vrensen GF, Graw J. Three murine cataract mutants (Cat2) are defective in different gamma-crystallin genes. Genomics 1998;52(2):152-8.

211. Gilbert SF. Chapter 6: Cell-cell communication in development. In: Developmental Biology. 6 ed. Sunderland, MA: Sinauer Associates, Inc; 2000. p. 143-181.

212. Gerido DA, White TW. Connexin disorders of the ear, skin, and lens. Biochimica et Biophysica Acta 2004;1662(1-2):159-170.

213. Xia CH, Liu H, Cheung D, Cheng C, Wang E, Du X, Beutler B, Lo WK, Gong X. Diverse gap junctions modulate distinct mechanisms for fiber cell formation during lens development and cataractogenesis. Development 2006;133(10):2033-2040.

214. Graw J, Loster J. Developmental genetics in ophthalmology. Ophthalmic Genetics 2003;24(1):1-33.

215. Gong X, Li E, Klier G, Huang Q, Wu Y, Lei H, Kumar NM, Horwitz J, Gilula NB. Disruption of alpha3 connexin gene leads to proteolysis and cataractogenesis in mice. Cell 1997;91(6):833-43.

216. White TW, Goodenough DA, Paul DL. Targeted ablation of connexin50 in mice results in microphthalmia and zonular pulverulent cataracts. J Cell Biol 1998;143(3):815-25.

217. Vanita V, Hennies HC, Singh D, Nurnberg P, Sperling K, Singh JR. A novel mutation in GJA8 associated with autosomal dominant congenital cataract in a family of Indian origin. Mol Vis 2006;12:1217-1222.

218. Devi RR, Vijayalakshmi P. Novel mutations in GJA8 associated with autosomal dominant congenital cataract and microcornea. Mol Vis 2006;12:190-195.

219. Arora A, Minogue PJ, Liu X, Reddy MA, Ainsworth JR, Bhattacharya SS, Webster AR, Hunt DM, Ebihara L, Moore AT, Beyer EC, Berthoud VM. A novel GJA8 mutation is associated with autosomal dominant lamellar pulverulent cataract: further evidence for gap junction dysfunction in human cataract. Journal of Medical Genetics 2006;43(1):e2.

220. Willoughby CE, Arab S, Gandhi R, Zeinali S, Luk D, Billingsley G, Munier FL, Heon E. A novel GJA8 mutation in an Iranian family with progressive autosomal dominant congenital nuclear cataract. J Med Genet 2003;40(11):e124.

221. Shiels A, Mackay D, Ionides A, Berry V, Moore A, Bhattacharya S. A missense mutation in the human connexin50 gene (GJA8) underlies autosomal dominant "zonular pulverulent" cataract, on chromosome 1q. Am J Hum Genet 1998;62(3):526-32.

222. Chang B, Wang X, Hawes NL, Ojakian R, Davisson MT, Lo WK, Gong X. A Gja8 (Cx50) point mutation causes an alteration of alpha 3 connexin (Cx46) in semi-dominant cataracts of Lop10 mice. Hum Mol Genet 2002;11(5):507-13.

223. Graw J, Loster J, Soewarto D, Fuchs H, Meyer B, Reis A, Wolf E, Balling R, Hrabe de Angelis M. Characterization of a mutation in the lens-specific MP70 encoding gene of the mouse leading to a dominant cataract. Experimental Eye Research 2001;73(6):867-876.

224. Rong P, Wang X, Niesman I, Wu Y, Benedetti LE, Dunia I, Levy E, Gong X. Disruption of Gja8 (alpha8 connexin) in mice leads to microphthalmia associated with retardation of lens growth and lens fiber maturation. Development 2002;129(1):167-174.

225. Steele ECJ, Lyon MF, Favor J, Guillot PV, Boyd Y, Church RL. A mutation in the connexin 50 (Cx50) gene is a candidate for the No2 mouse cataract. Curr Eye Res 1998;17(9):883-889.

226. Rees MI, Watts P, Fenton I, Clarke A, Snell RG, Owen MJ, Gray J. Further evidence of autosomal dominant congenital zonular pulverulent cataracts

linked to 13q11 (CZP3) and a novel mutation in connexin 46 (GJA3). Hum Genet 2000;106(2):206-9.

227. Jiang H, Jin Y, Bu L, Zhang W, Liu J, Cui B, Kong X, Hu L. A novel mutation in GJA3 (connexin46) for autosomal dominant congenital nuclear pulverulent cataract. Mol Vis 2003;9:579-583.

228. Li Y, Wang J, Dong B, Man H. A novel connexin46 (GJA3) mutation in autosomal dominant congenital nuclear pulverulent cataract. Mol Vis 2004;10:668-671.

229. Bennett TM, Mackay DS, Knopf HL, Shiels A. A novel missense mutation in the gene for gap-junction protein alpha3 (GJA3) associated with autosomal dominant "nuclear punctate" cataracts linked to chromosome 13q. Mol Vis 2004;10:376-382.

230. Hansen L, Yao W, Eiberg H, Funding M, Riise R, Kjaer KW, Hejtmancik JF, Rosenberg T. The congenital "ant-egg" cataract phenotype is caused by a missense mutation in connexin46. Mol Vis 2006;12:1033-1039.

231. Addison PK, Berry V, Holden KR, Espinal D, Rivera B, Su H, Srivastava AK, Bhattacharya SS. A novel mutation in the connexin 46 gene (GJA3) causes autosomal dominant zonular pulverulent cataract in a Hispanic family. Mol Vis 2006;12:791-795.

232. Verkman AS. Role of aquaporin water channels in eye function. Experimental Eye Research 2003;76(2):137-143.

233. Gonen T, Sliz P, Kistler J, Cheng Y, Walz T. Aquaporin-0 membrane junctions reveal the structure of a closed water pore. Nature 2004;429(6988):193-197.

234. Varadaraj K, Kumari S, Shiels A, Mathias RT. Regulation of aquaporin water permeability in the lens. Invest Ophthalmol Vis Sci 2005;46(4):1393-1402.

235. Varadaraj K, Kumari SS, Mathias RT. Functional expression of aquaporins in embryonic, postnatal, and adult mouse lenses. Developmental Dynamics 2007;236(5):1319-1328.

236. Francis P, Chung JJ, Yasui M, Berry V, Moore A, Wyatt MK, Wistow G, Bhattacharya SS, Agre P. Functional impairment of lens aquaporin in two families with dominantly inherited cataracts. Human Molecular Genetics 2000;9(15):2329-2334.

237. Berry V, Francis P, Kaushal S, Moore A, Bhattacharya S. Missense mutations in MIP underlie autosomal dominant 'polymorphic' and lamellar cataracts linked to 12q. Nat Genet 2000;25(1):15-7.

238. Sidjanin DJ, Parker-Wilson DM, Neuhauser-Klaus A, Pretsch W, Favor J, Deen PM, Ohtaka-Maruyama C, Lu Y, Bragin A, Skach WR, Chepelinsky AB, Grimes PA, Stambolian DE. A 76-bp deletion in the Mip gene causes autosomal dominant cataract in Hfi mice. Genomics 2001;74(3):313-319.

239. Shiels A, Bassnett S. Mutations in the founder of the MIP gene family underlie cataract development in the mouse. Nat Genet 1996;12(2):212-5.

240. Okamura T, Miyoshi I, Takahashi K, Mototani Y, Ishigaki S, Kon Y, Kasai N. Bilateral congenital cataracts result from a gain-of-function mutation in the gene for aquaporin-0 in mice. Genomics 2003;81(4):361-368.

241. Zhou L, Chen T, Church RL. Temporal expression of three mouse lens fiber cell membrane protein genes during early development. Mol Vis 2002;8:143-148.

242. Chen T, Li X, Yang Y, Church RL. Localization of lens intrinsic membrane protein MP19 and mutant protein MP19(To3) using fluorescent expression vectors. Mol Vis 2002;8:372-388.

243. Steele EC, Jr., Kerscher S, Lyon MF, Glenister PH, Favor J, Wang J, Church RL. Identification of a mutation in the MP19 gene, Lim2, in the cataractous mouse mutant To3. Mol Vis 1997;3:5.

244. Steele ECJ, Wang JH, Lo WK, Saperstein DA, Li X, Church RL. Lim2(To3) transgenic mice establish a causative relationship between the mutation identified in the lim2 gene and cataractogenesis in the To3 mouse mutant. Mol Vis 2000;6:85-94.

245. Shiels A, King JM, Mackay DS, Bassnett S. Refractive defects and cataracts in mice lacking lens intrinsic membrane protein-2. Invest Ophthalmol Vis Sci 2007;48(2):500-508.

246. Percin E, Ploder L, Yu J, Arici K, Horsford D, Rutherford A, Bapat, Cox D, Duncan A, Kalnins V, Kocak-Altintas A, ., Sowden J, Trabousli E, Sarfarazi M, McInnes R. Human microphthalmia associated with mutations in the retinal homeobox gene CHX10. Nat Genet 2000;25:397-401.

247. Xu PX, Woo I, Her H, Beier DR, Maas RL. Mouse Eya homologues of the Drosophila eyes absent gene require Pax6 for expression in lens and nasal placode. Development 1997;124(1):219-231.

248. Xu PX, Cheng J, Epstein JA, Maas RL. Mouse Eya genes are expressed during limb tendon development and encode a transcriptional activation function. Proc Natl Acad Sci U S A 1997;94(22):11974-11979.

249. Rayapureddi JP, Kattamuri C, Steinmetz BD, Frankfort BJ, Ostrin EJ, Mardon G, Hegde RS. Eyes absent represents a class of protein tyrosine phosphatases. Nature 2003;426(6964):295-298.

250. Buller C, Xu X, Marquis V, Schwanke R, Xu PX. Molecular effects of Eya1 domain mutations causing organ defects in BOR syndrome. Human Molecular Genetics 2001;10(24):2775-2781.

251. Azuma N, Hirakiyama A, Inoue T, Asaka A, Yamada M. Mutations of a human homologue of the Drosophila eyes absent gene (EYA1) detected in patients with congenital cataracts and ocular anterior segment anomalies. Hum Mol Genet 2000;9(3):363-6.

252. Blixt A, Mahlapuu M, Aitola M, Pelto-Huikko M, Enerback S, Carlsson P. A forkhead gene, FoxE3, is essential for lens epithelial proliferation and closure of the lens vesicle. Genes Dev 2000;14(2):245-54.

253. Semina EV, Brownell I, Mintz-Hittner HA, Murray JC, Jamrich M. Mutations in the human forkhead transcription factor FOXE3 associated with anterior segment ocular dysgenesis and cataracts. Hum Mol Genet 2001;10(3):231-6.

254. Valleix S, Niel F, Nedelec B, Algros MP, Schwartz C, Delbosc B, Delpech M, Kantelip B. Homozygous nonsense mutation in the FOXE3 gene as a cause of congenital primary aphakia in humans. American Journal of Human Genetics 2006;79(2):358-364.

255. Chi N, Epstein JA. Getting your Pax straight: Pax proteins in development and disease. Trends in Genetics 2002;18(1):41-47.

256. Grindley JC, Davidson DR, Hill RE. The role of Pax-6 in eye and nasal development. Development 1995;121(5):1433-42.

257. Chow RL, Altmann CR, Lang RA, Hemmati-Brivanlou A. Pax6 induces ectopic eyes in a vertebrate. Development 1999;126(19):4213-22.

258. Halder G, Callaerts P, Gehring WJ. Induction of ectopic eyes by targeted expression of the eyeless gene in Drosophila. Science 1995;267(5205):1788-92.

259. Chauhan BK, Reed NA, Yang Y, Cermak L, Reneker L, Duncan MK, Cvekl A. A comparative cDNA microarray analysis reveals a spectrum of genes regulated by Pax6 in mouse lens. Genes To Cells 2002;7(12):1267-83.

260. Chauhan BK, Zhang W, Cveklova K, Kantorow M, Cvekl A. Identification of differentially expressed genes in mouse Pax6 heterozygous lenses. Invest Ophthalmol Vis Sci 2002;43(6):1884-1890.

261. Cvekl A, Yang Y, Chauhan BK, Cveklova K. Regulation of gene expression by Pax6 in ocular cells: a case of tissue-preferred expression of crystallins in lens. The International Journal of Developmental Biology 2004;48(8-9):829-844.

262. Chauhan BK, Yang Y, Cveklova K, Cvekl A. Functional interactions between alternatively spliced forms of Pax6 in crystallin gene regulation and in haploinsufficiency. Nucleic Acids Research 2004;32(5):1696-1709.

263. Duncan MK, Xie L, David LL, Robinson ML, Taube JR, Cui W, Reneker L. Ectopic Pax6 expression disturbs lens fiber cell differentiation. Invest Ophthalmol Vis Sci 2004;45(10):3589-3598.

264. Plaza S, Dozier C, Saule S. Quail Pax-6 (Pax-QNR) encodes a transcription factor able to bind and trans-activate its own promoter. Cell Growth and Differentiation 1993;4(12):1041-1050.

265. Ton CC, Miwa H, Saunders GF. Small eye (Sey): cloning and characterization of the murine homolog of the human aniridia gene. Genomics 1992;13(2):251-6.

266. St-Onge L, Sosa-Pineda B, Chowdhury K, Mansouri A, Gruss P. Pax6 is required for differentiation of glucagon-producing alpha-cells in mouse pancreas. Nature 1997;387(6631):406-409.

267. Gerard M, Abitbol M, Delezoide AL, Dufier JL, Mallet J, Vekemans M. PAX-genes expression during human embryonic development, a preliminary report. Comptes rendus de l'Académie des sciences. Série III, Sciences de la vie 1995;318(1):57-66.

268. Quiring R, Walldorf U, Kloter U, Gehring WJ. Homology of the eyeless gene of Drosophila to the Small eye gene in mice and Aniridia in humans. Science 1994;265(5173):785-9.

269. Davis A, Cowell JK. Mutations in the PAX6 gene in patients with hereditary aniridia. Hum Mol Genet. 1993;2(12):2093-2097.

270. Hanson IM, Seawright A, Hardman K, Hodgson S, Zaletayev D, Fekete G, van Heyningen V. PAX6 mutations in aniridia. Hum Mol Genet 1993;2(7):915-20.

271. Glaser T, Jepeal L, Edwards JG, Young SR, Favor J, Maas RL. PAX6 gene dosage effect in a family with congenital cataracts, aniridia, anophthalmia and central nervous system defects. Nature Genetics 1994;7(4):463-71.

272. Martha A, Strong LC, Ferrell RE, Saunders GF. Three novel aniridia mutations in the human PAX6 gene. Human Mutation 1995;6(1):44-49.

273. Azuma N, Hotta Y, Tanaka H, Yamada M. Missense mutations in the PAX6 gene in aniridia. Investigative Ophthalmology and Visual Science 1998;39(13):2524-2528.

274. Nakai A, Tanabe M, Kawazoe Y, Inazawa J, Morimoto RI, Nagata K. HSF4, a new member of the human heat shock factor family which lacks properties of a transcriptional activator. Molecular And Cellular Biology 1997;17(1):469-481.

275. Min JN, Zhang Y, Moskophidis D, Mivechi NF. Unique contribution of heat shock transcription factor 4 in ocular lens development and fiber cell differentiation. Genesis 2004;40(4):205-217.

276. Fujimoto M, Izu H, Seki K, Fukuda K, Nishida T, Yamada S, Kato K, Yonemura S, Inouye S, Nakai A. HSF4 is required for normal cell growth and differentiation during mouse lens development. The EMBO Journal 2004;23(21):4297-306. Epub 2004 Oct 14.

277. Bu L, Jin Y, Shi Y, Chu R, Ban A, Eiberg H, Andres L, Jiang H, Zheng G, Qian M, Cui B, Xia Y, Liu J, Hu L, Zhao G, Hayden MR, Kong X. Mutant DNA-binding domain of HSF4 is associated with autosomal dominant lamellar and Marner cataract. Nat Genet 2002b;31(3):276-8. Epub 2002 Jun 24.

278. Smaoui N, Beltaief O, BenHamed S, M'Rad R, Maazoul F, Ouertani A, Chaabouni H, Hejtmancik JF. A homozygous splice mutation in the HSF4 gene is associated with an autosomal recessive congenital cataract. Invest Ophthalmol Vis Sci 2004;45(8):2716-21.

279. Talamas E, Jackson L, Koeberl M, Jackson T, McElwee JL, Hawes NL, Chang B, Jablonski MM, Sidjanin DJ. Early transposable element insertion in intron 9 of the Hsf4 gene results in autosomal recessive cataracts in lop11 and ldis1 mice. Genomics 2006;88(1):44-51.

280. Shi X, Luo Y, Howley S, Dzialo A, Foley S, Hyde DR, Vihtelic TS. Zebrafish foxe3: roles in ocular lens morphogenesis through interaction with pitx3. Mechanisms of Development 2006;123(10):761-782.

281. Khosrowshahian F, Wolanski M, Chang WY, Fujiki K, Jacobs L, Crawford MJ. Lens and retina formation require expression of Pitx3 in Xenopus pre-lens ectoderm. Developmental Dynamics 2005;234(3):577-589.

282. Pommereit D, Pieler T, Hollemann T. Xpitx3: a member of the Rieg/Pitx gene family expressed during pituitary and lens formation in Xenopus laevis. Mechanisms of Development 2001;102(1-2):255-257.

283. Semina EV, Reiter RS, Murray JC. Isolation of a new homeobox gene belonging to the Pitx/Rieg family: expression during lens development and mapping to the aphakia region on mouse chromosome 19. Human Molecular Genetics 1997;6(12):2109-2116.

284. Burdon KP, McKay JD, Wirth MG, Russell-Eggit IM, Bhatti S, Ruddle JB, Dimasi D, Mackey DA, Craig JE. The PITX3 gene in posterior polar congenital cataract in Australia. Molecular Vision 2006;12:367-371.

285. Bidinost C, Matsumoto M, Chung D, Salem N, Zhang K, Stockton DW, Khoury A, Megarbane A, Bejjani BA, Traboulsi EI. Heterozygous and homozygous mutations in PITX3 in a large Lebanese family with posterior polar cataracts and neurodevelopmental abnormalities. Invest Ophthalmol Vis Sci 2006;47(4):1274-1280.

286. Finzi S, Li Y, Mitchell TN, Farr A, Maumenee IH, Sallum JM, Sundin O. Posterior polar cataract: genetic analysis of a large family. Ophthalmic Genetics 2005;26(3):125-130.

287. Donner AL, Ko F, Episkopou V, Maas RL. Pax6 is misexpressed in Sox1 null lens fiber cells. Gene Expression Patterns 2007;7(5):606-613.

288. Ijichi N, Tsujimoto N, Iwaki T, Fukumaki Y, Iwaki A. Distal Sox binding elements of the alpha B-crystallin gene show lens enhancer activity in transgenic mouse embryos. Journal of Biochemistry 2004;135(3):413-420.

289. Muta M, Kamachi Y, Yoshimoto A, Higashi Y, Kondoh H. Distinct roles of SOX2, Pax6 and Maf transcription factors in the regulation of lens-specific delta1-crystallin enhancer. Genes Cells 2002;7(8):791-805.

290. Blank V, Andrews NC. The Maf transcription factors: regulators of differentiation. Trends in Biochem Sci 1997;22(11):437-441.

291. Ring BZ, Cordes SP, Overbeek PA, Barsh GS. Regulation of mouse lens fiber cell development and differentiation by the Maf gene. Development 2000;127(2):307-317.

292. Vanita V, Singh D, Robinson PN, Sperling K, Singh JR. A novel mutation in the DNA-binding domain of MAF at 16q23.1 associated with autosomal

dominant "cerulean cataract" in an Indian family. American Journal of Medical Genetics 2006;140(6):558-566.

293. Jamieson RV, Munier F, Balmer A, Farrar N, Perveen R, Black GC. Pulverulent cataract with variably associated microcornea and iris coloboma in a MAF mutation family. Br J Ophthalmol 2003;87(4):411-412.

294. Jamieson RV, Perveen R, Kerr B, Carette M, Yardley J, Heon E, Wirth MG, van Heyningen V, Donnai D, Munier F, Black GC. Domain disruption and mutation of the bZIP transcription factor, MAF, associated with cataract, ocular anterior segment dysgenesis and coloboma. Hum Mol Genet 2002;11(1):33-42.

295. Perveen R, Favor J, Jamieson RV, Ray DW, Black GC. A heterozygous c-Maf transactivation domain mutation causes congenital cataract and enhances target gene activation. Hum Mol Genet 2007;16(9):1030-1038.

296. Lyon MF, Jamieson RV, Perveen R, Glenister PH, Griffiths R, Boyd Y, Glimcher LH, Favor J, Munier FL, Black GC. A dominant mutation within the DNA-binding domain of the bZIP transcription factor Maf causes murine cataract and results in selective alteration in DNA binding. Human Molecular Genetics 2003;12(6):585-594.

297. Hoskins BE, Cramer CH, Silvius D, Zou D, Raymond RM, Orten DJ, Kimberling WJ, Smith RJ, Weil D, Petit C, Otto EA, Xu PX, Hildebrandt F. Transcription factor SIX5 is mutated in patients with branchio-oto-renal syndrome. American Journal of Human Genetics 2007;80(4):800-804.

298. Sarkar PS, Appukuttan B, Han J, Ito Y, Ai C, Tsai W, Chai Y, Stout JT, Reddy S. Heterozygous loss of Six5 in mice is sufficient to cause ocular cataracts. Nat Genet 2000;25(1):110-4.

299. Kawakami K, Ohto H, Takizawa T, Saito T. Identification and expression of six family genes in mouse retina. Federation of European Biochemical Societies, Letters 1996;393(2-3):259-263.

300. Winchester CL, Ferrier RK, Sermoni A, Clark BJ, Johnson KJ. Characterization of the expression of DMPK and SIX5 in the human eye and implications for pathogenesis in myotonic dystrophy. Human Molecular Genetics 1999;8(3):481-492.

301. Klesert TR, Cho DH, Clark JI, Maylie J, Adelman J, Snider L, Yuen EC, Soriano P, Tapscott SJ. Mice deficient in Six5 develop cataracts: implications for myotonic dystrophy. Nat Genet 2000;25(1):105-109.

302. Matise TC, Perlin M, Chakravarti A. Automated construction of genetic linkage maps using an expert system (MultiMap): a human genome linkage map. Nat Genet 1994;6(4):384-90.

303. Azuma N, Yamaguchi Y, Handa H, Hayakawa M, Kanai A, Yamada M. Missense mutation in the alternative splice region of the PAX6 gene in eye anomalies. Am J Hum Genet 1999;65(3):656-63.

304. Favor J, Peters H, Hermann T, Schmahl W, Chatterjee B, Neuhauser-Klaus A, Sandulache R. Molecular characterization of Pax6(2Neu) through Pax6(10Neu): an extension of the Pax6 allelic series and the identification of two possible hypomorph alleles in the mouse Mus musculus. Genetics 2001;159(4):1689-700.

305. Prosser J, van Heyningen V. PAX6 mutations reviewed. Human Mutation 1998;11(2):93-108.

306. Beauchamp GR, Meisler DM. An alternative hypothesis for iris maldevelopment (aniridia). Journal of Pediatric Ophthalmology and Strasbismus 1986;23(6):281-283.

307. Villagrasa M. Aplasia-hipoplasia de iris con carácter hereditario en el gos d'atura. Clinica Veterinaria de Pequeños Animales 1996;16(4):201-205.

308. Koroma BM, Yang JM, Sundin OH. The Pax-6 homeobox gene is expressed throughout the corneal and conjunctival epithelia. Investigative Ophthalmology and Visual Science 1997;38(1):108-120.

309. Ashery-Padan R, Gruss P. Pax6 lights-up the way for eye development. Current opinion in cell biology 2001;13(6):706-714.

310. Jensen AM. Potential roles for BMP and Pax genes in the development of iris smooth muscle. Developmental Dynamics 2005;232(2):385-392.

311. Nishina S, Kohsaka S, Yamaguchi Y, Handa H, Kawakami A, Fujisawa H, Azuma N. PAX6 expression in the developing human eye. British Journal of Ophthalmology 1999;83(6):723-727.

312. Zhang W, Cveklova K, Oppermann B, Kantorow M, Cvekl A. Quantitation of PAX6 and PAX6(5a) transcript levels in adult human lens, cornea, and monkey retina. Molecular Vision 2001;7:1-5.

313. Stanescu D, Iseli HP, Schwerdtfeger K, Ittner LM, Reme CE, Hafezi F. Continuous expression of the homeobox gene Pax6 in the ageing human retina. Eye 2007;21(1):90-93.

314. Callaerts P, Halder G, Gehring WJ. PAX-6 in development and evolution. Annual Reviews in Neuroscience 1997;20:483-532.

315. Hanson IM, Fletcher JM, Jordan T, Brown A, Taylor D, Adams RJ, Punnett HH, van Heyningen V. Mutations at the PAX6 locus are found in heterogeneous anterior segment malformations including Peters' anomaly. Nat Genet 1994;6(2):168-73.

316. Epstein JA, Glaser T, Cai J, Jepeal L, Walton DS, Maas RL. Two independent and interactive DNA-binding subdomains of the Pax6 paired domain are regulated by alternative splicing. Genes and Development 1994;8(17):2022-34.

317. Cook CS, Ozanics V, Jakobiec FA. Prenatal Development of the Eye and its Adnexa. In: Tasman W, Jaeger EA, editors. Duane's Foundations of Clinical Ophthalmology. Philadelphia: Lippincott, Williams & Wilkins; 2004. p. 1-48.

318. Ito M, Yoshioka M. Regression of the hyaloid vessels and pupillary membrane of the mouse. Anatomy and Embryology 1999;200(4):403-411.

319. Mitchell CA, Risau W, Drexler HC. Regression of vessels in the tunica vasculosa lentis is initiated by coordinated endothelial apoptosis: a role for vascular endothelial growth factor as a survival factor for endothelium. Developmental Dynamics 1998;213(3):322-333.

320. Roberts SR, Bistner SI. Persistent pupillary membrane in Basenji dogs. Journal of the American Veterinary Medical Association 1968;153(5):533-542.

321. Barnett KC, Knight GC. Persistent pupillary membrane and associated defects in the Basenji. Veterinary Research 1969;85(9):242-248.

322. Bistner SI, Rubin LF, Roberts SR. A review of persistent pupillary membranes in the Basenji dog. Journal of the American Animal Hospital Association 1971;7:143-157.

323. Mason TA. Persistent pupillary membrane in the Basenji. Australian Veterinary Journal 1976;52(8):343-344.

324. James RW. Persistent pupillary membrane in basenji dogs. Veterinary Research 1991;128(12):287-288.

325. Hamming N, Wilensky J. Persistent pupillary membrane associated with aniridia. American Journal of Ophthalmology 1978;86(1):118-120.

326. Hamming NA, Miller MT, Rabb M. Unusual variant of familial aniridia. Journal of Pediatric Ophthalmology and Strasbismus 1986;23(4):195-200.

327. Gronskov K, Rosenberg T, Sand A, Brondum-Nielsen K. Mutational analysis of PAX6: 16 novel mutations including 5 missense mutations with a mild aniridia phenotype. European Journal of Human Genetics 1999;7(3):274-286.

328. Willcock C, Grigg J, Wilson M, Tam P, Billson F, Jamieson R. Congenital iris ectropion as an indicator of variant aniridia. Br J Ophthalmol 2006;90(5):658-659.

329. Azuma N, Yamaguchi Y, Handa H, Tadokoro K, Asaka A, Kawase E, Yamada M. Mutations of the PAX6 gene detected in patients with a variety of optic-nerve malformations. am J Hum Genet. 2003;72(6):1565-1570.

330. van der Woerdt A, Stades FC, van der Linde-Sipman JS, Boeve MH. Multiple ocular anomalies in two related litters of soft coated wheaten terriers. Veterinary and Comparative Ophthalmololgy 1995;5(2):78-82.

331. Vincent MC, Pujo AL, Olivier D, Calvas P. Screening for PAX6 gene mutations is consistent with haploinsufficiency as the main mechanism leading to various ocular defects. European Journal of Human Genetics 2003;11(2):163-169.

332. Neethirajan G, Krishnadas SR, Vijayalakshmi P, Shashikant S, Sundaresan P. PAX6 gene variations associated with aniridia in south India. BMC Medical Genetics 2004;5(9).

# CHAPTER 2

## RADIATION HYBRID MAPPING OF CATARACT GENES IN THE DOG*


### *Abstract*

Purpose: To facilitate the molecular characterization of naturally occurring cataracts in dogs by providing the radiation hybrid location of 21 cataract-associated genes along with their closely associated polymorphic markers. These can be used for segregation testing of the candidate genes in canine cataract pedigrees. Methods: Twenty-one genes with known mutations causing hereditary cataracts in man and/or mouse were selected and mapped to canine chromosomes using a canine:hamster radiation hybrid RH5000 panel. Each cataract gene ortholog was mapped in relation to over 3000 markers including microsatellites, expressed sequence tags (ESTs), genes, and bacterial artificial chromosome (BAC) clones. The resulting independently determined RH-map locations were compared with the corresponding gene locations from the draft sequence of the canine genome. Results: Twenty-one cataract orthologs were mapped to canine chromosomes. The genetic locations and nearest polymorphic markers were determined for 20 of these orthologs. In addition, the resulting cataract gene locations, as determined experimentally by this study, were compared with those determined by the canine genome project. All genes mapped within or near chromosomal locations with previously established homology to the corresponding human gene locations based on canine:human chromosomal synteny.

Conclusion: The location of selected cataract gene orthologs in the dog, along with their nearest polymorphic markers, serves as a resource for association and linkage testing in canine pedigrees segregating inherited cataracts. The recent development of canine genomic resources make canine models a practical and valuable resource for


* Hunter et. al., 2006. Molecular Vision Volume 12, pages 588-596.

the study of human hereditary cataracts. Canine models can serve as large animal models intermediate between mouse and man for both gene discovery and the development of novel cataract therapies.

***Introduction***

As the leading cause of worldwide blindness and low vision, cataracts affect millions of individuals, and billions of dollars are spent annually on cataract medical and surgical expenses [1]. The etiology of cataracts varies; they can be hereditary, traumatic or secondary to ocular inflammatory or systemic diseases, or as a sequelae to taking certain pharmaceuticals/medications. The onset of cataract also varies. Congenital cataracts occur in over 2 out of 10,000 live births [2] and are the leading cause of treatable visual impairment in children worldwide [3, 4]. Approximately 1/3 of all congenital cataracts are inherited [5]. Age-related cataracts, however, are the most common type of cataract; approximately 26.6 million Americans older than 40 years have cataract or have had cataract surgery, and this number is projected to increase to 39.6 million by the year 2020 [6]. The risk factors associated with the development of age-related cataract include ultraviolet light exposure [7], cigarette smoking [8], alcohol consumption [9], and nutrition [10]. In addition, the role of genetics in age-related cataract has been reviewed suggesting an interaction between genetic background and environmental risk factors [11].

Most of our knowledge of cataractogenesis comes from genetic studies of hereditary cataracts in man and mice. Mutations causing non-syndromic inherited cataract have been identified in at least 15 genes in man [12], and at least 18 genes in the mouse (Mouse Genome Informatics [MGI]: http://www.informatics.jax.org/). Here, we propose the development of the dog as a complementary large animal model for molecular studies of cataracts to facilitate gene discovery and the development of

novel and alternative cataract therapies. There are over 300 breeds of dog, and of these, 20 breeds are known to have hereditary cataracts while another 125 breeds are suspected of having hereditary cataract [13]. It is likely that some hereditary cataracts in dogs will be caused by mutations in cataract genes already identified in humans or mice. However, to date no mutations causing cataract have been identified in any canine pedigrees. Because of the recent progress in canine genomics [14-19], and the success in identifying canine models for retinal diseases [20-22] it is likely that similar progress will be possible with molecular studies of canine cataracts.

To begin the molecular identification of cataract phenotypes in the dog we have selected 21 genes known to cause cataracts in man and/or mouse. These include genes encoding; structural proteins (6), crystallin proteins (6) and transcription factors (9). We have determined the canine chromosomal locations of each gene using a radiation hybrid (RH) 5000 rad panel [23] and compared our experimentally derived chromosomal locations for each gene with that of the draft sequence of the canine genome. RH-mapping and genome sequencing are complementary procedures which identify gene locations, order and distance, along with regions of conserved synteny across species. Combining data from RH-maps with that from genomic sequences, maximizes the information obtained from both methodologies [24] and helps to resolve discrepancies that might arise with the draft sequence information currently available. The identification of cataract gene locations along with their nearest polymorphic markers provides an integrated resource essential for segregation analysis of cataract phenotypes in canine cataract pedigrees. This resource will aid in the development of the dog as a complementary large animal model for the molecular study of cataracts and will help to advance our knowledge of naturally occurring cataracts in mammalian species. This may one day contribute to the development of new therapies to prevent, delay or even reverse cataracts.

## *Methods*

### *Selection Of Cataract Gene Orthologs*

Twenty-one gene orthologs were selected as cataract candidate genes in dogs based on their ability to cause cataracts in man and/or mouse. These candidate genes include STRUCTURAL PROTEIN GENES: *Beaded filament structural protein 2* (*BFSP2*), *Connexin 46* (*CX46*), *Connexin 50* (*CX50*), *Lens intrinsic membrane protein 2* (*LIM2*), *Major intrinsic protein of lens fiber* (*MIP*), and *Secreted protein acidic cysteine-rich* (*SPARC*); CRYSTALLIN GENES: *Beta crystallin B2* (*CRYBB2*), *Gamma crystallin A* (*CRYGA*), *Gamma crystallin B* (*CRYGB*), *Gamma crystallin C* (*CRYGC*), *Gamma crystallin D* (*CRYGD*) and *Gamma crystallin S* (*CRYGS*); TRANSCRIPTION FACTOR GENES: *CEH10 homeodomain-containing homolog* (*CHX10*), *Homolog of Drosophila eyes absent 1* (*EYA1*), *Forkhead Box E3* (*FOXE3*), *Heat shock transcription factor 4* (*HSF4*), *Avian musculoaponeurotic fibrosarcoma oncogene homologue* (*MAF*), *Paired-box 6 transcription factor* (*PAX6*), *Paired-like homeodomain transcription factor 3* (*PITX3*), *Homologue of Drosophila sine oculis homeobox* (*SIX5*), and *Sex determining region-Y (SRY)-box 1* (*SOX1*).

### *Canine Orthologous Sequences*

Human gene cDNAs obtained from the National Center for Biotechnology Information (NCBI) database were analyzed against drafts of the canine genome to obtain orthologous sequences. The corresponding accession numbers for the human cDNA sequences are listed in Table 2.1.

Table 2.1. PCR primer sequences used to place cataract orthologs on canine chromosomes using an RH5000 panel. Primer melting temperature (Tm), PCR product size, and corresponding NCBI reference accession numbers are represented. (NCBI-National Center for Biotechnology Information).

| GENE | REFERENCE ACCESSION NO. | CANINE PRIMER SEQUENCES | Tm °C | PRO-DUCT SIZE (bp) |
|---|---|---|---|---|
| Structural Protein Genes | | | | |
| *1. BFSP2* | NM003571 | F: CCT CTT CAT AGT TCC TTG AC | 50.7 | 419 |
| | | R: CCC TAC AGT TCT ATG CTT CCA G | 55.8 | |
| *2. CX46* | NM021954 | F: CCA GAG AAT GCT AAT TTG TCC C | 54.9 | 365 |
| | | R: CAG CAC ATG CAC TTA CAC AGG | 57.6 | |
| *3. CX50* | NM005267 | F: GGG ATA ACC AGA GGG TAG CAC | 57.8 | 386 |
| | | R: GGA TCT CGA AGT TCT CCT ACC | 54.9 | |
| *4. LIM2* | NM030657 | F: GGC AAC AAG TGC TAC CTG C | 56.9 | 353 |
| | | R: CCC AGT TTC CAA CCT AGT TC | 53.0 | |
| *5. MIP* | NM012064 | F: GGG CAC GAG TAC GAG CAC TG | 61.0 | 308 |
| | | R: GCC TGC ACG CTT CGC AAG C | 63.5 | |
| *6. SPARC* | NM003118 | F: CTG ATC ATG TGG CCT TGA GC | 56.2 | 343 |
| | | R: GGC CTA ATC TGA TCT GCT AAG | 52.5 | |
| Crystallin Genes | | | | |
| *7. CRYBB2* | NM000496 | F: GGA GAG CAG TTT GTG TTC GAG | 55.9 | 356 |
| | | R: GTG CAA TGT GGC AAC CCT TAG | 56.9 | |
| *8. CRYGA* | NM014617 | F: CCT ACG AAG GAA TCC CTT TTG | 53.2 | 349 |
| | | R: GAG TGG AGC TCA TTG AGC CG | 58.1 | |
| *9. CRYGB* | NM005210 | F: GCT CCT GGC ATC CAG TGG G | 61.0 | 404 |
| | | R: CTG CTC CTG CTG CTC TAC TC | 57.3 | |
| *10. CRYGC* | NM020989 | F: CTC TAA CCC AGA CTC TGA ACC | 54.3 | 373 |
| | | R: GGA CCC AGC AGC CCT CCA G | 63.3 | |
| *11. CRYGD* | NM006891 | F: GAC AGC GGC TGC TGG ATG C | 62.1 | 381 |
| | | R: CCA GGA CAG GAC CTA TTG CTG | 57.4 | |
| *12. CRYGS* | NM017541 | F: CAG CTC ATC CCA AGA CTG AAT G | 55.7 | 390 |
| | | R: GAC ACC ATC CAG CAC CTT ACT G | 57.7 | |
| Transcription Factors | | | | |
| *13. CHX10* | NM182894 | F: CGT AAG TTA AGT ACC AGA GGG | 52.1 | 390 |
| | | R: CTA AAC CTG TGA TTT CTG TGC C | 54.0 | |
| *14. EYA1* | NM172060 | F: CTA CTG CCC AAA CTC ATC AC | 53.2 | 386 |
| | | R: CCC ACA GAA AGA ATG TAG ATG | 50.7 | |
| *15. FOXE3* | NM012186 | F: GCA AGT CAC TGC AGG GAC TG | 58.6 | 342 |
| | | R: GTT CTT TAG TGG TGC TGG AGG | 55.5 | |
| *16. HSF4* | NM001538 | F: GAT TCC TGA GCT CTA CCA TAG | 51.7 | 463 |
| | | R: GCC AGG GTC TGG TTG AAG C | 58.9 | |
| *17. MAF* | NM005360 | F: GTT AAC AGC ACG GAG GTT ACA C | 55.9 | 340 |
| | | R: CCC TTC CAC TGC ATC TGA GTC | 57.6 | |
| *18. PAX6* | NM001604 | F: GCC ACA TCT TCA GTA CAA AG | 49.6 | 300 |
| | | R: TAG TTC AGG CAT TGA CTG ATG | 50.3 | |
| *19. PITX3* | NM005029 | F: CCT CCC TGA ACA GGG TGA TAG | 57.5 | 304 |
| | | R: CCG CAC CAT TGC ACA CCA CG | 63.0 | |
| *20. SIX5* | NM175875 | F: GAC CCG CAG CTT CTC AAG C | 59.0 | 371 |
| | | R: CCT TCC TAC TGC AAA GTG AGC | 55.8 | |
| *21. SOX1* | NM005986 | F: CTC AAG AAT GAT ATC CAC TGC TTC | 53.5 | 299 |
| | | R: GTA CAT TTC AGA GTC AAT GTG GC | 54.1 | |

Human gene cDNAs for *BFSP2, CX46, CX50, MIP, PAX6,* and *PITX3* were analyzed against the original 1.5X (poodle) canine genome sequence through collaboration with The Institute for Genomic Research (TIGR). Human gene cDNAs for *CHX10, CRYBB2, CRYGA, CRYGB, EYA1, FOXE3, HSF4, MAF, SIX5, SOX1,* and *SPARC* were analyzed against the publicly available 1.5X (poodle) canine genome using the Blast function (http://www.ncbi.nlm.nih.gov/genome/seq/CfaBlast.html), and cDNAs for *CRYGC, CRYGD, CRYGS* and *LIM2* were analyzed against the 7.5X (boxer) canine whole genome shotgun sequence using the Blat function (http://genome.ucsc.edu/cgibin/hgBlat?command=start&org=Dog&db=canFam1&hgsid=60802051). Primers were designed from putative intronic or untranslated regions of canine orthologs of each cataract candidate gene using Amplify® software (Bill Engels, University of Wisconsin, Madison, WI). Primers were designed to amplify canine-specific sequences suitable for RH mapping and are summarized in Table 2.1. The average melting temperature of the primers was 56.2°C, and the average PCR product size was 363bp. All PCRs were performed on the MJ Research Tetrad 2 thermocycler (Global Medical Instrumentation Inc., Ramsey, MN) using *Taq* DNA polymerase (Invitrogen Corporation, Carlsbad, CA). To ensure canine specificity, initial PCRs were carried out at 25µl volume on control canine, hamster and canine:hamster (1:5 ratio) DNA. PCR conditions were as follows: 2 min 94°C, followed by 30 cycles of (30 sec 94°C, 30 sec 56°C, 30 sec 72°C), and a final extension of 5 min 72°C. The PCR product sizes ranged from 144-463bp. PCRs were optimized by adjusting the annealing temperature where needed.

*RH5000 Panel*

Canine cataract candidate genes were positioned on a canine radiation hybrid map using an RH5000 panel consisting of 118 cell lines made by fusing 5000 rad-irradiated canine fibroblast cells with TK-HTK3 hamster cells [23]. Information on the RH5000 panel may be obtained from the following web site: http://www-recomgen.univ-rennes1.fr/doggy.html. The RH5000 panel has a retention frequency of 22% and a resolution limit of 600kb [17]. The PCR reactions on the RH5000 panel were performed at 15µl volume using the same PCR conditions described above, and run in duplicate or triplicate. PCR products were analyzed on 2% agarose gels containing 0.05% ethidium bromide at 50-65 volts. Gel bands were visualized using a UV transilluminator, and images were taken of each gel. Gels were then scored for presence, absence, or ambiguity of the band of interest in each of the 118 cell lines.

*Radiation Hybrid Map Construction*

Radiation hybrid data collected from the 21 cataract gene orthologs was merged with previous data from 3270 markers [17], and analyzed using Multimap® software [25]. Two-point linkage analysis was performed for each canine ortholog to determine its nearest markers and chromosomal location. A subset of the linked markers was selected and used as a framework map based on their map locations as previously provided [17]. Multimap's® multipoint mapping algorithm was then used to place the cataract gene orthologs on canine chromosomes in relation to the markers within the framework map. The May 2005, 7.5X canine draft sequence predicted locations of each cataract ortholog were compared with the corresponding locations of each PCR amplicon used for RH-mapping. The resulting genome locations for each ortholog and corresponding sequence-tagged site (STS) are listed in Table 2.2

Table 2.2. Twenty-one cataract genes mapped to the canine genome.

PCR primers (Table 2.1) from 21 cataract genes were used for RH-mapping using an RH5000 panel. Multimap® two-point linkage analysis was used to identify the chromosome location and 2 nearest markers [17] along with the corresponding logarithm of odds (LOD) score and theta value (distance). To confirm these locations, PCR amplicons were analyzed against the 7.5X canine draft sequence to obtain sequence tagged site (STS) locations which were compared with the corresponding ortholog locations within the draft sequence.

| Gene | Chromosome | Closest Markers | LOD | Theta | STS Location | Canine Ortholog Location |
|---|---|---|---|---|---|---|
| *BFSP2* | CFA23 | REN156G20 | 22.448 | 0.086 | 33427673 - 33428089 | 33388029 - 33450927 |
| | | REN210D03 | 17.827 | 0.169 | | |
| *CX46* | CFA 25 | EST18C6 | 9.688 | 0.276 | 20988791 - 20989147 | 20986634 - 20987933 |
| | | BAC_372_A23 | 9.617 | 0.261 | | |
| *CX50* | CFA 17 | CFOR12C10 | 20.47 | 0.056 | 61506499 - 61506884 | 61498923 - 61505209 |
| | | PEZ8 | 19.834 | 0.058 | | |
| *LIM2* | CFA 1 | KLK2 | 18.201 | 0.035 | 108473188 - 108473537 | 108472780 - 08479290 |
| | | REN06N11 | 17.642 | 0.066 | | |
| *MIP* | CFA 10 | FH2537 | 25.039 | 0.09 | 3684287 - 3684594 | 3684852 - 3689232 |
| | | ATP5B | 21.428 | 0.132 | | |
| *SPARC* | CFA 4 | FH4018 | 14.097 | 0.048 | 60879945 - 60880285 | 60873070 - 60887224 |
| | | BAC_374_E21 | 12.897 | 0.093 | | |
| *CRYBB2* | CFA 26 | CRYBB1 | 25.249 | 0.043 | 22335395 - 22335748 | 22331283 - 22338858 |
| | | REN131L06 | 24.11 | 0.064 | | |
| *CRYGA* | CFA 37 | AHT133 | 20.482 | 0.092 | 19453604 - 19453950 | 19453388 - 19455353 |
| | | REN105M20 | 20.482 | 0.092 | | |
| *CRYGB* | CFA 37 | BAC_381_J22 | 15.426 | 0.123 | 20124535 - 20124930 | 19440507 - 19442393 |
| | | FH2708 | 13.738 | 0.157 | | |
| *CRYGC* | CFA 37 | BAC_381_J22 | 24.954 | 0 | 19431676 - 19432046 | 19431504 - 19433284 |
| | | EST22D1 | 23.468 | 0.026 | | |
| *CRYGD* | CFA37 | CRYGB | 15.027 | 0.045 | 19425779 - 19426157 | 19424588 - 19426264 |
| | | BAC_374_E1 | 8.03 | 0.354 | | |
| *CRYGS* | CFA 34 | BAC_374_K23 | 27.708 | 0.021 | 22165843 - 22166230 | 22165569 - 22166681 |
| | | REN266K05 | 27.283 | 0.022 | | |
| *CHX10* | CFA 8 | EST10D4 | 23.799 | 0.025 | 50510969 - 50511356 | 50492693 - 50511026 |
| | | EST27E3 | 21.735 | 0.051 | | |

Table 2.2. (Continued)

| | | | | | | |
|---|---|---|---|---|---|---|
| *EYA1* | CFA 29 | STS246A16 | 19.01 | 0.119 | 23177126 - 23177509 | 23176722 - 23342854 |
| | | C29_188 | 18.473 | 0.138 | | |
| *FOXE3* | CFA 15 | FH3888 | 23.211 | 0.046 | 16294587 - 16294926 | 16295972 - 16298254 |
| | | FH3886 | 22.806 | 0.047 | | |
| *HSF4* | CFA 5 | AHTH201REN | 13.127 | 0.052 | 85205320 - 85205780 | 85204186 - 85208678 |
| | | REN122J03 | 11.927 | 0.1 | | |
| *MAF* | CFA 5 | FH3450 | 9.517 | 0.244 | 74976764 - 74977099 | 74970434 - 74976948 |
| | | FH3113 | 9.427 | 0.224 | | |
| *PAX6* | CFA 18 | WT1 | 17.245 | 0.148 | 38687699 - 38688008 | 38671041 - 38693640 |
| | | FH3824 | 17.15 | 0.148 | | |
| *PITX3* | CFA 28 | EST3H1 | 19.137 | 0.083 | 17763487 - 17763792 | 17761261 - 17772191 |
| | | COL17A1 | 18.606 | 0.085 | | |
| *SIX5* | CFA 1 | BAC_375_N13 | 21.594 | 0 | 112730879 - 112731247 | 112726865 - 12731063 |
| | | FH2598 | 21.594 | 0 | | |
| *SOX1* | CFA 22 | EST3G2 | 26.711 | 0.022 | 62864830 - 62865127 | 62861615 - 62864949 |
| | | BAC_376_O1 | 24.774 | 0.045 | | |

***Results and Discussion***

*Two-Point Linkage Analysis*

Twenty-one cataract gene orthologs were positioned on canine chromosomes using an RH5000 panel of 118 cell lines. Orthologs were located on 16 of the 39 canine chromosomes with more than one ortholog represented on 3 chromosomes (CFA1, 5, and 37) (Table 2.2). The nearest chromosomal markers were determined for each cataract gene ortholog using Multimap® two-point linkage analysis [25]. Logarithm of odds (LOD) scores for the 2 closest linked markers ranged from 8.0 (*CRYGD*:BAC_374_E1) to 27.7 (*CRYGS*:BAC_374_K23), with an average LOD score of 18.9 (Table 2.2). Theta (θ), a measure of the frequency of breakage between two markers, varies from 0 (no breakage between markers) to 1 (complete breakage between markers), and represents the distance between markers. Theta ranged from 0 (*CRYGC*:BAC_381_J22, *SIX5*:BAC_375_N13 and *SIX5*:FH2598) to 0.354 (*CRYGD*:BAC_374_E1) with an average theta of 0.095 for the 2 closest linked markers (Table 2.2).

Two-point linkage analysis placed the gamma crystallin genes (*CRYGA, CRYGB, CRYGC* and *CRYGD*) on CFA 37. There are estimated to be 7 gamma crystallin genes in man; these include *gamma A-D,* and *S*, and two pseudogenes, *CRYGE* and *CRYGF*. There is sequence homology between *gamma crystallins A-F*, and these genes form a cluster at HSA 2q33-35, and in mouse they form a cluster on chromosome 1 (MMU1). In man, *CRYGS* maps to 3q25-qter, and in mouse to MMU 16. Similarly, canine *CRYGS* was not part of the gamma crystallin cluster on CFA37, but mapped to CFA 34 near BAC_374_K23 and marker REN266K05. Mutations causing cataracts have previously been identified in murine *Cryga* [26, 27], *Crygb* [26], *Crygc* [27], *Crygd* [27, 28], and *Crygs* [29, 30] as well as human *CRYGC* [31],

*CRYGD* [31], and *CRYGS* [32]. As a result, there is a high likelihood that the gamma crystallins will also be involved in canine cataracts.

LOD scores for the two closest linked markers to gamma crystallin genes A, B, C, and D ranged from 8.0 (*CRYGD*:BAC_374_E1) to 24.95 (*CRYGC*:BAC_381_J22) and theta ranged from 0 (*CRYGC*:BAC_381_J22) to 0.354 (*CRYGD*:BAC_374_E1) (Table 2.2). The two closest linked markers to *CRYGD* were *CRYGB* from a previous study [17] (LOD=15.027, theta=0.045) and BAC_374_E1 (LOD=8.03, theta=0.354). Although in the previous study, the *CRYGB* marker was "unlinked" to any other marker, the corresponding 171 bp amplicon was located on CFA37 (19,425,908-19,426,078). Also, in the previous study, markers were incorporated into a 1500 marker map using Multimap® pairwise calculation at a threshold of LOD > 8 [33]. The *CRYGB* marker in that study may have linked to other markers in the data set at a lower threshold. Decreased marker density in the vicinity of a gene's map location can also result in unlinked gene markers. However, marker density in the vicinity of *CRYGB* should have been sufficient in the previous study since they mapped the same markers which linked to the gamma crystallins in this study.

The next closest linked marker to *CRYGD* (BAC_374_E1: LOD=8.03, theta= 0.354) was also on CFA37. The decrease in LOD score from 15.027 (*CRYGD:CRYGB*) to 8.03 supports linkage but the increase in theta from 0.045 (*CRYGD:CRYGB*) to 0.354 indicates an increase in the distance between these two markers. All of the markers which linked to *CRYGD* with LOD> 4 were located on CFA37 (data not shown). In addition, the *CRYGD* PCR amplicon was located on CFA37 (19,425,779-19,426,157) within the predicted location for *CRYGD* based on reference sequence NM006891 (19,424,588-19,426,264). Thus, based on two-point linkage analysis results, and the location of the *CRYGD* PCR amplicon we place *CRYGD* on CFA37.

*Alpha crystallins A* and *B* were previously mapped to CFA31 (*CRYAA*) and CFA5 (*CRYAB*) [34], and *beta crystallins A1* and *B1* to CFA9 (*CRYBA1*) [17] and CFA26 (*CRYBB1*) [17, 34]. Here we placed *CRYBB2* on CFA26 near *CRYBB1* and REN131L06. Similarly, *CRYBB1* and *CRYBB2* both map to 22q11.2-12.2 in man, and chromosome 5 in mouse (MMU5). *MIP* was mapped to CFA10 near FH2537 and *ATP5B*, in agreement with previously reported data [34]. Both *LIM2* and *SIX5* mapped to CFA1, and *HSF4* and *MAF* to CFA 5. All other orthologs (excluding the gamma crystallins) mapped to individual chromosomes as summarized in Table 2.2

*Sequenced Tagged Sites*

Sequence-tagged sites (STS) for each cataract ortholog were obtained by analyzing the corresponding PCR amplicons against the May 2005, 7.5X canine draft sequence. With the exception of *CRYGB*, all of the resulting STSs were located inside, or within 1,300 bp of the predicted gene location based on human reference sequences (Table 2.2). The *CRYGB* STS (20,124,535-20,124,930) was not within the predicted location for canine *CRYGB* (19,440,507-19,442,393) based on the human reference sequence (NM005210). Primers used to amplify *CRYGB* were designed from the 1.5X (poodle) whole genome shotgun reference sequence AACN010184836. This sequence was selected from 1.5X canine sequences having homology to human *CRYGB* mRNA (NM005210). When analyzed against the 7.5X (boxer) canine genomic sequence, AACN010184836 had sequence homology to 4 unique sites on CFA37 (19,417,160-19,418,711; 19,426,006-19,426,485; 19,432,821-19,455,395; 20,124,527-20,126,527). These included the human reference sequence (NM005210) *CRYGB* predicted site (19,440,507-19,442,393). However, the actual AACN010184836 sequence was located on CFA37 from 20,124,527-20,126,527, and the 396bp portion of this sequence which corresponded to the *CRYGB* amplicon only

had homology to CFA37 at 20,124,535-20,124,930 (which is the *CRYGB* amplicon location). Therefore, even though the *CRYGB* primers were designed from the AACN010184836 sequence which had homology to human *CRYGB*, this sequence and the PCR amplicon derived from it were >682kb downstream from the expected *CRYGB* site.

Furthermore, there are four *CRYGB* predicted sites on CFA37 based on human protein homology (19,415,025-19,433,068; 19,424,652-19,455,135; 19,440,575-19,442,393 and 20,126,034-20,128,506). Human protein sequence homology is determined by analyzing human protein sequences against the human genome to find exonic sequences corresponding to amino acid sequences. The amino acid sequences are then analyzed against the canine genomic sequence using tBLASTn to find predicted canine exons (http://genome.ucsc.edu/cgi-bin/hgTrackUi?hgsid=67540273&g=blastHg17KG). Three of the four *CRYGB* predicted sites based on protein homology overlap and cover a 40kb region (19,415,026-19,455,135). This region is 670kb upstream of the fourth predicted *CRYGB* site (20,126,033-20,128,569). The *CRYGB* STS amplified here was located 1,104bp upstream to this fourth site. Because there are multiple predicted sites for *CRYGB* on CFA37 in the dog genome, and these sites share sequence homology, it is difficult to design primers specific for any single *CRYGB* predicted site. The multiple sites of *CRYGB* sequence homology make the actual location of the canine *CRYGB* gene unclear. As a result, our *CRYGB* STS should not be used to predict the exact location of canine *CRYGB*.

*Radiation Hybrid Mapping*

Markers linked to cataract orthologs, as determined by two-point linkage analysis, were used to create a framework map with previously established marker positions [17]. This framework map was then used to determine the map locations of the cataract orthologs (Figure 2.1). The orthologs were positioned between the 2 closest markers using the multipoint mapping algorithm of Multimap® software. In two cases, the cataract orthologs mapped to the same exact position as a BAC end marker in the framework map (theta = 0). For example, *SIX5* mapped to CFA1 at the same location as BAC_375_N13, and *CRYGC* mapped to CFA37 at the same location as BAC_381_J22. Since BACs represent large ( 155kb) DNA fragments [35], the mapping of these 2 genes to the same location as the 2 BACs suggests that these genes may be located within the BACS.

The RH maps generated by Multimap's® multipoint mapping algorithm were generally consistent with the results of two-point linkage analysis, and the orthologs mapped on top of, between, or very near the closest linked markers as determined by two-point linkage. An exception was *CRYGD* which was placed on CFA37 based on two-point linkage results and the location of the *CRYGD* STS (Table 2.2) but could not be accurately localized within the framework map. The framework map used to localize the gamma crystallin genes on CFA37 included the gamma crystallin gene vectors (*CRYGA, B, C, D*) along with framework markers whose locations were previously determined [17]. As a result, the framework map did not include the unlinked *CRYGB* marker from the previous study [17], which was the closest linked marker to *CRYGD* based on two-point linkage analysis. Instead, the closest linked marker to *CRYGD* in the framework map was BAC_374_E1 which linked to *CRYGD* with LOD=8.03, and theta=0.354. All of the other markers in the framework map which linked to *CRYGD* had a LOD score <8.03 and theta value > 0.354. These theta

Figure 2.1. Radiation hybrid maps locating 20 cataract genes to canine chromosomes. In each *Canis Familiaris* (CFA) chromosome representation, unboxed markers on left represent framework markers [17]. Markers with an asterisk are polymorphic. Boxed markers indicate locations of canine orthologs of cataract associated genes. Numbers on right are distances in centiRays from the top framework marker.

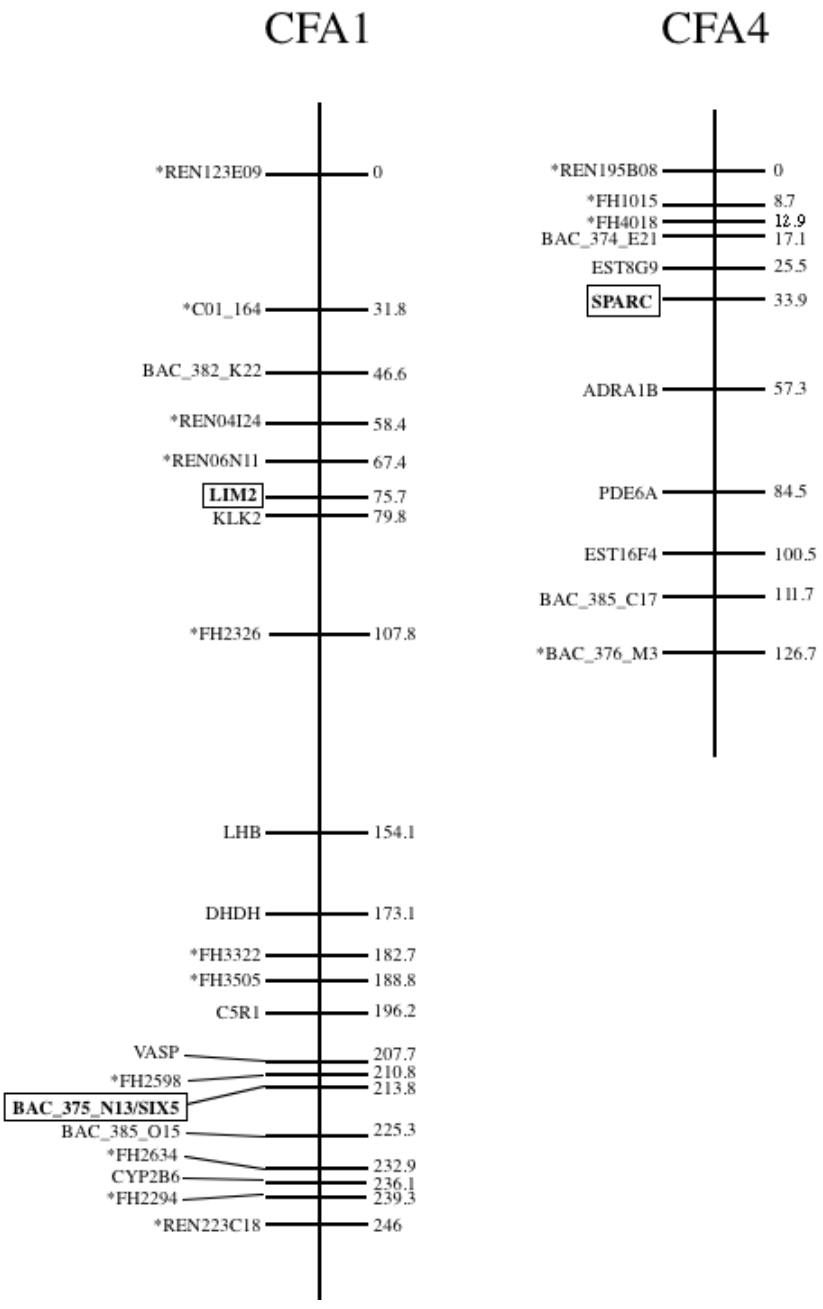
CFA1
*REN123E09 0
*C01_164 31.8
BAC_382_K22 46.6
*REN04I24 58.4
*REN06N11 67.4
LIM2 75.7
KLK2 79.8
*FH2326 107.8
LHB 154.1
DHDH 173.1
*FH3322 182.7
*FH3505 188.8
C5R1 196.2
VASP 207.7
*FH2598 210.8
BAC_375_N13/SIX5 213.8
BAC_385_O15 225.3
*FH2634 232.9
CYP2B6 236.1
*FH2294 239.3
*REN223C18 246
CFA4
*REN195B08 0
*FH1015 8.7
*FH4018 12.9
BAC_374_E21 17.1
EST8G9 25.5
SPARC 33.9
ADRA1B 57.3
PDE6A 84.5
EST16F4 100.5
BAC_385_C17 111.7
*BAC_376_M3 126.7

Figure 2.1. (Continued)

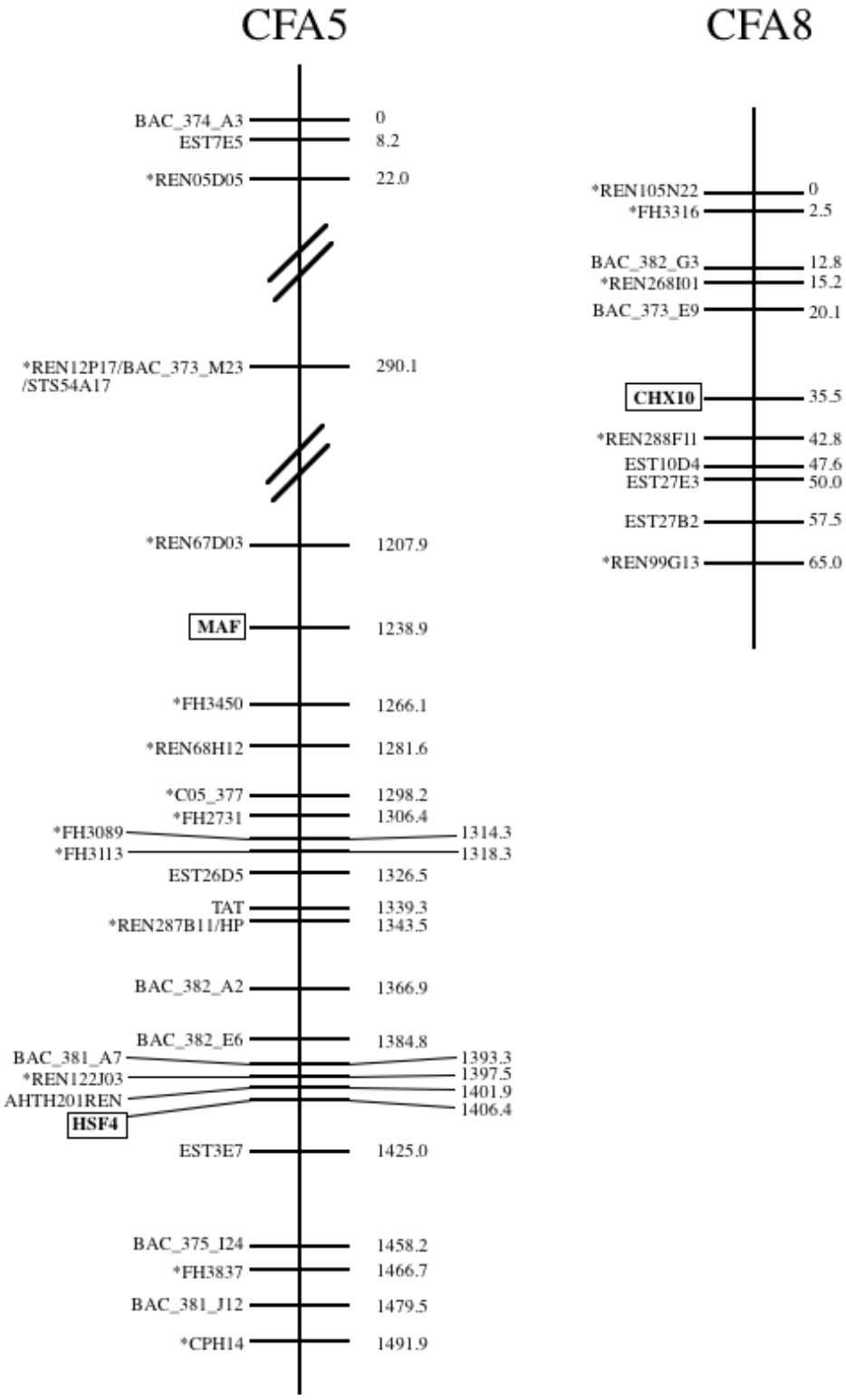

Figure 2.1. (Continued)

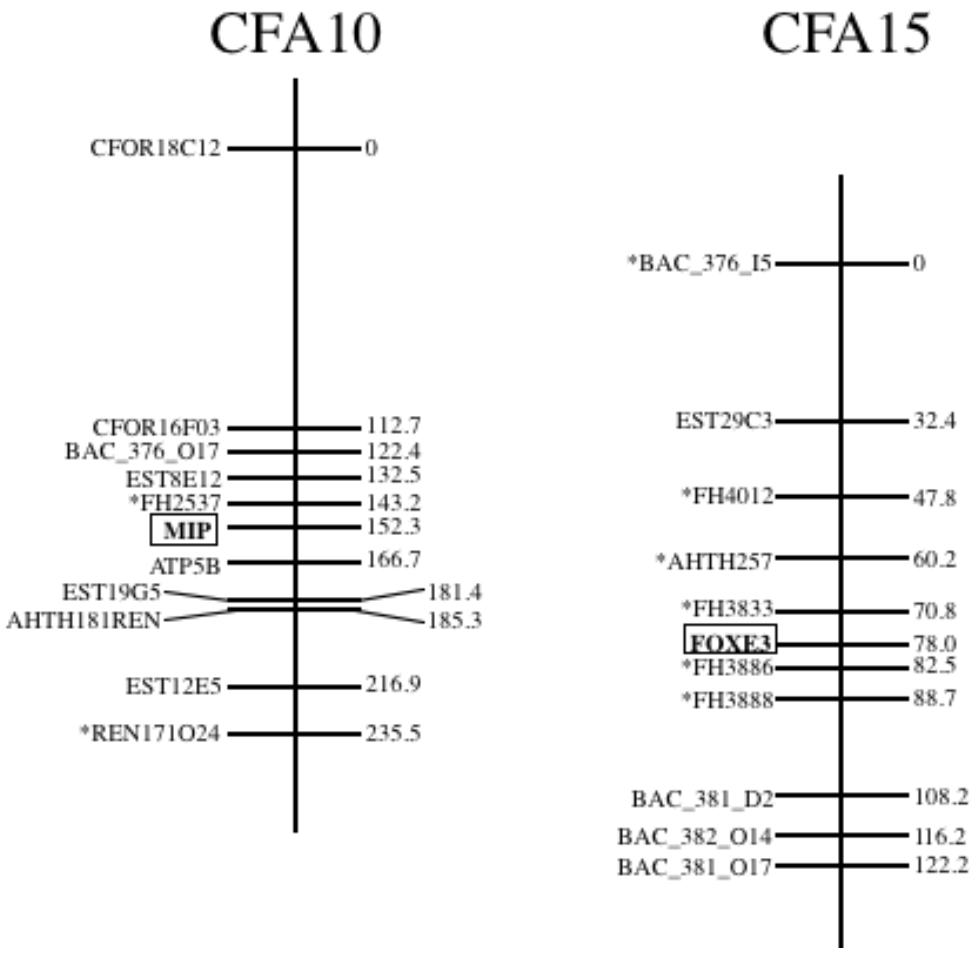

Figure 2.1. (Continued)

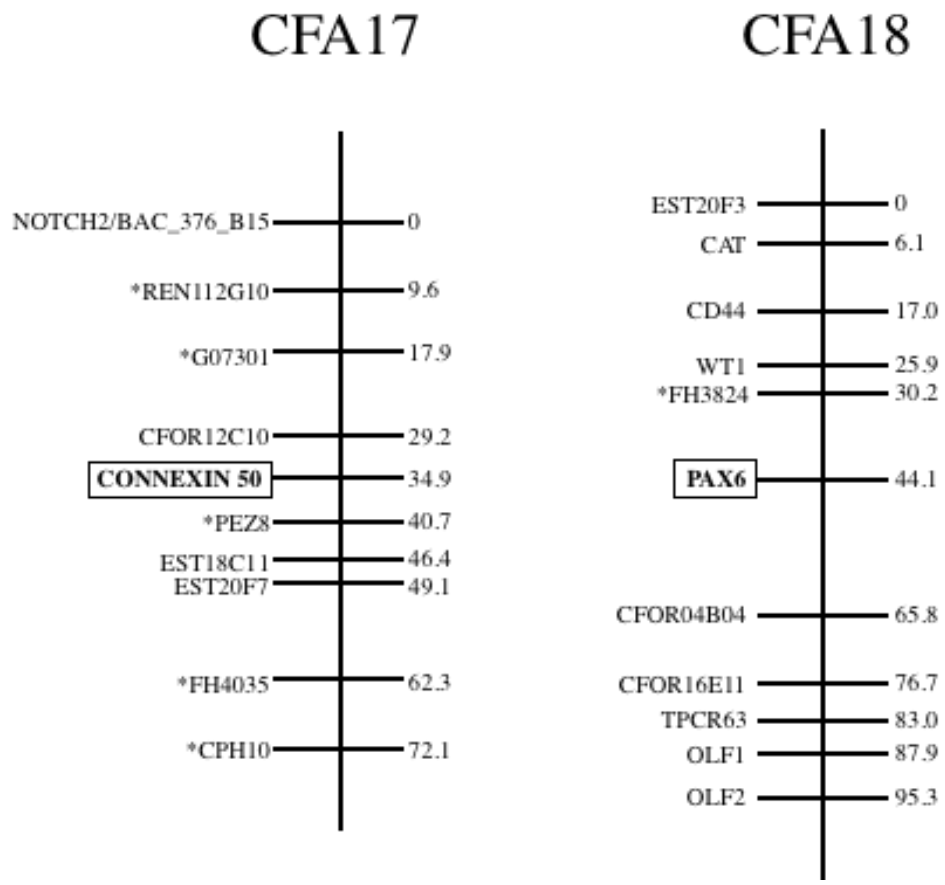

Figure 2.1. (Continued)

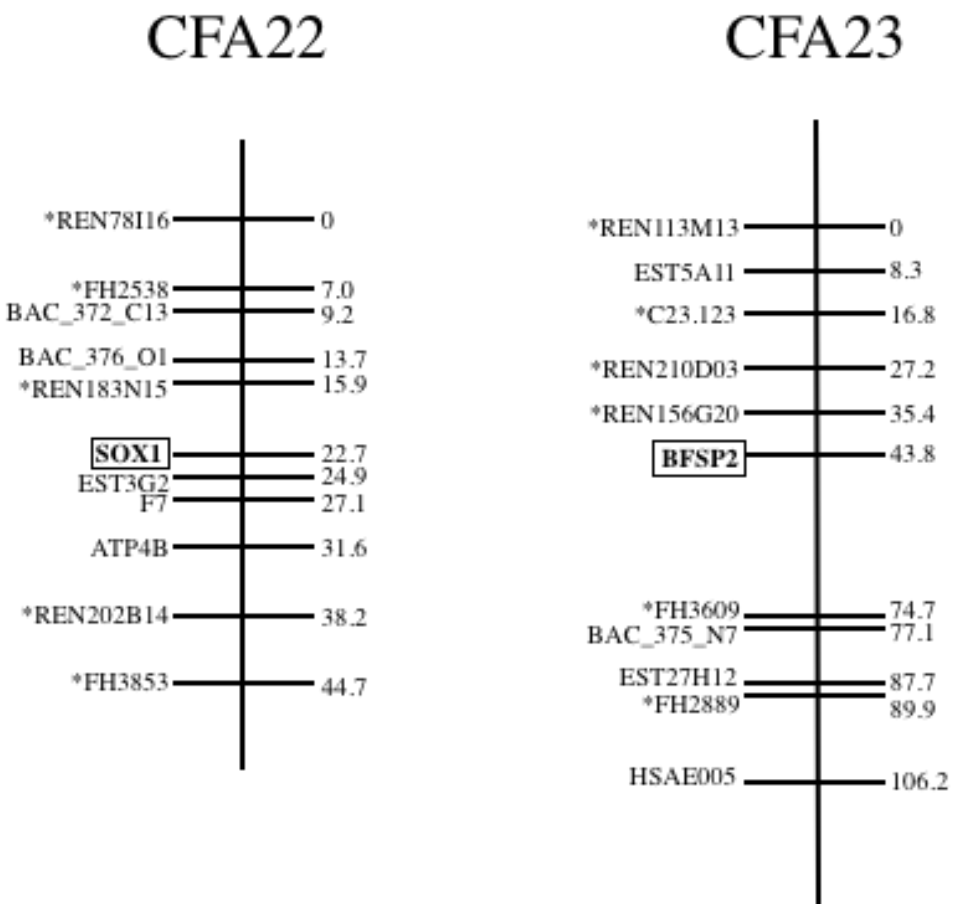

Figure 2.1. (Continued)

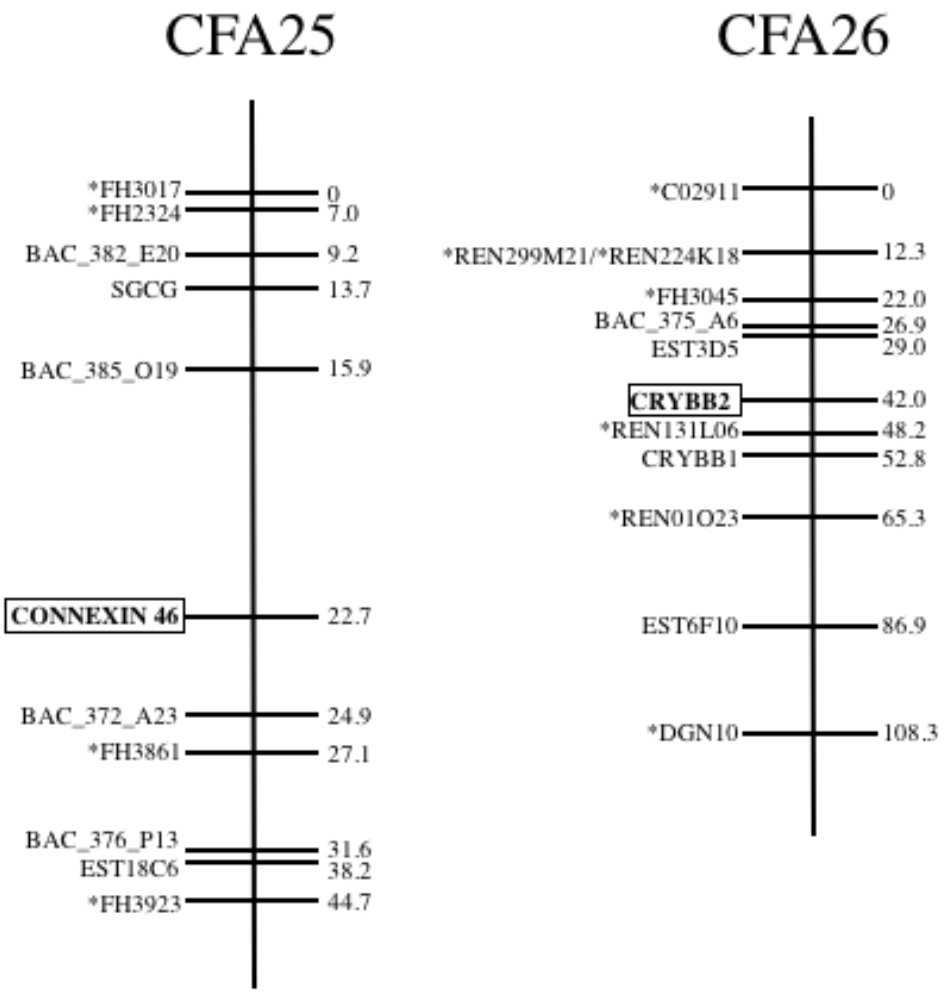

Figure 2.1. (Continued)

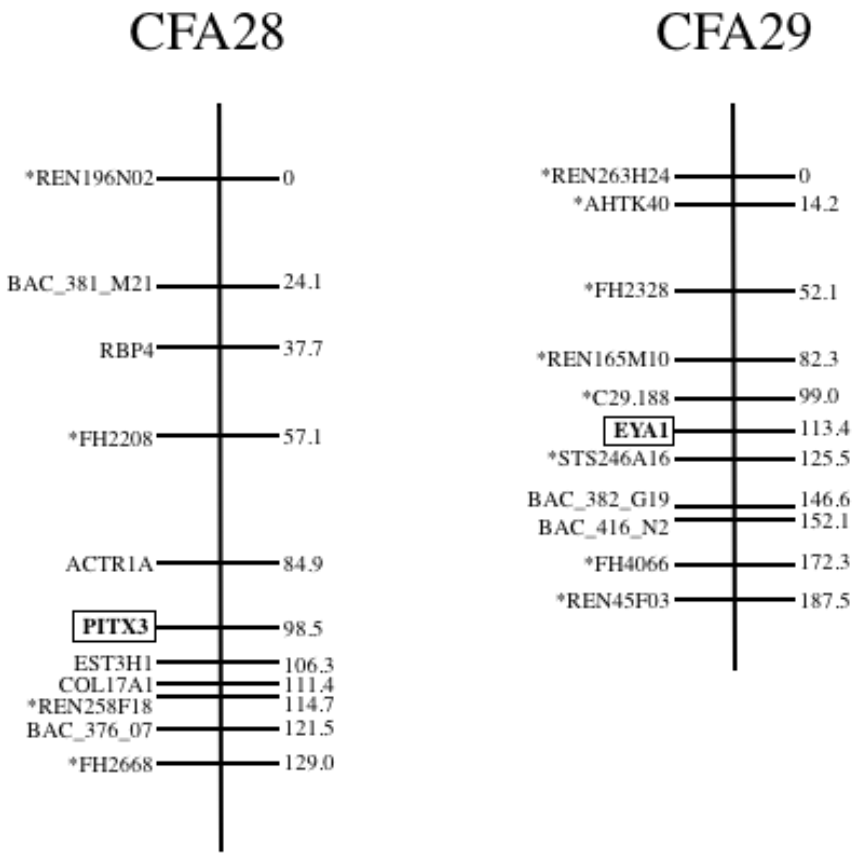

Figure 2.1. (Continued)

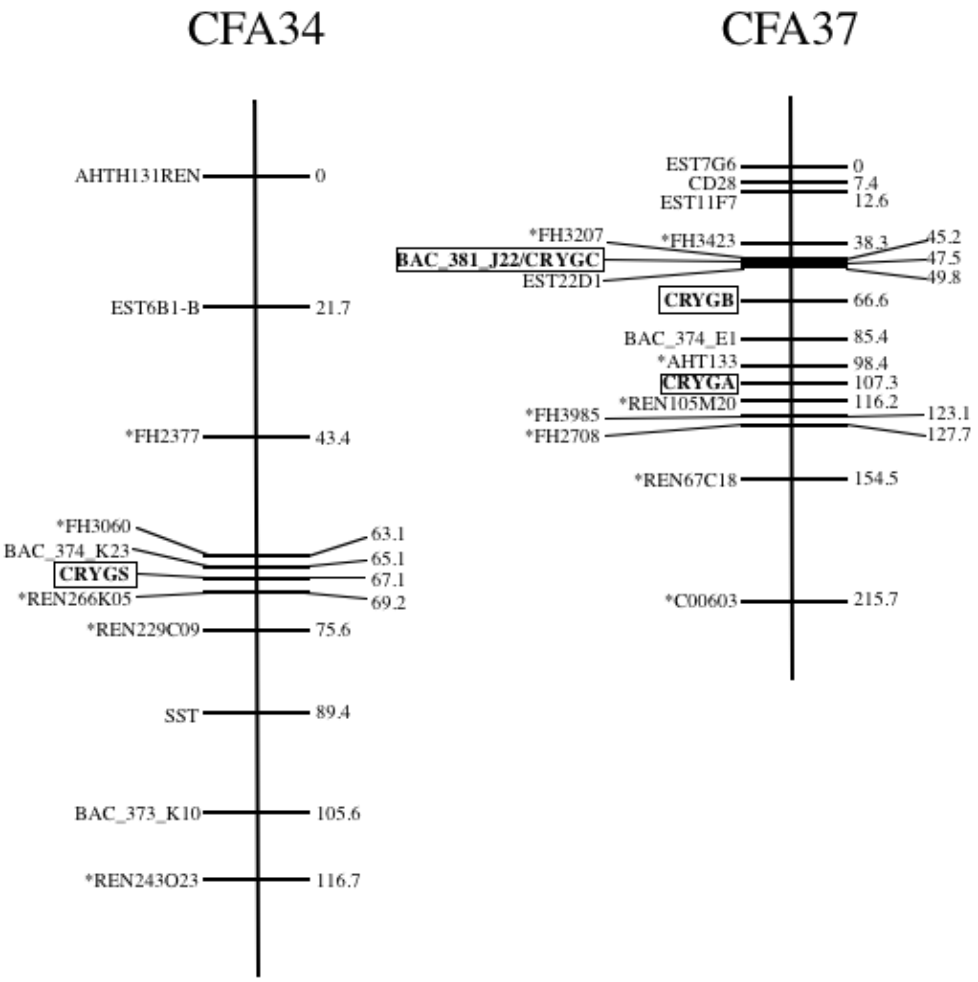

values indicated an increased frequency of breakage (increased distance) between *CRYGD* and the markers on the framework map and decreased the likelihood of accurately localizing *CRYGD* on the map. As a result, although we placed *CRYGD* on CFA37 based on two-point linkage analysis and the location of the *CRYGD* amplicon, we were unable to accurately localize this gene on the framework map using Multimap's® multipoint mapping algorithm due to the decreasing LOD scores and increasing theta values of the markers linked to *CRYGD*. The lack of markers linked to *CRYGD* with high LOD scores and low theta values may indicate low marker density in the vicinity of *CRYGD*. Even though all of the gamma crystallins orthologs (*CRYGA, B, C, D*) were located on CFA37 and were mapped against each other, this did not resolve the problem of marker density in the vicinity of *CRYGD*. To resolve this problem *CRYGD* should be mapped on the new RH9000 panel [24].

*Gamma crystallins A, B,* and *C* mapped to CFA37 as expected based on results of two-point-linkage analysis. The 5'→ 3' RH-map order on CFA37 (*CRYGC, CRYGB, CRYGA*) (Figure 2.1) matched the order of the predicted gene locations within the 7.5X draft sequence (Table 2.2). However, this RH-map order did not correspond with the order of the STS locations within the 7.5X draft sequence (*CRYGC, CRYGA, CRYGB*) (Table 2.2). Two-point linkage analysis linked the *CRYGB* ortholog to multiple markers on CFA37. The two closest linked markers were: BAC_381_J22 (LOD=15.426, theta=0.123), and FH2708 (LOD=13.738, theta=0.157). Multimap's® multipoint mapping algorithm placed the *CRYGB* ortholog on CFA37 between EST22D1 and BAC_374_E1, which are also between BAC_381_J22 and FH2708. Thus, two-point linkage analysis and radiation hybrid mapping results are consistent and place *CRYGB* on CFA37 in the same region, however this location does not correspond with the *CRYGB* STS location.

Radiation hybrid maps are physical maps based on the statistical analysis of the pattern of marker retention in a panel of RH-cell lines. As a result, the order and location of markers within RH-maps do not always correspond exactly with the order and location of markers within genomic sequences. Marker order and position on the canine RH5000 map [17] for example, are not equivalent with their order and position in the 7.5X canine genomic sequence in all instances. Thus, it is not surprising that the *CRYGB* marker in this study mapped to a location on the RH-map that does not exactly correspond to the physical location of this marker within the canine genome. Nevertheless, RH-maps are valuable in localizing markers and genes to specific regions and providing statistically close markers for association and linkage testing.

Furthermore, the discrepancy between the order of *CRYGA, B,* and *C* on the RH-map and their STSs in the draft sequence may also reflect the limited power for fine resolution of the RH5000 panel which has a resolution limit of 600kb. The distance between *CRYGA* and *CRYGB* STSs is about 670kb, and the distance between *CRYGB* and *CRYGC* STSs is about 692kb. These distances are close to the resolution limit for the RH5000 panel. Further, the distance between *CRYGA* and CRYGC STSs is only 21,558bp and is outside the resolution limit for the panel. Therefore, the inconsistency between the RH-map order and the STS order for *CRYGA, B* and *C* may be due to the resolution limit of the RH5000 panel. The new RH9000 panel has a resolution of 200kb [24] and can be used to resolve mapping issues for the gamma crystallin genes in the dog.

The canine chromosomal locations of the 21 cataract orthologs were consistent with human and canine established chromosomal synteny [36-38]. All of the cataract orthologs mapped to canine chromosomal locations which are syntenic with the corresponding human gene locations, except for 4 orthologs (*SPARC, HSF4, CX46,* and *PITX3*) which mapped to locations which are directly adjacent to the

corresponding syntenic region of the human gene location. Although *CRYGD* was not localized on the RH-map, the results of the two-point linkage analysis did place this gene on CFA37 in a region with homology to HSA2q33-35 where the gene is located in man.

To facilitate the molecular characterization of naturally occurring cataracts in the dog we have provided the radiation hybrid location of 20 cataract-associated genes along with their associated polymorphic markers (Figure 2.1). Primers for selected polymorphic markers near cataract-associated genes can be obtained from the RH5000 website (http://idefix.univ-rennes1.fr:8080/Dogs/RH3270-page.html) and serve as a resource for association and linkage testing in canine pedigrees segregating inherited cataracts. Although *CRYGD* is not represented in Figure 2.1, two-point linkage analysis did link *CRYGD* to BAC_374_E1 which localizes it on CFA37 to some degree. Also, the *CRYGD* STS location (19,425,779-19,426,157) can be used to identify proximal markers in the canine genome sequence. Though the RH5000 panel was used to map cataract-associated genes in this study, these results have not been incorporated into the RH5000 map. Nevertheless, the RH5000 map can be used to locate the markers referred to in this study (Table 2.2 and Figure 2.1). In addition, while the RH5000 and RH9000 maps will not be merged, a subset of 545 BACs has been mapped on both RH-panels and is part of both maps allowing navigation between the RH5000 and RH9000 maps (http://idefix.univ-rennes1.fr:8080/Dogs/RH10K-SOM-web.html).

Animal models provide a tremendous tool in the study of cataract, and molecular studies in mice have been instrumental in advancing our knowledge of the mechanisms of cataract formation. The dog has recently emerged as a promising model organism for gene discovery and genomic studies, and is a complementary species to the mouse for molecular genetic studies. There are over 300 known breeds

of dogs, and most function as genetic isolates due to restricted mating. As a result, there is a decrease in genetic diversity within breeds and an increase in diversity between breeds such that genetic diseases within one breed tend to be caused by the same mutations (founder effect). This facilitates the mapping of disease loci. In addition, developments in canine genomic resources which include integrated RH maps [14-17, 24], the availability of the canine genomic sequence [18, 19] , and comparative chromosome maps of the human and dog genomes which identify homologous segments and conserved synteny between canine and human karyotypes [36-38] make it practical to develop and use canine models.

Although mutations causing human cataracts have been identified in 15 genes there are many other genes with mutations yet to be identified. The study of naturally occurring cataracts in the dog could reveal novel genes and/or mutations not yet identified in either man or the mouse. The dog represents a valuable yet largely untapped resource to study the molecular genetics of cataracts. This study takes some initial steps towards developing the tools needed to begin studies on the canine cataract model. We have identified the chromosomal locations of 20 canine orthologs of cataract-associated genes and their nearest polymorphic markers (Figure 2.1) which can be used for association and linkage testing in cataract pedigrees. This resource, along with the recent advances in canine genomics, will help facilitate the development of such models for the study of naturally occurring inherited cataracts. Once developed, canine cataract models should help to identify new cataract genes and disease causing mutations, assist in the development of new therapies, and provide an intermediate large animal model between mouse and man for pre-clinical trials of new therapies.

APPENDIX

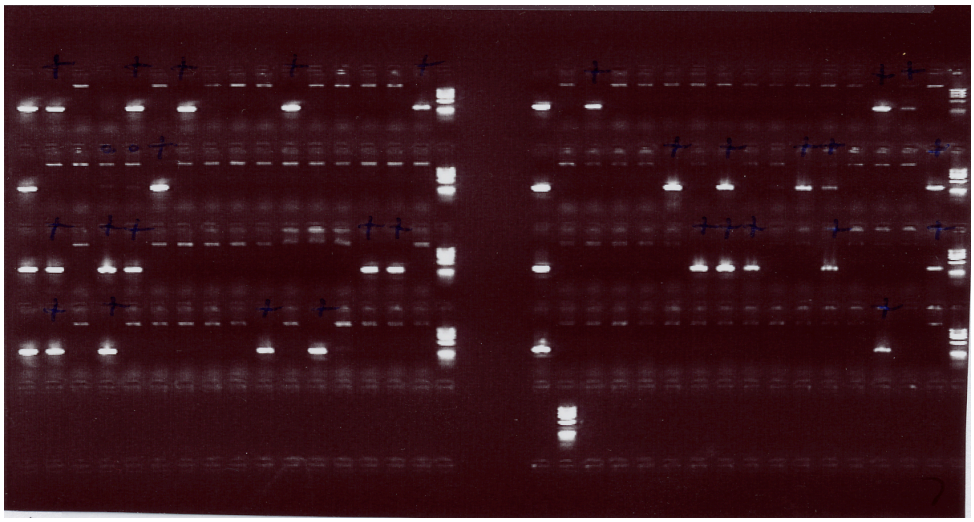


Figure A2.2. Representative 2% agarose gel showing PCR products generated from different cell lines in the RH5000 panel to identify those containing canine gamma crystallin A (CRYGA). There are 8 rows containing 17 columns (wells) each. The first column of each row contains a positive canine control (350bp band) and the last column of each row contains a phiX174 DNA marker. CRYGA was amplified in 29 cell lines and was localized to canine chromosome 37.

# REFERENCES


1. Resnikoff S, Pascolini D, Etya'ale D, Kocur I, Pararajasegaram R, Pokharel GP, et al. Global data on visual impairment in the year 2002. Bull World Health Organ 2004;82(11):844-51. Epub 2004 Dec 14.

2. Wirth MG, Russell-Eggitt IM, Craig JE, Elder JE, Mackey DA. Aetiology of congenital and paediatric cataract in an Australian population. Br J Ophthalmol 2002;86(7):782-6.

3. Evans CA. 1995 Presidential Address. Public health: vision and reality. Am J Public Health 1996;86(4):476-9.

4. Evans J, Rooney C, Ashwood F, al e. Blindness and Partial Sight in England and Wales: April 1990 - March 1991. Health Trends 1996;28:5-12.

5. He W, Li S. Congenital cataracts: gene mapping. Hum Genet 2000;106(1):1-13.

6. Congdon N, Vingerling JR, Klein BE, West S, Friedman DS, Kempen J, et al. Prevalence of cataract and pseudophakia/aphakia among adults in the United States. Arch Ophthalmol. 2004;122(4):487-94.

7. McCarty CA, Taylor HR. A review of the epidemiologic evidence linking ultraviolet radiation and cataracts. Dev Ophthalmol 2002;35:21-31.

8. Klein BE, Klein R, Lee KE, Meuer SM. Socioeconomic and lifestyle factors and the 10-year incidence of age-related cataracts. Am J Ophthalmol 2003;136(3):506-12.

9. Morris MS, Jacques PF, Hankinson SE, Chylack LT, Jr., Willett WC, Taylor A. Moderate alcoholic beverage intake and early nuclear and cortical lens opacities. Ophthalmic Epidemiol 2004;11(1):53-65.

10. Mares-Perlman JA, Lyle BJ, Klein R, Fisher AI, Brady WE, VandenLangenberg GM, et al. Vitamin supplement use and incident cataracts in a population-based study. Arch Ophthalmol 2000;118(11):1556-63.

11. Hejtmancik JF, Kantorow M. Molecular Genetics of Age-related Cataract. Experimental Eye Research 2004;79(1):3-9.

12. Reddy MA, Francis PJ, Berry V, Bhattacharya SS, Moore AT. Molecular Genetic Basis of Inherited Cataract and Associated Phenotypes. Survey of Ophthalmology 2004;49(3):300-315.

13. Gelatt KN, Wallace MR, Andrew SE, MacKay EO, Samuelson DA. Cataracts in the Bichon Frise. Vet Ophthalmol 2003;6(1):3-9.

14. Priat C, Hitte C, Vignaux F, Renier C, Jiang Z, Jouquand S, et al. A whole-genome radiation hybrid map of the dog genome. Genomics 1998;54(3):361-78.

15. Breen M, Jouquand S, Renier C, Mellersh CS, Hitte C, Holmes NG, et al. Chromosome-specific single-locus FISH probes allow anchorage of an 1800-marker integrated radiation-hybrid/linkage map of the domestic dog genome to all chromosomes. Genome Res 2001;11(10):1784-95.

16. Breen M, Hitte C, Lorentzen TD, Thomas R, Cadieu E, Sabacan L, et al. An integrated 4249 marker FISH/RH map of the canine genome. BMC Genomics 2004;5(1):65.

17. Guyon R, Lorentzen TD, Hitte C, Kim L, Cadieu E, Parker HG, et al. A 1-Mb resolution radiation hybrid map of the canine genome. Proc Natl Acad Sci U S A 2003;100(9):5296-301. Epub 2003 Apr 16.

18. Kirkness EF, Bafna V, Halpern AL, Levy S, Remington K, Rusch DB, et al. The dog genome: survey sequencing and comparative analysis. Science 2003;301(5641):1898-903.

19. Lindblad-Toh K, Wade CM, Mikkelsen TS, Karlsson EK, Jaffe DB, Kamal M, et al. Genome sequence, comparative analysis and haplotype structure of the domestic dog. Nature. 2005;438(7069):803-19.

20. Kijas JW, Cideciyan AV, Aleman TS, Pianta MJ, Pearce-Kelling SE, Miller BJ, et al. Naturally occurring rhodopsin mutation in the dog causes retinal dysfunction and degeneration mimicking human dominant retinitis pigmentosa. Proc Natl Acad Sci U S A 2002;99(9):6328-33. Epub 2002 Apr 23.

21. Sidjanin DJ, Lowe JK, McElwee JL, Milne BS, Phippen TM, Sargan DR, et al. Canine CNGB3 mutations establish cone degeneration as orthologous to the human achromatopsia locus ACHM3. Hum Mol Genet 2002;11(16):1823-33.

22. Zhang Q, Acland GM, Wu WX, Johnson JL, Pearce-Kelling S, Tulloch B, et al. Different RPGR exon ORF15 mutations in Canids provide insights into photoreceptor cell degeneration. Hum Mol Genet 2002;11(9):993-1003.

23. Vignaux F, Hitte C, Priat C, Chuat JC, Andre C, Galibert F. Construction and optimization of a dog whole-genome radiation hybrid panel. Mamm Genome 1999;10(9):888-94.

24. Hitte C, Madeoy J, Kirkness EF, Priat C, Lorentzen TD, Senger F, et al. Facilitating genome navigation: survey sequencing and dense radiation-hybrid gene mapping. Nat Rev Genet 2005;6(8):643-8.

25. Matise TC, Perlin M, Chakravarti A. Automated construction of genetic linkage maps using an expert system (MultiMap): a human genome linkage map. Nat Genet 1994;6(4):384-90.

26. Klopp N, Favor J, Loster J, Lutz RB, Neuhauser-Klaus A, Prescott A, et al. Three murine cataract mutants (Cat2) are defective in different gamma-crystallin genes. Genomics 1998;52(2):152-8.

27. Graw J, Neuhauser-Klaus A, Klopp N, Selby PB, Loster J, Favor J. Genetic and allelic heterogeneity of Cryg mutations in eight distinct forms of dominant cataract in the mouse. Invest Ophthalmol Vis Sci 2004;45(4):1202-13.

28. Smith RS, Hawes NL, Chang B, Roderick TH, Akeson EC, Heckenlively JR, et al. Lop12, a mutation in mouse Crygd causing lens opacity similar to human Coppock cataract. Genomics 2000;63(3):314-20.

29. Sinha D, Wyatt MK, Sarra R, Jaworski C, Slingsby C, Thaung C, et al. A temperature-sensitive mutation of Crygs in the murine Opj cataract. J Biol Chem. 2001;276(12):9308-15. Epub 2000 Dec 19.

30. Bu L, Yan S, Jin M, Jin Y, Yu C, Xiao S, et al. The gamma S-crystallin gene is mutated in autosomal recessive cataract in mouse. Genomics 2002a;80(1):38-44.

31. Heon E, Priston M, Schorderet DF, Billingsley GD, Girard PO, Lubsen N, et al. The gamma-crystallins and human cataracts: a puzzle made clearer. Am J Hum Genet 1999;65(5):1261-7.

32. Sun H, Ma Z, Li Y, Liu B, Li Z, Ding X, et al. Gamma-S crystallin gene (CRYGS) mutation causes dominant progressive cortical cataract in humans. J Med Genet 2005;42(9):706-10.

33. Breen M, Jouquand S, Renier C, Mellersh CS, Hitte C, Holmes NG, et al. Chromosome-specific single-locus FISH probes allow anchorage of an 1800-marker integrated radiation-hybrid/linkage map of the domestic dog genome to all chromosomes. Genome Res. 2001;11(10):1784-95.

34. Parker HG, Yuhua X, Mellersh CS, Khan S, Shibuya H, Johnson GS, et al. Meiotic linkage mapping of 52 genes onto the canine map does not identify significant levels of microrearrangement. Mamm Genome 2001;12(9):713-8.

35. Li R, Mignot E, Faraco J, Kadotani H, Cantanese J, Zhao B, et al. Construction and characterization of an eightfold redundant dog genomic bacterial artificial chromosome library. Genomics. 1999;58(1):9-17.

36. Breen M, Thomas R, Binns MM, Carter NP, Langford CF. Reciprocal chromosome painting reveals detailed regions of conserved synteny between the karyotypes of the domestic dog (Canis familiaris) and human. Genomics 1999;61(2):145-55.

37. Yang F, O'Brien PC, Milne BS, Graphodatsky AS, Solanky N, Trifonov V, et al. A complete comparative chromosome map for the dog, red fox, and human and its integration with canine genetic maps. Genomics 1999;62(2):189-202.

38. Sargan DR, Yang F, Squire M, Milne BS, O'Brien PC, Ferguson-Smith MA. Use of flow-sorted canine chromosomes in the assignment of canine linkage, radiation hybrid, and syntenic groups to chromosomes: refinement and verification of the comparative chromosome map for dog and human. Genomics 2000;69(2):182-95.

# CHAPTER 3

## CLONING AND CHARACTERIZATION OF CANINE *PAX6* AND EVALUATION AS A CANDIDATE GENE IN A CANINE MODEL OF ANIRIDIA*


### *Abstract*

Purpose: Mutations in *PAX6* cause human aniridia. The *small eye* (*sey*) mouse represents an animal model for aniridia; however, no large animal model currently exists. We cloned and characterized canine *PAX6*, and evaluated *PAX6* for causal associations with inherited aniridia in dogs. Methods: Canine *PAX6* was cloned from a retinal cDNA library using primers designed from human and mouse *PAX6* consensus sequences. An RH3000 radiation hybrid panel was used to localize *PAX6* within the canine genome. Genomic DNA was extracted from whole blood from dogs with inherited aniridia, and association testing was performed using markers on CFA18. Fourteen *PAX6* exons were sequenced and scanned for mutations, and a Southern blot was used to test for large deletions. Results: Like the human gene, canine *PAX6* has 13 exons and 12 introns, plus an alternatively spliced exon (5a). *PAX6* nucleotide and amino acid sequences were highly conserved between dog, human, and mouse. The canine *PAX6* cDNA sequence determined in this study spans 2 large gaps present in the current canine genomic sequence. Radiation hybrid mapping placed canine *PAX6* on CFA18 in a region with synteny to HSA11p13. Exon-scanning revealed single nucleotide polymorphisms, but no pathological mutations, and Southern blot analysis revealed no differences between normal and affected animals. Conclusion: Canine *PAX6* was cloned and characterized, and results


* Hunter et. al., 2007. Molecular Vision, volume 13, pages 431-442

provide sequence information for gaps in the current canine genome sequence. Canine *PAX6* nucleotide and amino acid sequences, as well as gene organization and map location, were highly homologous with that of the human gene. *PAX6* was evaluated in dogs with an inherited form of aniridia, and sequence analysis indicated no pathological mutations in the coding regions or splice sites of aniridia- affected dogs, and Southern blot analysis showed no large deletions within the regions analyzed.

***Introduction***

Mutations in the paired-box 6 (*PAX6*) gene cause aniridia in man, a panocular disorder primarily characterized by complete or partial absence of iris tissue. Aniridia is often associated with other ocular abnormalities including corneal dystrophy, cataract, and glaucoma. The disease has a high penetrance, but variable expressivity, and, within pedigrees, phenotypes can vary in patients having the same mutation [1]. The incidence of aniridia is 1:65,000-1:100,000 in man, and approximately 2/3 of aniridia cases are inherited. In addition to aniridia, *PAX6* mutations can also cause Peter's anomaly, cataract, corneal dystrophy, keratitis, coloboma, ectopic pupillae, foveal hypoplasia, and optic nerve hypoplasia (http://www.ncbi.nlm.nih.gov/entrez/query.fcgi?db=OMIM). Over 300 *PAX6* mutations have been described in man, and can be viewed at the Human *PAX6* Allelic Variant Database (http://*PAX6*.hgu.mrc.ac.uk/). *PAX6* mutations are dominant to semidominant and homozygous lethal; homozygous or compound heterozygous patients have anophthalmia and multiple, severe CNS malformations [2, 3].

*PAX6* is expressed during embryogenesis in the developing CNS, eye, nose, pituitary and pancreas [4-8]. It functions as a master control gene in ocular development across species, both vertebrate and invertebrate, and is able to induce ectopic eye development in *Drosophila melanogaster* [9] and *Xenopus laevis* [10].

Mutations in the *Drosophila PAX6* homologue *eyeless* cause partial to complete loss of the compound eye, and surrounding sensory bristles [11]. *Pax6* mutations in mouse are dominant, and result in the *small eye* (*sey*) phenotype characterized by microphthalmia and small body size [12]. Experimentally induced mutations in mouse *Pax6* exhibit a range of phenotypes including partial to complete aniridia, iris abnormalities, cataract, and corneal adhesions [13]. Homozygous *Pax6* mutations are lethal in the mouse, and, as in man, result in small embryos with anopthalmia and severe CNS malformations [3, 12].

PAX6 is a highly conserved member of the PAX family of DNA-binding transcription factors. It contains a paired domain (PD), a linker region, a homeodomain (HD), and a proline-serine-threonine rich (PST) region which functions as a transcription activator [3]. Both the paired and homeo domains of the PAX6 protein recognize and bind to DNA target sequences. The paired domain is further divided into an N-terminal subdomain (NTS) and a C-terminal subdomain (CTS). An alternatively spliced form of PAX6 inserts an additional 14 amino acids, encoded by exon 5a, into the NTS of the paired domain, thereby altering its binding ability [14, 15]. In the shorter PAX6, the NTS binds to DNA targets while in the longer PAX6(5a) the CTS preferentially binds. Thus, the alternatively spliced exon 5a acts as a molecular switch which can determine DNA-binding targets [14, 16].

In an effort to identify the causal gene, and mutation responsible for canine aniridia, a family of Spanish Catalan sheepdogs with an inherited form of aniridia was analyzed. Affected dogs presented with partial to nearly complete absence of the iris with or without keratitis, cataract, and glaucoma. Because limited pedigree information and samples precluded a genome wide scan, a candidate gene approach was used. *PAX6* was selected for evaluation because it is the primary aniridia gene in man. The canine *PAX6* has not been cloned, and the current draft of the canine

genomic sequence [17] (http://genome.ucsc.edu/cgi-bin/hgGateway) does not contain an annotated *PAX6*. Moreover, the canine draft genomic sequence does not contain the entire sequence for this gene. As a result, *PAX6* was cloned from a canine retinal cDNA library, characterized and evaluated for mutations that could be causally associated with the disease.

## ***Methods***

### *Animals and DNA*

Catalan sheepdogs (Gos d'Atura) with an inherited form of aniridia were ascertained by Dr. Manuel Villagrasa at the Veterinary Ophthalmology Center in Madrid, Spain [18]. The dogs were privately owned pets or working sheepedogs, and were not part of a research colony. Dogs were examined using direct and indirect ophthalmoscopy and slit lamp biomicroscopy. Clinical signs included partial to nearly complete absence of the iris with ciliary processes visible at the circumferential border (Figure 3.1). Some canine patients also exhibited persistent remnants from the pupillary membrane, corneal edema, keratitis, cataract, and glaucoma. A total of 10 dogs were examined, including 7 which were part of one pedigree (GD2, GD3, GD5, GD6, GD8, GD9, GD10) (Figure 3.2), and 3 which were unrelated (GD12, GD13, GD14). Six dogs were affected with aniridia (GD5, GD6, GD9, GD10, GD12, GD14), and 4 were normal (GD2, GD3, GD8, GD13). Although the pedigree information available was very limited, the disease appeared to segregate as an autosomal recessive trait in that aniridia-affected dogs were produced from phenotypically normal parents (Figure 3.2) [18]. Whole blood was collected in EDTA-anticoagulant tubes, and total genomic

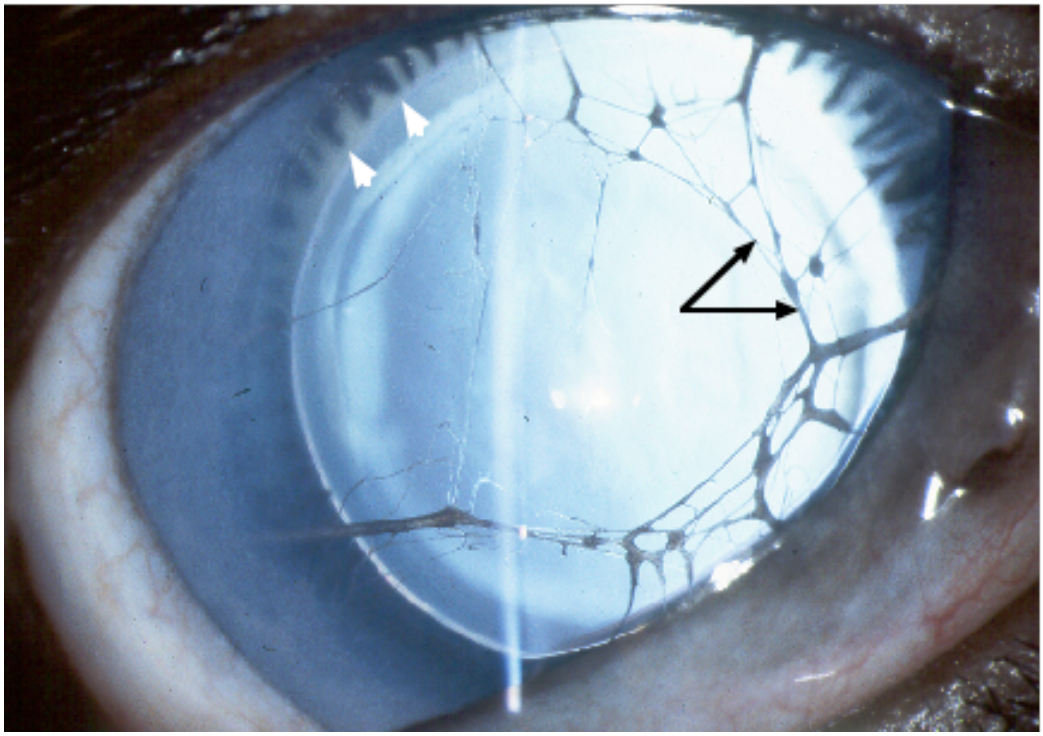

Figure 3.1. The canine aniridia phenotype. Note absence of the iris, visible ciliary processes located near the lens equator (white arrowheads) and pupillary membrane remnants (black arrows).

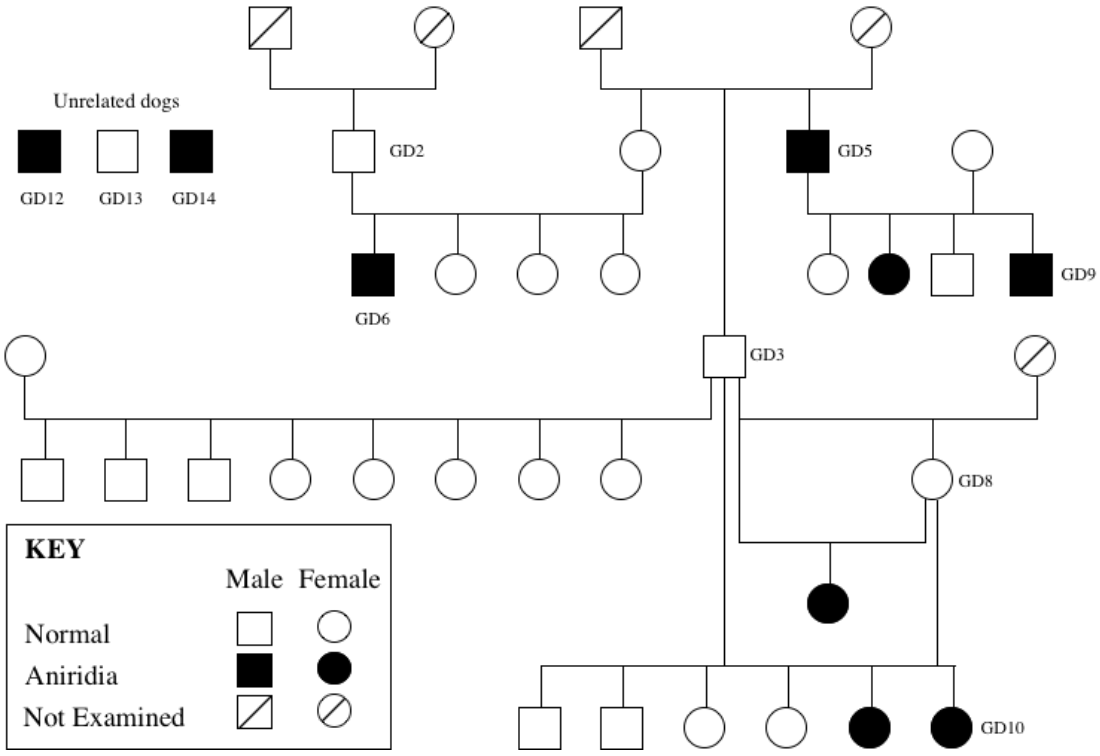


Figure 3.2. Spanish Catalan sheepdog pedigree showing aniridia-affected dogs. Note that the parents of affected dogs in 3 litters were clinically normal.

DNA (gDNA) was extracted from blood lymphocytes using standard phenol:chloroform extraction protocols with ethanol precipitation [19].

*Cloning and characterization of canine PAX6*

Oligonucleotide primers were designed based on human (XM_012065) and mouse (X63963) *PAX6* consensus sequences using Amplify© software (Bill Engels, University of Wisconsin, Madison, WI). *PAX6* was amplified from a canine retinal cDNA library made with the pBK-CMV phagemid vector (Stratagene, LaJolla, CA), using primers listed in Table 3.1. Vector primers PBKIII and PBKVI from the cDNA library were used to extend the resulting *PAX6* sequence in the 5' and 3' directions, respectively. Additional sequence information was obtained from The Institute For Genomic Research (TIGR) 1.5X (Poodle) canine genomic sequence [20]. Additional primers were designed to cross introns in gDNA in order to obtain the intron/exon boundary sequences which were then used to design primers for exon scanning. Intron/exon boundaries were analyzed, and intronic sizes were determined for 9 of the 13 introns. For the larger introns (2, 4, 7, and 11), which could not be amplified directly, genomic sequence at the intron/exon boundaries was obtained from TIGR (Poodle) canine genomic sequence [20], and used to design primers for exon scanning.

PCRs for the cloning of *PAX6* were run in a 25μl reaction volume using *Taq* DNA polymerase (Invitrogen Corporation, Carlsbad, CA), with the following conditions: 2 min 94°C followed by 30 cycles of (60 sec 94°C, 60 sec 58°C, 60 sec 72°C), and a final extension of 7 min 72°C. PCRs were run on Amplitron II® Thermolyne thermocyclers (Barnstead Thermolyne Co., Dubuque, IA), and amplified products were electrophoresed on 2% agarose gels (Invitrogen, Carlsbad, CA) with 1X TAE buffer (0.04 M Tris-acetate buffer, pH 8, 100 mM EDTA) at 60V. Gels were

Table 3.1. Primer Sequences Used To Clone *PAX6* From A Canine Retinal cDNA Library

| **PRIMER (location)** | **SEQUENCE** | **Tm (°C)** | **PRODUCT SIZE (bp)** |
|---|---|---|---|
| PAX6-1F (exons 4-5) | GCAGAACAGTCACAGCGGAGTG | 60.4 | 464 |
| PAX6-3R (exon 7) | CCGTCTGCGCCCATCTGTTG | 61.4 | |
| PAX6-4F (exon 7) | GTCATCAATAAACAGAGTTCTTCGC | 54.3 | 485 |
| PAX6-5R (exon 10) | GTGTTGCTGGCCTGTCTTCTCTG | 60.1 | |
| PAX6-6F (exon 9) | GATCTACCTGAAGCAAGAATACAGG | 54.9 | 380 |
| PAX6-7R (exon 12) | GGTGTAGGTATCATAACTCCG | 51.9 | |
| **Primers used to clone 5' end of *PAX6*** | | | |
| PBKIII F(vector) | GGTCGACACTAGTGGATCCAAAG | 57.1 | 550 |
| PAX6-3R (exon 7) | CCGTCTGCGCCCATCTGTTG | 61.4 | |
| **Primers used to clone 3' end of *PAX6*** | | | |
| PAX6-6F (exon 9) | GATCTACCTGAAGCAAGAATACAGG | 54.9 | 600 |
| PBKVI R (vector) | GCTCTCATGAAGATCTCGCCG | 57.7 | |
| PAX6-27F (exon 12) | AACAGTCAGCCAATGGGCAC | 53.7 | 200 |
| PBKVI R (vector) | GCTCTCATGAAGATCTCGCCG | 57.7 | |
| **Primers used to amplify alternatively transcribed EXON 5a** | | | |
| PAX6-14F (exon 5) | CTCGGTGGTGTCTTTGTCAAC | 54.2 | 250 |
| PAX6-15R (exon 6) | CTACTCTCGGTTTACTACCACC | 54.7 | |

stained with ethidium bromide, visualized using an ultraviolet transilluminator (Spectronics Corporation, Westbury, NY), and digitally photographed.
PCR products were purified using the Concert™ PCR purification kit (Gibco, BRL, Gaithersburg, MD), or gel bands were excised and purified using the Qiaex II® Gel Extraction kit (QIAGEN Inc., Valencia, CA). Purified PCR products were then sequenced on the Applied Biosystems Automated 3730 DNA Analyzer using Big Dye Terminator chemistry and Ampli Taq-FS DNA Polymerase. Sequence assembly and analysis were performed using Sequencher™ software (Gene Codes Corporation, Ann Arbor, MI).

*Exon scanning*

*PAX6* exons, along with their intron/exon junctions, were scanned using PCR amplification of genomic DNA from 4 aniridia-affected dogs (GD5, GD6, GD9, GD10), and 3 non-affected dogs (GD2, GD3, GD8) from the same pedigree. In addition, one non-affected, unrelated Beagle (B15) was scanned as a control. Primers were designed in introns near the intron/exon boundaries (Table 3.2) using Amplify© software. PCR and electrophoresis conditions were the same as those described earlier. Gel bands corresponding to exon sizes were excised and gel purified using the QIAquick® Gel Extraction kit (QIAGEN Inc., Valencia, CA). Gel-purified PCR products were sequenced and analyzed as previously described.

*Radiation Hybrid Mapping*

Canine *PAX6* was positioned on a radiation hybrid map using a canine/hamster radiation hybrid (RH3000) panel consisting of 92 cell lines made by fusing 3000 rad-irradiated canine fibroblast cells with TK-HTK3 hamster cells (Research Genetics, Inc., Huntsville, AL). Canine *PAX6* was linked to CFA18 in relation to 7 gene

Table 3.2. *PAX6* Primer Sequences Used For Exon Scanning

| EXON | PRIMER (location) | PRIMER SEQUENCE | Tm (°C) | PRODUCT SIZE (bp) |
|---|---|---|---|---|
| 1 | PX6-40F (5'UTR) | TCAGGCGCAGGAGGAAGTG | 59.9 | 194 |
| | PX6-41R (intron 1) | TCAGCGGCTGGAGAGTGAG | 59.3 | |
| 2 | PX6-42F (intron 1) | CTCACTCTCCAGCCGCTGAC | 60.1 | 400 |
| | PX6-43R (intron 2) | CTCTCCCGGCGTGGCAGTG | 63.6 | |
| 3 | PX6-44F (intron 2) | GAGAGTCCATGGGCCTGTGC | 60.6 | 200 |
| | PX6-45R (intron 3) | CTTCTCCCATGTGAACAATGAAG | 53.9 | |
| 4 | PX6-84F (intron 3) | GCGACTGAGTGGATCCCTTC | 58.2 | 302 |
| | PX6-83R (intron 4) | CCCTCCAGCCGGACTGC | 61.0 | |
| 5 | PX6-86F (intron 4) | CCGCATGGACGTGTGGTCC | 61.7 | 558 |
| | PX6-79R (intron 5) | GGAGTTATCTTATGTGACTGAC | 51.4 | |
| 5A | PX6-50F (intron 5) | CTCTCTACAGTAAGTTCTCATAC | 49.6 | 210 |
| | PX6-39R (exon 6) | CCAGTCTCGTAATACCTGCC | 53.7 | |
| 6 | PAX6-34F (exon 5A) | GTCCAAGTGCTGGACAATC | 51.0 | 917 |
| | PAX6-29R (intron 6) | AACAAGCTCCCAGCCATCCT | 53.7 | |
| 7 | PX6-51F (intron 6) | GTTGTTCTTTAAGAGAGTGGGTG | 53.5 | 310 |
| | PX6-52R (intron 7) | CCAGTGGCTGCCTATATGGAG | 57.3 | |
| 8 | PX6-53F (intron 7) | GCCTCTTTGGGAGGCTCCAAG | 60.4 | 300 |
| | PX6-54R (intron 8) | CTGGCTAAATATAGCTCTTTGTAC | 51.2 | |
| 9 | PAX6-30F (intron 8) | GCCACATCTTCAGTACAAAG | 49.6 | 800 |
| | PX6-21R (exon 10) | GCCTGTCTTCTCTGGTTCC | 53.1 | |
| 10 | PAX6-6F (exon 9) | GATCTACCTGAAGCAAGAATACAGG | 54.9 | 590 |
| | PX6-23R (exon 11) | GTGTTTGTGAGGGCTGTGTC | 53.7 | |
| 11 | PX6-22F (exon 10) | CCCAGTCACATCCCCATCAG | 55.8 | 350 |
| | PX6-55R (intron 11) | CCCACTCCTCGCTTCTCCG | 60.1 | |
| 12 | PX6-61F (intron 11) | CGATCATCAGGCTATCATAC | 49.9 | 415 |
| | PX6-62R (intron 12) | CCAGGAGGTTTCTCTTAAGG | 52.2 | |
| 13 | PX6-63F (intron 12) | CATAGTCCATGCTTGTCTCTC | 52.7 | 318 |
| | PX6-88R (3'UTR) | CACAGGACACAACTGCAGAAC | 57.4 | |

markers (*WT1, CD44, COLF1, COLF2, DLA79, ROM1, TPCR63*) and 7 microsatellite markers (Wilms-TF, REN47J11, REN248C19, C18.156, C18.460, AHT130, FH2356). All of these markers were previously mapped and positioned on CFA18 [21, 22]. Primers for RH mapping are listed in Table 3.3. *PAX6* primers 30F and 21R, which amplify intron 8, were used to amplify *PAX6* in the RH3000 panel.

PCR reactions were run on the 92 cell lines of the RH3000 panel, in duplicate or triplicate, at 25 μl volume using *Taq* DNA polymerase (Invitrogen Corporation, Carlsbad, CA). PCR conditions were as follows: 2 min 94°C, followed by 30 cycles of (30 sec 94°C, 30 sec 56°C, 30 sec 72°C), and a final extension of 5 min 72°C. PCRs were optimized by adjusting the annealing temperature as needed. PCR products were electrophoresed and analyzed as described earlier. Gel images were recorded for each gel, and scored for presence or absence of the band of interest in each of the 92 cell lines. Radiation hybrid data was analyzed using Multimap® software [23].

*Association Testing*

Ten dogs, 6 affected and 4 non-affected, were used to test for association of aniridia with the *PAX6* locus. Seven of the ten animals were part of one small pedigree, and 3 were unrelated (Figure 3.3). Autosomal recessive inheritance was assumed based on a previous report [18], and limited pedigree information, but phenotypic variability prevented the exclusion of dominant inheritance with incomplete penetrance. In addition, a founder effect mutation was hypothesized based on the small breed size. This mutation appears to have occurred recently in that the previous clinical [18] report is the first and only description of aniridia in the breed, and, as this is a working dog breed, the visual impairment caused by aniridia would be readily recognized in these dogs once it occurred.

Table 3.3. Primers Used For Radiation Hybrid Mapping

| PRIMER (location) | PRIMER SEQUENCE | Tm (°C) | PRODUCT SIZE (bp) |
|---|---|---|---|
| PAX6-30F (intron 8) | GCCACATCTTCAGTACAAAG | 49.6 | 300 |
| PAX6-31R (intron 8) | TAGTTCAGGCATTGACTGATG | 50.3 | |
| WT1 (Wilms tumor 1)-F | GGTGCCTGGAAACGTCCG | 59.2 | 155 |
| WT1 (Wilms tumor 1)-R | ACCGGGAGAACTTTCGCTGAC | 59.5 | |
| CD44 (Cell differentiation antigen 44 variant)-F | TGGAAGAGAAGGTGGACATCTTCC | 58.2 | 106 |
| CD44 (Cell differentiation antigen 44 variant)-R | GGTCACCGGGATGAGGGTC | 60.1 | |
| COLF1 (Canine olfactory receptor gene 1) -F | GTCTCGGGGCATCTGTGTAT | 57.4 | 357 |
| COLF1 (Canine olfactory receptor gene 1) -R | GATGGCCACAGAAGTCAGGT | 57.4 | |
| COLF2 (Canine olfactory receptor gene 2)-F | AGAGTGTGCTCCCTGCTGAT | 57.4 | 357 |
| COLF2 (Canine olfactory receptor gene 2)-R | TGCAACAGCAGTTAAGTGGG | 55.4 | |
| DLA79 (MHC class IB) -F | TCTATTCTGGCATTGGGGAC | 55.4 | 270 |
| DLA79 (MHC class IB) -R | TGAGTAGCTCCCTCCTTTTCTG | 58.1 | |
| ROM1 –F | CTCTTTGATCCTCGTCAGCC | 57.4 | 230 |
| ROM1 –R | TGAGGGTCAGTAGGTCCCTG | 59.5 | |
| TPCR63 (Putative olfactory receptor)-F | AGGATACGTTCCTCAGAGGGCC | 61.9 | 129 |
| TPCR63 (Putative olfactory receptor)-R | ATCTAATGAGTGGTTGGTCCCTGGT | 60.6 | |
| Wilms-TF (tetra repeat)-F | CCCAATCTCCAGAGATTTTCC | 52.3 | 300 |
| Wilms-TF (tetra repeat)-R | CCAGTCTCAGCTGTGTCCAA | 53.7 | |
| REN47J11-F (CA)11 | TCTCCTCGCGTGTTTCTG | 50.2 | 163 |
| REN47J11-R (CA)11 | GGGGACACTCAGAAGGACG | 55.3 | |
| REN248C19-F (CA)10 | TGACTGTGGCAAGCAAGAAC | 51.7 | 319 |
| REN248C19-R (CA)10 | GGCAAAGAAAGATGGACTGG | 51.7 | |
| C18.156-F (AC)15 | ACAACCAACACACACAAAAACC | 54.7 | 136 |
| C18.156-R (AC)15 | TGTTATCCCAGTGGCATTAGG | 54.5 | |
| C18.460-F (TG)17 | CTTCCCATTATAGCCCTGTCC | 54.8 | 147 |
| C18.460-R (TG)17 | GGTGTCAGGAAAATGAGACCA | 54.8 | |
| AHT130-F (GT)19 | CCTCTCCTGGTAAGTGCTGC | 57.6 | 113 |
| AHT130-R (GT)19 | TGGAACACTGGTCCCCAG | 57.0 | |
| FH2356-F (tetra repeat) | CTTGCATTCCCGCTCTCACT | 57.6 | 235 |
| FH2356-R (tetra repeat) | TCCTGAAATAGCTCCAGCGC | 57.4 | |

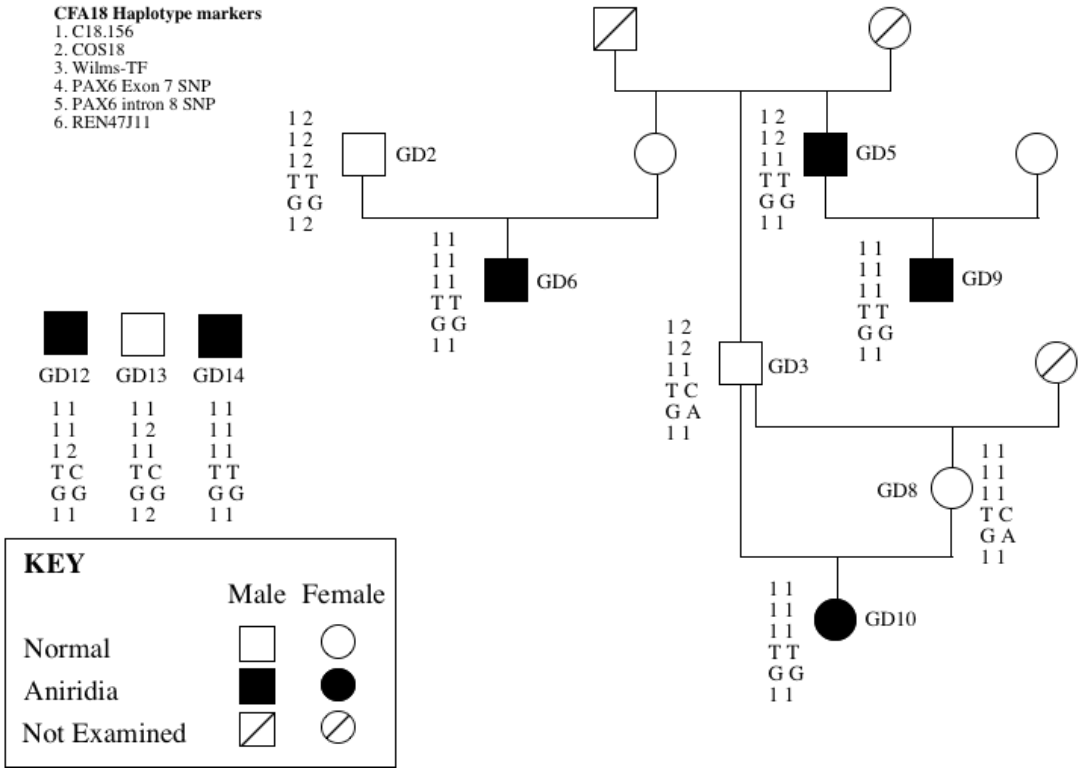


Figure 3.3. Test for association of aniridia phenotypes with CFA18 markers. Four microsatellites and 2 single nucleotide polymorphisms were analyzed in 10 dogs (6 affected, and 4 non-affected). Two of the 6 affected dogs were heterozygous; one of these was heterozygous for the PAX6 exon 7 SNP.

Four microsatellite markers (C18.156, COS18, Wilms-TF, REN47J11) which were previously mapped to CFA18 using an RH5000 panel [21, 22] were used for association testing along with 2 SNPs identified within canine *PAX6*: one in exon 7 and one in intron 8. In exon 7 there is a T→C change (ACT>ACC) at nucleotide 501 of the 1311bp coding sequence (PAX6(5a)) that does not alter the translated amino acid (threonine). In intron 8 (which is 484bp), there is a G →A change at intronic nucleotide position 351.

Primers used for association testing, along with PCR product sizes, genomic locations, and inter-marker distances are listed in Table 3.4. The previous RH5000 map placement of the 4 microsatellite markers gives 22.0 cRays between C18.156 and COS18, 57.5 cRays between COS18 and Wilms-TF, and 64.7 cRays between Wilms-TF and REN47J11 [22]. According to the current genomic sequence, *PAX6* lies between Wilms-TF and REN47J11 (Table 3.4). PCRs were run as previously described, and products for microsatellite markers were electrophoresed on 6% polyacrylamide gels, and microsatellite sizes were scored for each dog. PCR products for the exon 7 SNP were electrophoresed on 2% agarose gels (Invitrogen, Carlsbad, California), gel purified, sequenced and analysed as previously described. Intron 8 PCR products were digested with *Bst*NI (New England Biolabs, Ipswich, MA) and electrophoresed on 6% polyacrylamide gels. Dogs homozygous (G/G) for the intron 8 SNP had 230bp and 220bp bands, while heterozygous dogs (G/A) had 230bp, 220bp, and 450bp bands after enzyme digestion. Homozygous (A/A) dogs would have a 450bp band, but there were none in this pedigree.

*Southern blot*

Southern (DNA) analysis was performed using ten micrograms (10μg) of gDNA from 2 non-affected dogs (GD2 and GD8), 2 affected progeny (GD6 and

Table 3.4. Primer sequences used for association testing and genomic location of amplicons. The exact location of COS18* and *PAX6* exon 7** could not be determined in the current canine genome draft sequence. The site given for COS18 represents the region between its flanking markers BAC_375-H17 and BAC_373-K16 (24,25). The site given for exon 7 represents the boundaries of the gap in the canine genome which begins in *PAX6* intron 4 and ends in intron 8.

| PRIMER NAME | PRIMER SEQUENCE | Tm (°C) | PRODUCT SIZE (bp) | CANINE GENOMIC SEQ. LOCATION | DIST. BTWN MARKERS |
|---|---|---|---|---|---|
| C18.156-F (AC)15 | ACAACCAACACACAC AAAAACC | 54.7 | 136 | Chr18:25401870+ 25402003 | |
| C18.156-R (AC)15 | TGTTATCCCAGTGGC ATTAGG | 54.5 | | | 2.2MB |
| COS-18-F (TC)19 | CGTGGTGCCGGCCCT TTGAT | 63.4 | 360 | Chr18:27577535-30076377* | |
| COS-18-R (TC)19 | TTTAGCGCCTGCCTTT GGAC | 58.4 | | | 8.1MB |
| Wilms-TF-F (tetra repeat) | CCCAATCTCCAGAGA TTTTCC | 52.3 | 300 | Chr18:38163822+ 38164112 | |
| Wilms-TF-R (tetra repeat) | CCAGTCTCAGCTGTG TCCAA | 53.7 | | | 510KB |
| PAX6-51F (exon 7 SNP) | GTTGTTCTTTAAGAG AGTGGGTG | 53.5 | 310 | Chr18:38675041-38687664** | |
| PAX6-52R (exon 7 SNP) | CCAGTGGCTGCCTATA TGGAG | 57.3 | | | 2.8KB |
| PAX6-30F (intron 8 SNP) | GCCACATCTTCAGTA CAAAG | 49.6 | 824 | Chr18:38687699+ 38688522 | |
| PAX6-21R (intron 8 SNP) | GCCTGTCTTCTCTGGTT CC | 53.1 | | | 6.6MB |
| REN47J11-F (CA)11 | TCTCCTCGCGTGTTTC TG | 50.2 | 163 | Chr18:45329434-45329603 | |
| REN47J11-R (CA)11 | GGGGACACTCAGAAG GACG | 55.3 | | | |

agarose gel, and transferred to a nylon hybridization transfer membrane (GeneScreen Plus® Perkin Elmer, Boston, MA). The nylon membrane was prehybridized and hybridized with ExpressHyb™ (Clontech, Palo Alto, California). Probes were labeled with αP32 dCTP (3000Ci/mmol, 10mCi/ml) using the RadPrime DNA Labeling System (Life Technologies™, Inc Palo Alto, California).

Two probes were designed from the canine *PAX6*. A 580bp fragment including all of exon 1, intron 1, exon 2 and part of intron 2 was used as a 5'UTR probe. This probe was amplified using primers *PAX6*-40F and 43R (Table 3.2). A 373bp fragment in the PST domain, including part of intron 11, all of exon 12 and part of intron 12, was used as a 3' end probe. This probe was amplified using *PAX6*-61F and 62R (Table 3.2). Each probe was amplified in gDNA, gel purified using the QIAquick® Gel Extraction kit (QIAGEN Inc., Valencia, CA), and verified by sequencing.

***Results***

*Characterization of canine PAX6*

A 1072bp fragment of canine *PAX6* cDNA, representing the 3' end of exon 4 through the 5' end of exon 12, was amplified from a canine retinal cDNA library using primers designed from human/mouse *PAX6* consensus sequence (Table 3.1). cDNA library vector primers, PBKIII and PBKVI, were used to extend the sequence to 1472bp which included the 3' end of exon 2 through the 5' end of exon 13. This fragment contained the complete *PAX6* coding sequence for isoform a, which does not contain the alternatively transcribed exon 5a. This 1269bp coding sequence began at the ATG start codon in exon 4, and ended at the TAA stop codon in exon 13. A poly-A sequence of at least 20 residues followed the stop codon, and it was unclear where non-coding exon 13 ended. Similarly, in man the ATG start codon occurs in exon 4,

and the TAA stop codon in exon 13 is followed by a poly-A sequence of 21 residues. Exon 13 in man is estimated to be 1110bp (NM_001604). Unlike the human and canine genes, mouse *Pax6* contains 12 exons instead of 13, and mouse exons 2-12 correspond with human and canine exons 3-13 (Figure 3.4). As a result, the mouse ATG start codon is in exon 3 (instead of exon 4), and the TAA stop codon is in exon 12 (instead of exon 13), and it is not followed by a poly-A sequence (NM_013627).

A 42bp alternatively transcribed exon 5a was amplified from the canine retinal cDNA library, and was located between exons 5 and 6, as in man; this alternatively transcribed exon is located between exons 4 and 5 in the mouse. The coding sequence for canine *PAX6* isoform b, which includes this alternatively transcribed exon, was 1311bp, and was the same length as the human and mouse *PAX6*(5a) coding sequences.

Sequences for exon 1 and the 5' end of exon 2 could not be amplified from the cDNA library, and were obtained from TIGR 1.5X (Poodle) canine genomic sequence [20]. Within the 5'UTR, the predicted sizes for canine exons 1 and 2, and introns 1 and 2, were similar in size to the corresponding human exons and introns (Table 3.5). Exon 1 was predicted to be 103bp based on the TIGR canine genomic sequence, and sequences amplified from genomic DNA in canine patients. In man, *PAX6* exon 1 is 119bp (NM_001604) or 196bp (NM_000280). *PAX6* exon 2 is 188bp in man (NM_001604 and NM_000280), and predicted to be 224bp in the dog. The additional 36bp in canine exon 2 included a 23bp poly-A sequence near the center of the exon followed by highly repetitive sequence. In the mouse, the comparable exon 1 is 386pb (NM_013627), while exon 2 is 80bp and corresponds with human and canine exon 3 (77bp) (Figure 3.4 & Table 3.5).

Canine *PAX6* (EF_141016, EF_141017)

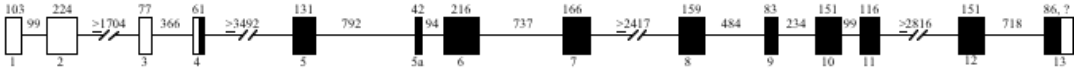


Human *PAX6* (NM_001604)

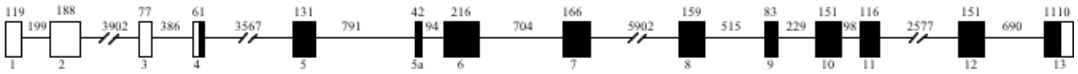


Mouse *Pax6* (NM_013627)

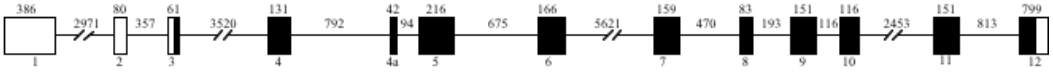


Figure 3.4. Comparison of canine, human, and mouse *PAX6* organization. Open boxes represent non-coding exons, and filled boxes represent coding exons. Exon sizes are given above exon boxes. Lines represent introns with sizes written above.

Table 3.5. Comparison Of Human, Canine And Mouse *PAX6* Exon And Intron Sizes. *Human sizes were determined using reference sequence NM_001604 and the UCSC human genome sequence. **Mouse sizes were determined using reference sequence NM_013627 and the UCSC mouse genome sequence. † Canine intron 2 and 7 estimates are based on the TIGR 1X (poodle) sequence. ΔCanine intron 4 and 11 estimates are based on UCSC 7.5X (boxer) sequence. The complete size of canine exon 13 is unknown. The ATG start codon is located in human and canine exon 4, and mouse exon 3. The TAA stop codon is located in human and canine exon 13, and mouse exon 12.

| ***PAX6* EXONS & INTRONS** | **HUMAN* SIZES (bp)** | **CANINE SIZES (bp)** | **MOUSE EXONS/ INTRONS** | **MOUSE** SIZES (bp)** |
|---|---|---|---|---|
| EXON 1 | 119 | 103 | | |
| INTRON 1 | 197 | 99 | | |
| EXON 2 | 188 | 224 | EXON 1 | 386 |
| INTRON 2 | 3902 | $\geq$ 1704† | INTRON 1 | 2971 |
| EXON 3 | 77 | 77 | EXON 2 | 80 |
| INTRON 3 | 386 | 366 | INTRON 2 | 357 |
| EXON 4 (ATG) | 61 | 61 | EXON 3 (ATG) | 61 |
| INTRON 4 | 3567 | $\geq$3492 Δ | INTRON 3 | 3520 |
| EXON 5 | 131 | 131 | EXON 4 | 131 |
| INTRON 5 | 791 | 792 | INTRON 4 | 792 |
| EXON 5A | 42 | 42 | EXON 4a | 42 |
| INTRON 5A | 94 | 94 | INTRON 4a | 94 |
| EXON 6 | 216 | 216 | EXON 5 | 216 |
| INTRON 6 | 704 | 737 | INTRON 5 | 675 |
| EXON 7 | 166 | 166 | EXON 6 | 166 |
| INTRON 7 | 5902 | $\geq$ 2417 † | INTRON 6 | 5621 |
| EXON 8 | 159 | 159 | EXON 7 | 159 |
| INTRON 8 | 515 | 484 | INTRON 7 | 470 |
| EXON 9 | 83 | 83 | EXON 8 | 83 |
| INTRON 9 | 229 | 234 | INTRON 8 | 193 |
| EXON 10 | 151 | 151 | EXON 9 | 151 |
| INTRON 10 | 98 | 99 | INTRON 9 | 116 |
| EXON 11 | 116 | 116 | EXON 10 | 116 |
| INTRON 11 | 2577 | $\geq$2816 Δ | INTRON 10 | 2453 |
| EXON 12 | 151 | 151 | EXON 11 | 151 |
| INTRON 12 | 690 | 716 | INTRON 11 | 813 |
| EXON 13 (TAA) | 1110 | >99 | EXON 12 (TAA) | 799 |

The canine *PAX6* cDNA sequence (1786bp) representing exons 1-13, including exon 5a, and a 20bp poly-A 3'end, was analyzed against the 2005 canine 7.6X genomic sequence (Boxer) using the blat function: (http://genome.ucsc.edu/cgibin/hgBlat?command=start&org=Dog&db=canFam2&hgsid=73037822). As of November, 2006, there was 99.9% identity spanning >21kb in the genomic sequence (38,671,042-38,692,610) on chromosome 18. Matching sequences were identified for exons 3-4, and 9-13. However, *PAX6* exons 1-2 and 5-8 (including exon 5a) were missing from the current canine draft sequence. A 714bp gap in the canine sequence, from 38,666,389-38,667,102, included predicted exons 1 and 2, while a second, larger 12,622bp gap from 38,675,042-38,687,663, included exons 5-8. As a result, our cloned sequence provides the complete *PAX6* coding sequence (accession numbers EF141016, and EF141017) which was unavailable from the latest canine genomic sequence.

Primers designed to cross introns were used to determine intronic sizes for 9 of the 13 canine introns. The estimated sizes of the remaining 4 introns (2, 4, 7, and 11) were determined using genomic sequence information from TIGR 1.5X (Poodle) [20] and the 7.6X (Boxer) [17] public canine genome sequence (http://genome.ucsc.edu/cgi-bin/hgGateway) (Figure 3.4). Canine exons 3-12, and intron 5a are identical in size to the human counterparts, while exons 1, and 2, and introns 1-12 are similar in size (Table 3.5). Both canine and human isoform b (PAX6(5a)) nucleotide coding sequences were 1311bp and shared 97.3% identity, while the corresponding amino acid sequences shared 99.8% identity (Figure 3.5). Interestingly, the canine and mouse coding sequences were only 93.2% identical, and had 89 nucleotide differences: 15-PD, 13-Linker, 11-HD, 50-PST. Eighty-four of the 89 nucleotide differences between dog and mouse, occurred in the 3$^{rd}$ codon position

Figure 3.5. Comparison of the canine and human PAX6 coding (CDS), and amino acid sequences. First row is the human (NM_001604) CDS, second row is the canine CDS, and the third row is the corresponding amino acid sequence (436 aa). The first underlined region is the Paired domain (426bp), followed by the Linker region (234bp). The second underlined region is the homeodomain (183bp), followed by the PST domain (459bp). Asterisks (*) mark the 36 nucleotide differences between dog and man: 2 - PD, 3 - linker, 5 - HD, and 26 - PST domain. Thirty-five of the 36 nucleotide differences occurred in the third position of the triplet codon, and did not alter the translated amino acid. Only one nucleotide difference occurred at the first position of a codon (base pair 1213) resulting in an ACC (threonine) in man, and a GCC (alanine) in the dog. This change occurred in exon 12 which was part of the PST domain. As a result, the human and canine *PAX6* nucleotide coding sequences were 97.3% identical, and the corresponding amino acid sequences were 99.8% identical.

```
H:ATGCAGAACA GTCACAGCGG AGTGAATCAG CTCGGTGGTG TCTTTGTCAA 50
C:ATGCAGAACA GTCACAGCGG AGTGAATCAG CTCGGTGGTG TCTTTGTCAA
  METGlnAsnS erHisSerGl yValAsnGln LeuGlyGlyV alPheValAs

                                          *
H:CGGGCGGCCA CTGCCGGACT CCACCCGGCA GAAGATTGTA GAGCTAGCTC 100
C:CGGGCGGCCA CTGCCGGACT CCACCCGGCA GAAGATCGTA GAGCTAGCTC
  nGlyArgPro LeuProAspS erThrArgGl nLysIleVal GluLeuAlaH


H:ACAGCGGGGC CCGGCCGTGC GACATTTCCC GAATTCTGCA GACCCATGCA 150
C:ACAGCGGGGC CCGGCCGTGC GACATTTCCC GAATTCTGCA GACCCATGCA
  isSerGlyAl aArgProCys AspIleSerA rgIleLeuGl nThrHisAla


H:GATGCAAAAG TCCAAGTGCT GGACAATCAA AACGTGTCCA ACGGATGTGT 200
C:GATGCAAAAG TCCAAGTGCT GGACAATCAA AACGTGTCCA ACGGATGTGT
  AspAlaLysV alGlnValLe uAspAsnGln AsnValSerA snGlyCysVa


H:GAGTAAAATT CTGGGCAGGT ATTACGAGAC TGGCTCCATC AGACCCAGGG 250
C:GAGTAAAATT CTGGGCAGGT ATTACGAGAC TGGCTCCATC AGACCCAGGG
  lSerLysIle LeuGlyArgT yrTyrGluTh rGlySerIle ArgProArgA


H:CAATCGGTGG TAGTAAACCG AGAGTAGCGA CTCCAGAAGT TGTAAGCAAA 300
C:CAATCGGTGG TAGTAAACCG AGAGTAGCGA CTCCAGAAGT TGTAAGCAAA
  laIleGlyGl ySerLysPro ArgValAlaT hrProGluVa lValSerLys


H:ATAGCCCAGT ATAAGCGGGA GTGCCCGTCC ATCTTTGCTT GGGAAATCCG 350
C:ATAGCCCAGT ATAAGCGGGA GTGCCCGTCC ATCTTTGCTT GGGAAATCCG
  IleAlaGlnT yrLysArgGl uCysProSer IlePheAlaT rpGluIleAr

                                                      *
H:AGACAGATTA CTGTCCGAGG GGGTCTGTAC CAACGATAAC ATACCAAGCG 400
C:AGACAGATTA CTGTCCGAGG GGGTCTGTAC CAACGATAAC ATACCAAGTG
  gAspArgLeu LeuSerGluG lyValCysTh rAsnAspAsn IleProSerV


H:TGTCATCAAT AAACAGAGTT CTTCGCAACC TGGCTAGCGA AAAGCAACAG 450
C:TGTCATCAAT AAACAGAGTT CTTCGCAACC TGGCTAGCGA AAAGCAACAG
  alSerSerIl eAsnArgVal LeuArgAsnL euAlaSerGl uLysGlnGln


H:ATGGGCGCAG ACGGCATGTA TGATAAACTA AGGATGTTGA ACGGGCAGAC 500
C:ATGGGCGCAG ACGGCATGTA TGATAAACTA AGGATGTTGA ACGGGCAGAC
  MetGlyAlaA spGlyMetTy rAspLysLeu ArgMetLeuA snGlyGlnTh

                          *                       *
H:CGGAAGCTGG GGCACCCGCC CTGGTTGGTA TCCGGGGACT TCGGTGCCAG 550
C:CGGAAGCTGG GGCACCCGCC CCGGTTGGTA TCCGGGGACT TCTGTGCCAG
  rGlySerTrp GlyThrArgP roGlyTrpTy rProGlyThr SerValProG
```

Figure 3.5 (Continued)

```
H:GGCAACCTAC GCAAGATGGC TGCCAGCAAC AGGAAGGAGG GGGAGAGAAT 600
C:GGCAACCTAC GCAAGATGGC TGCCAGCAAC AGGAAGGAGG GGGAGAGAAT
  lyGlnProTh rGlnAspGly CysGlnGlnG lnGluGlyGl yGlyGluAsn

                                                *
H:ACCAACTCCA TCAGTTCCAA CGGAGAAGAT TCAGATGAGG CTCAAATGCG 650
C:ACCAACTCCA TCAGTTCCAA CGGAGAAGAT TCAGATGAGG CCCAAATGCG
  ThrAsnSerI leSerSerAs nGlyGluAsp SerAspGluA laGlnMetAr

                            *
H:ACTTCAGCTG AAGCGGAAGC TGCAAAGAAA TAGAACATCC TTTACCCAAG 700
C:ACTTCAGCTG AAGCGGAAGC TGCAGAGAAA TAGAACATCC TTTACCCAAG
  gLeuGlnLeu LysArgLysL euGlnArgAs nArgThrSer PheThrGlnG

             *
H:AGCAAATTGA GGCCCTGGAG AAAGAGTTTG AGAGAACCCA TTATCCAGAT 750
C:AGCAAATTGA AGCCCTGGAG AAAGAGTTTG AGAGAACCCA TTATCCAGAT
  luGlnIleGl uAlaLeuGlu LysGluPheG luArgThrHi sTyrProAsp

                               *         *
H:GTGTTTGCCC GAGAAAGACT AGCAGCCAAA ATAGATCTAC CTGAAGCAAG 800
C:GTGTTTGCCC GAGAAAGACT AGCGGCCAAA ATCGATCTAC CTGAAGCAAG
  ValPheAlaA rgGluArgLe uAlaAlaLys IleAspLeuP roGluAlaAr

                               *
H:AATACAGGTA TGGTTTTCTA ATCGAAGGGC CAAATGGAGA AGAGAAGAAA 850
C:AATACAGGTA TGGTTTTCTA ATCGGAGGGC CAAATGGAGA AGAGAAGAAA
  gIleGlnVal TrpPheSerA snArgArgAl aLysTrpArg ArgGluGluL

             *                 *              *      *  *  *
H:AACTGAGGAA TCAGAGAAGA CAGGCCAGCA ACACACCTAG TCATATTCCT 900
C:AACTGAGGAA CCAGAGAAGA CAGGCTAGCA ACACACCCAG TCACATCCCC
  ysLeuArgAs nGlnArgArg GlnAlaSerA snThrProSe rHisIlePro

                                                 *  *
H:ATCAGCAGTA GTTTCAGCAC CAGTGTCTAC CAACCAATTC CACAACCCAC 950
C:ATCAGCAGTA GTTTCAGCAC CAGTGTCTAC CAACCTATCC CACAACCCAC
  IleSerSerS erPheSerTh rSerValTyr GlnProIleP roGlnProTh

     *  *                *                          *
H:CACACCGGTT TCCTCCTTCA CATCTGGCTC CATGTTGGGC CGAACAGACA 1000
C:CACGCCTGTT TCCTCCTTCA CCTCTGGCTC CATGTTGGGC CGGACAGACA
  rThrProVal SerSerPheT hrSerGlySe rMetLeuGly ArgThrAspT

                    *                   *
H:CAGCCCTCAC AAACACCTAC AGCGCTCTGC CGCCTATGCC CAGCTTCACC 1050
C:CAGCCCTCAC AAACACGTAC AGCGCTCTGC CGCCCATGCC CAGCTTCACC
  hrAlaLeuTh rAsnThrTyr SerAlaLeuP roProMetPr oSerPheThr

       *
H:ATGGCAAATA ACCTGCCTAT GCAACCCCCA GTCCCCAGCC AGACCTCCTC 1100
C:ATGGCGAATA ACCTGCCTAT GCAACCCCCA GTCCCCAGCC AGACCTCCTC
  MetAlaAsnA snLeuProMe tGlnProPro ValProSerG lnThrSerSe
```

Figure 3.5 (Continued)

```
  *                                        *           *
H:ATACTCCTGC ATGCTGCCCA CCAGCCCTTC GGTGAATGGG CGGAGTTATG 1150
C:GTACTCCTGC ATGCTGCCCA CCAGCCCTTC GGTGAACGGG CGGAGTTACG
  rTyrSerCys MetLeuProT hrSerProSe rValAsnGly ArgSerTyrA

             *     *           *
H:ATACCTACAC CCCCCCACAT ATGCAGACAC ACATGAACAG TCAGCCAATG 1200
C:ATACCTACAC GCCCCCCCAT ATGCAGACCC ACATGAACAG TCAGCCAATG
  spThrTyrTh rProProHis MetGlnThrH isMetAsnSe rGlnProMet

               *        *
H:GGCACCTCGG GCACCACTTC AACAGGACTC ATTTCCCCTG GTGTGTCAGT 1250
C:GGCACCTCGG GCGCCACTTC CACAGGACTC ATTTCCCCTG GTGTGTCAGT
  GlyThrSerG ly   ThrSe rThrGlyLeu IleSerProG lyValSerVa

                  *                        *   *
H:TCCAGTTCAA GTTCCCGGAA GTGAACCTGA TATGTCTCAA TACTGGCCAA 1300
C:TCCAGTTCAA GTTCCTGGAA GTGAACCTGA TATGTCTCAG TATTGGCCAA
  lProValGln ValProGlyS erGluProAs pMetSerGln TyrTrpProA

H:GATTACAGTA A 1311
C:GATTACAGTA A
  rgLeuGlnST P
```

and represented silent changes. Of the 5 nucleotide differences which occurred in the first codon position, only two resulted in an amino acid change: *PAX6(5a)* coding sequence nucleotide position 178 in exon 5a (PD) coded for glutamine (CAA) in the dog and man, but glutamic acid (GAA) in mouse; nucleotide position 1213 in exon 12 (PST) coded for alanine (GCC) in the dog and threonine (ACC) in mouse and man.

*Exon Scanning*

The 14 exons of canine *PAX6* were scanned for mutations, including predicted exons 1 and 2, cloned exons 3-13, and the alternatively transcribed exon 5a. Splice sites at the intron/exon boundaries were also examined; at least 27 intronic nucleotides before each exon, and at least 30 intronic nucleotides after each exon were included in the analysis. *PAX6* exon scans were performed in 7 dogs that were part of one pedigree; this included 4 aniridia-affected dogs and 3 non-affected related dogs (Figure 3.2). Non-coding exon 2 (224 bp) contained a 23bp poly-A region followed by 6 AACC repeats. The first 133bp of exon 2 was scanned in all 7 dogs, and the complete exon 2 sequence was scanned in 2 affected dogs (GD 5, 6) and 2 normal dogs (GD 3, 8). These 4 dogs had an extra AACC repeat in non-coding exon 2.

*PAX6* exon scanning also revealed 2 single nucleotide polymorphisms (SNPs). The first was located in exon 7 at nucleotide position 501/1311, and involved a C to T change at the third position of the codon which did not alter the amino acid coded (ACC to ACT; threonine). The second SNP occurred in intron 8 (484bp) at intronic nucleotide position 351, and was an A to G transition. Both of these SNPs were silent changes which did not alter the translated amino acids. No pathological mutations were identified in all 14 exons scanned or in their exon/intron junctions.

*Radiation Hybrid Mapping*

A canine/hamster radiation hybrid (RH3000) panel was used to link canine *PAX6* to CFA 18 in relation to 7 gene markers and 7 microsatellite markers (Table 3.3) which were mapped in previous studies [21, 22]. Multimap analysis could only place 8 of the 15 markers at unique map positions. *PAX6* and 6 other markers were placed on CFA18, but could not be localized to a unique position in relation to the other markers. However, two-point linkage analysis linked canine *PAX6* to Wilms-TF and WT1 on CFA18, with LOD scores of 8.0 and 7.1, respectively. Wilms-TF and WT1 are both located on CFA18 in a region with homology to HSA11p13, [22, 24, 25] which is where human *PAX6* is located. Similar map locations between the canine and human *PAX6* genes further supports their homology.

*Association Testing*

Having excluded disease-associated changes in the coding sequence, we examined whether there was an association of *PAX6* with the disease locus. Ten Catalan sheepdogs (6 affected and 4 non-affected) were tested for association of *PAX6* with the aniridia phenotype. Seven of these dogs were related and part of the same pedigree, while 3 dogs were unrelated (Figure 3.3). Because of the limited genetic studies to date, it was not definitive whether this disease was recessive or dominant. Based on a prior report [18], and the production of affected dogs from non-affected parents, recessive inheritance was assumed. Furthermore, based on the small breed size, we hypothesized also that all aniridia-affected dogs resulted from a founder-effect mutation. Thus, if the disease is autosomal recessive, all affected dogs would be homozygous for a common haplotype segment of CFA18. Alternatively, if the disease is autosomal dominant with incomplete penetrance, all affected dogs would have at least one common haplotype segment of CFA18.

Six polymorphic markers on CFA18 were analyzed that included 4 microsatellite markers (C18.156, COS18, Wilms-TF, and REN47J11), and 2 *PAX6* SNPs (exon 7 and intron 8). All 10 dogs examined shared at least one common haplotype for all 6 markers (Figure 3.3: "111TG1"). Four of the 6 affected dogs (GD6, GD9, GD10, GD14) were homozygous for this common haplotype, while 2 affected dogs (GD5, GD12) were heterozygous. All affected dogs, regardless of homozygosity or heterozygosity for this haplotype, showed a broadly similar aniridia phenotype. Haplotypes for GD5 and GD12 were repeated to confirm their heterozygosity. All 4 unaffected dogs (GD2, GD3, GD8, GD13) were heterozygous for the common haplotype. At 4 of the 6 individual marker loci (C18.156, COS18, WILMS-TF, and exon 7 SNP) both normal and affected dogs shared common genotypes. For 2 marker loci (intron 8 SNP, and REN47J11) non-affected dogs had both homozygous and heterozygous genotypes while all affected dogs were homozygous. Furthermore, at each marker locus there were both affected and non-affected animals with identical genotypes. Such degree of haplotype sharing is not unexpected given the small breed size and degree of inbreeding.

Assuming recessive inheritance, our observations suggested no association of the *PAX6* locus with the aniridia phenotype. However, if aniridia segregates as a dominant disease in these dogs, our observations would suggest an association in that all affected dogs shared at least one common haplotype ("111TG1"). Incomplete penetrance could explain the presence of this commom haplotype in “non-affected” dogs (GD2, GD3, GD8, GD13) that did not manifest the aniridia phenotype.

*Southern Blot Analysis*

A Southern blot analysis was performed using probes designed from both the 5’UTR (exon 1, intron 1, exon 2 and the 5’ end of intron 2) and the 3’ PST domain (3’

end of intron 11, all of exon 12 and the 5' end of intron 12) of *PAX6*. Identical bands were found in affected and unaffected dogs from the aniridia pedigree, and a normal Beagle control using both probes. The 5'UTR probe hybridized at about 8500bp, while the 3' PST probe hybridized at about 7400bp (data not shown). The absence of any distinction between the *PAX6* bands of affected and non-affected dogs using both 5' and 3' end probes suggested that there were no large deletions present in these two regions of the gene.

***Discussion***

Human aniridia patients show varying degrees of iris loss including complete to partial absence of the iris, iris coloboma and thinning of the iris. They may also exhibit other related ocular abnormalities including cataract, keratitis, or glaucoma (http://www.ncbi.nlm.nih.gov/entrez/query.fcgi?db=OMIM). In this study, the clinical manifestation of aniridia in a canine model strongly resembled that seen in human patients. Canine subjects showed total to nearly complete absence of the iris with ciliary processes visible at the circumferential border; in some cases, cataracts, corneal edema and glaucoma also were present. The anatomical similarities between the dog and human eye, along with the clinical similarities in canine and human aniridia phenotypes, make the dog an important model for this disease.

Because the vast majority of aniridia cases in man are caused by mutations in the *PAX6* gene [26] we used the candidate gene approach to evaluate *PAX6* in the study population. *PAX6* was cloned from a canine retinal cDNA library, and linked to WT1 and Wilms-TF on CFA18 using an RH3000 panel. A previous study placed *PAX6* on CFA18 in the same region between markers FH3824 and CFOR04B04 using an RH5000 panel [27]. WT1 is just 4 cRays away from marker FH3824, and 14 cRays from CFOR04B04 on the RH5000, 4249-marker map [25]. Integrated canine

maps demonstrate homology between CFA18 and human chromosomes 7 and 11 [28-30]. *PAX6* is located in a region of CFA18 which has homology with human chromosome 11p13 where *PAX6* is located in man.

The canine *PAX6* cDNA sequence was 1786bp, and included predicted exons 1 and 2, and cloned exons 3-13, plus alternatively transcribed exon 5a (EF141016, EF141017). This cDNA has sequence identity with the current canine genomic sequence over a span >21kb in length (38,671,042-38,692,610) [17](http://genome.ucsc.edu/cgi-bin/hgGateway). This presumably represents the genomic length of the canine *PAX6* gene. The human *PAX6* genomic sequence is 22.4kb (NM001604), while the mouse genomic sequence is 20.6kb (NM013627). Canine *PAX6* exons 3-4 and 9-13 matched sequences in the current genomic sequence. However, exons 1-2 fell within a 714bp gap, and exons 5-8 fell within a second 12,622bp gap in the sequence. The exons that are missing in the current draft canine genomic sequence are provided by our cloning studies. Thus, this study fills in the gaps left by the draft canine genome sequence, and provides a complete canine *PAX6* sequence.

At the nucleotide level, the canine *PAX6(5a)* coding sequence (1311bp) had a higher degree of homology to the human (NM_001604) (97.3% identical) than to the mouse (NM_013627) (93.2% identical) sequence. Most of the nucleotide variations occurred within the PST domain: 26 of the 36 nucleotide differences between dog and human, and 50 of 89 differences between dog and mouse. Nevertheless, most of the nucleotide differences occurred in the third codon position and were synonymous changes that did not result in corresponding amino acid changes (Figure 3.5).

At the amino acid level, canine PAX6 is 99.8% and 99.5% identical, respectively, to the human and murine sequences. The one amino acid difference between canine and human sequences occurred in the PST region at codon 405

(nucleotide position 1213/1311) which codes for alanine in the dog, and threonine in man. The mouse also has threonine at codon 405, and, in addition, the mouse has glutamic acid in the PD at codon 60 (nucleotide position 178/1311) while the dog and human have glutamine. The extremely high *PAX6* nucleotide and amino acid sequence identities between dog, man and mouse suggest a consistency in protein structure and function.

Both canine (EF141016, EF141017) and human (NM_001604) *PAX6* contained 13 exons plus an alternatively transcribed exon 5a. Exons 3-12 and intron 5a were the same sizes in both species while intronic sizes were similar. The mouse (NM_013627) gene, however, only has 12 exons (plus exon 4a) with mouse exons 2-12 corresponding to canine and human exons 3-13. The mouse coding sequence (exons 3-12) was the same size as the corresponding coding sequences in dog and human (exons 4-13). Mouse exon 2, and introns 1-12 were also similar in size to canine and human, but mouse exon 1 was 386bp compared with 103bp (dog) and 119bp (human). Mouse exon 1 is more similar in size to canine and human exons 1 and 2 combined, 327 (canine) and 307 (human), and may explain why the mouse has one less exon than the canine and human genes.

No pathological mutations were detected in the canine *PAX6* coding sequence, non-coding exons, or in the intron/exon junctions of aniridia-affected dogs. This included coding exons 4-13, the alternatively transcribed exon 5a, and the non-coding exons 1-3 in the 5'UTR. Because the dogs used in this study were privately owned pets or working dogs, we were unable to obtain tissue samples to examine *PAX6* RNA products to detect splicing defects or other transcript variants. We also were unable to examine *PAX6* expression in normal and affected animals to rule out mutations in a promoter or enhancer.

Southern blot analysis showed no difference in normal from affected dogs using either 5' or 3' end probes. In the case of a recessively inherited deletion, normal and affected dogs would be distinguishable on Southern analysis because all affected dogs would be homozygous for the deletion, and have either no *PAX6* band (if the probe is in the deletion), or a smaller *PAX6* band (if the probe is not in the deletion, and the deletion is $\geq$ 50bp). Thus, if canine aniridia is a recessive trait, we have excluded a large deletion in *PAX6* at both the 5' and 3' ends of the gene. However, in the case of dominant inheritance, if the Southern blot probe lies within a deletion, the blot would not distinguish between heterozygous-affected, and normal dogs, making the results of the Southern analysis inconclusive. Regardless of the mode of inheritance, however, deletions in the region of exon 7 and intron 8 can be ruled out in dogs which were heterozygous for SNPs detected in these regions [exon 7 (GD3, GD8, GD12, GD13) and intron 8 (GD3, GD8)].

Limitations in access to a larger sample size of dogs, or the ability to carry out prospective matings, prevented confirmation of the mode of inheritance of canine aniridia, and created difficulties in interpreting the association test. If canine aniridia is inherited as a recessive trait, the association test suggests no association of the *PAX6* locus with the aniridia phenotype. However, if canine aniridia is a dominant disease, there appears to be association of *PAX6* with aniridia in that all affected dogs share at least one common haplotype ("111TG1"). Dominance with incomplete penetrance could account for the presence of this common haplotype in the "non-affected" dogs (GD2, GD3, GD8, GD13). Nonetheless, the broadly similar aniridia phenotype present in dogs homozygous or heterozygous for the "111TG1" haplotype argues against dominant inheritance. Furthermore, the frequent occurrence of the "111TG1 haplotype may not be associated with the aniridia phenotype, but may instead result from the degree of relatedness among dogs.

This emphasizes the need for further analysis of animals to establish the mode of inheritance, and to conduct a more complete association test and segregation analysis.

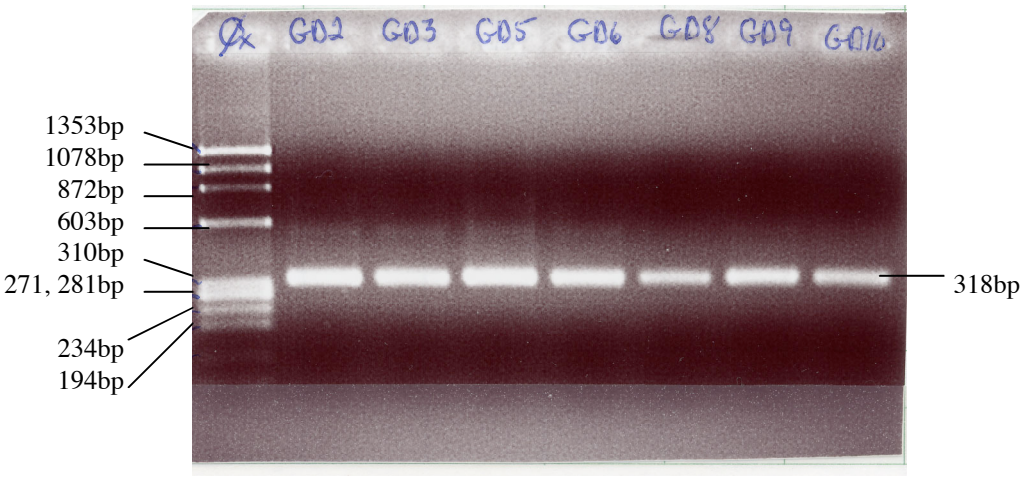


Figure A3.6. Representative 2% agarose gel showing PCR products amplified from genomic DNA from Spanish Catalan sheepdogs using primers specific for *PAX6* exon 13. The first column contains a PhiX174 DNA marker, and columns 2-8 show a 318bp band representing exon 13 in dogs featured in pedigrees (Figures 3.2 and 3.3.).

# REFERENCES


1. Sale MM, Craig JE, Charlesworth JC, FitzGerald LM, Hanson IM, Dickinson JL, et al. Broad phenotypic variability in a single pedigree with a novel 1410delC mutation in the PST domain of the PAX6 gene. Human Mutation 2002;20(4):322.

2. Hodgson SV, Saunders KE. A probable case of the homozygous condition of the aniridia gene. Journal of Medical Genetics 1980;17(6):478-80.

3. Glaser T, Jepeal L, Edwards JG, Young SR, Favor J, Maas RL. PAX6 gene dosage effect in a family with congenital cataracts, aniridia, anophthalmia and central nervous system defects. Nature Genetics 1994;7(4):463-71.

4. Walther C, Gruss P. Pax-6, a murine paired box gene, is expressed in the developing CNS. Development 1991;113(4):1435-49.

5. Ton CC, Hirvonen H, Miwa H, Weil MM, Monaghan P, Jordan T, et al. Positional cloning and characterization of a paired box- and homeobox-containing gene from the aniridia region. Cell 1991;67(6):1059-74.

6. Ton CC, Miwa H, Saunders GF. Small eye (Sey): cloning and characterization of the murine homolog of the human aniridia gene. Genomics 1992;13(2):251-6.

7. Gerard M, Abitbol M, Delezoide AL, Dufier JL, Mallet J, Vekemans M. PAX-genes expression during human embryonic development, a preliminary report. Comptes rendus de l'Académie des sciences. Série III, Sciences de la vie 1995;318(1):57-66.

8. Grindley JC, Davidson DR, Hill RE. The role of Pax-6 in eye and nasal development. Development 1995;121(5):1433-42.

9. Halder G, Callaerts P, Gehring WJ. Induction of ectopic eyes by targeted expression of the eyeless gene in Drosophila. Science 1995;267(5205):1788-92.

10. Chow RL, Altmann CR, Lang RA, Hemmati-Brivanlou A. Pax6 induces ectopic eyes in a vertebrate. Development 1999;126(19):4213-22.

11. Lindsley D, Zimm G. The Genome of Drosophila Melanogaster. New York: Academic Press; 1992.

12. Hill RE, Favor J, Hogan BL, Ton CC, Saunders GF, Hanson IM, et al. Mouse small eye results from mutations in a paired-like homeobox-containing gene. Nature 1991;354(6354):522-5.

13. Favor J, Peters H, Hermann T, Schmahl W, Chatterjee B, Neuhauser-Klaus A, et al. Molecular characterization of Pax6(2Neu) through Pax6(10Neu): an extension of the Pax6 allelic series and the identification of two possible hypomorph alleles in the mouse Mus musculus. Genetics 2001;159(4):1689-700.

14. Epstein JA, Glaser T, Cai J, Jepeal L, Walton DS, Maas RL. Two independent and interactive DNA-binding subdomains of the Pax6 paired domain are regulated by alternative splicing. Genes and Development 1994;8(17):2022-34.

15. Azuma N, Yamaguchi Y, Handa H, Hayakawa M, Kanai A, Yamada M. Missense mutation in the alternative splice region of the PAX6 gene in eye anomalies. American Journal of Human Genetics 1999;65(3):656-663.

16. Yamaguchi Y, Sawada J, Yamada M, Handa H, Azuma N. Autoregulation of Pax6 transcriptional activation by two distinct DNA-binding subdomains of the paired domain. Genes to Cells 1997;2(4):255-61.

17. Lindblad-Toh K, Wade CM, Mikkelsen TS, Karlsson EK, Jaffe DB, Kamal M, et al. Genome sequence, comparative analysis and haplotype structure of the domestic dog. Nature 2005;438(7069):803-819.

18. Villagrasa M. Aplasia-hipoplasia de iris con carácter hereditario en el gos d'atura. Clinica Veterinaria de Pequeños Animales 1996;16(4):201-205.

19. Sambrook J, Fritsch EF, Maniatis T. Molecular Cloning: A Laboratory Manual. Cold Spring Harbor, NY: Cold Spring Harbor Laboratory Press; 1989.

20. Kirkness EF, Bafna V, Halpern AL, Levy S, Remington K, Rusch DB, et al. The dog genome: survey sequencing and comparative analysis. Science 2003;301(5641):1898-1903.

21. Mellersh CS, Hitte C, Richman M, Vignaux F, Priat C, Jouquand S, et al. an integrated linkage-radiation hybrid map of the canine genome. Mammalian Genome 2000;11:120-130.

22. Breen M, Jouquand S, Renier C, Mellersh CS, Hitte C, Holmes NG, et al. chromosome-specific single-locus FISH probes allow anchorage of an 1800-marker integrated radiation-hybrid/linkage map of the domestic dog genome to all chromosomes. Genome Research 2001;11:1784-1795.

23. Matise TC, Perlin M, Chakravarti A. Automated construction of genetic linkage maps using an expert system (MultiMap): a human genome linkage map. Nature Genetics 1994;6(4):384-90.

24. Guyon R, Lorentzen TD, Hitte C, Kim L, Cadieu E, Parker HG, et al. A 1-Mb resolution radiation hybrid map of the canine genome. Proceedings of the National Academy of Sciences of the U S A 2003;100(9):5296-5301.

25. Breen M, Hitte C, Lorentzen TD, Thomas R, Cadieu E, Sabacan L, et al. An integrated 4249 marker FISH/RH map of the canine genome. BMC Genetics 2004;5(1):65.

26. Prosser J, van Heyningen V. PAX6 mutations reviewed. Human Mutation 1998;11(2):93-108.

27. Hunter LS, Sidjanin DJ, Johnson JL, Zangerl B, Galibert F, Andre C, et al. Radiation hybrid mapping of cataract genes in the dog. Molecular Vision 2006;12:588-596.

28. Breen M, Thomas R, Binns MM, Carter NP, Langford CF. Reciprocal chromosome painting reveals detailed regions of conserved synteny between the karyotypes of the domestic dog (Canis familiaris) and human. Genomics 1999;61(2):145-55.

29. Yang F, O'Brien PC, Milne BS, Graphodatsky AS, Solanky N, Trifonov V, et al. A complete comparative chromosome map for the dog, red fox, and human and its integration with canine genetic maps. Genomics 1999;62(2):189-202.

30. Sargan DR, Yang F, Squire M, Milne BS, O'Brien PC, Ferguson-Smith MA. Use of flow-sorted canine chromosomes in the assignment of canine linkage, radiation hybrid, and syntenic groups to chromosomes: refinement and verification of the comparative chromosome map for dog and human. Genomics 2000;69(2):182-95.

# CHAPTER 4

## EVALUATION OF *PAX6* AS A CANDIDATE GENE IN CANINE MODELS OF CATARACT, PERSISTENT PUPILLARY MEMBRANES AND MULTIPLE CONGENITAL DEFECTS


### *Abstract*

Purpose: Mutations that result in premature termination of the PAX6 protein cause aniridia, while missense mutations are associated with non-aniridia ocular phenotypes in man. Because aniridia phenotypes are most commonly selected for *PAX6* evaluation, there is an over-representation of premature termination mutations, and a relative paucity of missense mutations. To try to identify missense mutations associated with non-aniridia phenotypes, we evaluated *PAX6* in dog breeds with inherited ocular diseases including cataract, persistent pupillary membrane, sclero-cornea, and choroidal hypoplasia.

Methods: *PAX6* coding regions and splice sites were analyzed for mutations by direct sequencing in affected dogs from three breeds with inherited ocular diseases. Genomic DNA was extracted from whole blood from Siberian huskies with inherited cataract, Basenjis with persistent pupillary membranes and Soft-coated wheaten terriers with persistent pupillary membranes, sclero-cornea and choroidal hypoplasia.

Results: Evaluation of canine *PAX6* in three breeds identified four single nucleotide polymorphisms (SNPs), and two microsatellite expansions. Two SNPs, and both microsatellite expansions occurred within the 5' untranslated region, while the remaining two SNPs occurred within coding exons 7 and 12.

Conclusion: Although the sequence changes identified in this study were either present in non-coding regions, or represented synonymous changes in coding exons,

additional pedigree information is needed to rule out the association of *PAX6* with the disease phenotypes studied.

***Introduction***

The transcription factor PAX6 is a member of the PAX family of DNA-binding transcription factors, and is highly conserved across species (1). PAX6 contains both paired (PD), and homeo (HD) domains which function as binding sites for DNA targets, as well as a proline-serine-threonine rich (PST) domain which functions as a transactivator (2). *PAX6* is expressed in the developing CNS, eye, and nose during embryogenesis (3-7). Within the eye, it is expressed in the developing cornea, conjunctiva, lens, ciliary body, and retina (8-11). *PAX6* is a master control gene for the development of ocular structures in both vertebrates and invertebrates, and is essential for normal eye morphology. Misexpression of *Pax6* in *Xenopus laevis*, or the *PAX6* homologue *eyeless* in *Drosophila,* is sufficient for the formation of ectopic eyes (12, 13).

*PAX6* mutations are inherited as autosomal dominant or semidominant, and are homozygous lethal. In mouse, *Pax6* mutations cause microphthalmia (*small eye*), cataract, abnormal iris, and anophthalmia (14, 15). In man, *PAX6* mutations cause aniridia (OMIM#106210), a panocular disease characterized by partial to complete absence of the iris, which often occurs with: corneal opacity, cataract, nystagmus, foveal hypoplasia, optic nerve hypoplasia, or glaucoma. Because aniridia phenotypes have been most commonly associated with *PAX6* mutations, these phenotypes have been preferentially selected for *PAX6* mutation screening (16, 17). Analysis of the *PAX6* Allelic Variant Database (http://pax6.hgu.mrc.ac.uk/) reveals that mutations which cause a premature termination in the PAX6 protein are predominantly associated with aniridia, while missense mutations are associated with non-aniridia

phenotypes (16, 18). The over-selection of aniridia phenotypes for *PAX6* mutation analysis has, therefore, resulted in the over-representation of mutations which cause premature termination of the PAX6 protein (17). Conversely, there is an under-representation of missense mutations which may be associated with non-aniridia phenotypes (19). Thus, there is a need to select non-aniridia phenotypes for *PAX6* mutation screening to try to identify other missense mutations.

Non-aniridia *PAX6* phenotypes have been described including Peter's anomaly (20), autosomal dominant keratitis (21), ectopic pupil with optic nerve and macular hypoplasia (19), and ectopic pupil with iris atrophy (22). Isolated foveal hypoplasia (23), as well as foveal hypoplasia with nystagmus and cataracts (19), and foveal hypoplasia with nystagmus, iridocorneal adhesion, corneal opacity, microphthalmos, sclero-cornea, exotropia and embryotoxon (24), have also been described. *PAX6* mutations affecting the optic nerve have been identified which cause optic nerve hypoplasia/aplasia, optic nerve coloboma, and morning glory disc anomaly (25). Although cataracts often occur with aniridia, *PAX6* mutations resulting in cataracts without iris abnormalities have also been described (2, 19, 22, 24, 26). The spectrum of ocular phenotypes observed in non-aniridia *PAX6* mutations, as well as those observed in conjunction with aniridia, provide a clue as to which phenotypes may be worth considering as candidates for *PAX6* mutation screening. These include phenotypes affecting the cornea, iris, pupil, lens, retina, and optic nerve.

In an attempt to identify *PAX6* mutations associated with non-aniridia phenotypes, we have evaluated *PAX6* sequences in canine models with inherited non-aniridia ocular phenotypes. Canine *PAX6* (accession #s EF141016, and EF141017) was cloned and characterized in a previous study (27). Both the human and canine *PAX6* genes contain 13 exons plus an alternatively transcribed exon 5a located between exons 5 and 6 (24, 26, 27). Human and canine coding sequences are 97.3%

identical, and the corresponding amino acid sequences are 99.8% identical; only one amino acid difference occurs in the PST region at codon 405 which codes for threonine (ACC) in man, and alanine (GCC) in the dog (27). *PAX6* is located on *Canis familiaris* autosome 18 (CFA18) in an area homologous to the location of PAX6 on HSA 11p13 (27-29). Thus, the homology between human and canine *PAX6*, with regard to nucleotide and amino acid sequences, as well as gene organization, and gene location, make the dog a reasonable animal model for molecular analysis of this gene. In addition, naturally occurring diseases in dogs are clinically, physiologically, and histologically similar to their corresponding human diseases, and this has contributed to the successful use of dogs as models of many human genetic diseases (30, 31).

In an effort to identify non-aniridia phenotypes with possible *PAX6* missense mutations, we have selected three dog breeds with phenotypes consistent with those observed in patients with *PAX6* mutations. These include: (a) Siberian huskies with inherited cataracts (32, 33), (b) Basenjis with inherited, congenital, persistent pupillary membrane (PPM) (34-38), and (c) Soft-coated wheaten terriers (SCWT) with an inherited ocular syndrome characterized by PPM, sclero-cornea, and choroidal hypoplasia. In man, *PAX6* mutations are associated with cataract (2, 19, 22, 24, 26), and PPM (39, 40). In addition, *PAX6* is expressed in the developing (9), and adult (10) cornea, and mutations are associated with corneal dystrophy (2, 19), keratitis (21), microcornea (41), and sclero-cornea (42, 43). As well, *PAX6* mutations have been associated with ocular coloboma affecting the choroid, retina, and optic nerve (25).

Lack of pedigree information and samples prevented association and linkage studies, and necessitated using an exon scanning approach for molecular evaluation of these phenotypes. *PAX6* was chosen as a candidate gene for analysis because all three

breeds had ocular phenotypes involving anatomical structures which have been associated with *PAX6* mutations. Fourteen *PAX6* exons (including exon 5a) were evaluated by direct sequencing of genomic DNA from each breed. Four single nucleotide polymorphisms (SNPs) were identified; two in the 5' untranslated region (5'UTR), and two within the translated region. Two microsatellite expansions were identified in the 5'UTR as well.

***Methods***

*Animals and DNA*

All dogs used in this study were examined by board-certified veterinary ophthalmologists using indirect ophthalmoscopy and slit lamp biomicroscopy, after mydriasis. Whole blood was collected in EDTA anticoagulant tubes, and stored at –70°C until analyzed. Total genomic DNA (gDNA) was extracted from blood lymphocytes using standard phenol:chloroform extraction protocols (44). Limited pedigree information made it impossible to perform genome wide scans, linkage or association studies. Thus, to analyze the molecular basis of disease in these dogs, a direct sequencing approach was used. Three breeds with inherited ocular diseases were examined including:

(a) Siberian huskies with inherited cataracts. These cataracts occur approximately between 8 months – 1.5 years of age, and affect the posterior cortex. They form a characteristic large triangular plaque in the posterior cortex with a prominent central inverted Y-suture. Two unrelated, one-year-old male dogs (H-1, and H–2) with bilateral, posterior cortical cataracts were selected for *PAX6* sequence analysis.

(b) Basenjis with PPMs. Two, 3 year-old, full sibling male dogs with congenital, unilateral, iris-to-iris PPMs were selected for *PAX6* analysis. B-1 was affected in the left eye, and B-2, in the right eye.

(c) Soft-coated wheaten terriers (SCWT) with a congenital, autosomal recessive syndrome characterized by PPMs, sclero-cornea, and choroidal hypoplasia. Two, 4 month-old, full sibling SCWTs, one female (SCWT-1) and one male (SCWT-2), with bilateral, iris-to-iris, PPMs were selected for *PAX6* analysis. Both dogs also had ventral sclero-cornea such that the ventral margins of the normally transparent cornea were invaded by opaque white scleral tissue. SCWT-1 had mild, bilateral, choroidal hypoplasia, while SCWT-2 had choroidal hypoplasia that was moderate and localized in the right eye, and severe and localized in the left eye.

*Exon scanning*

Fourteen *PAX6* exons along with their intron/exon boundaries, were sequenced using PCR amplification of genomic DNA from two affected dogs from each breed, and one non-affected, normal beagle as a control. Exon 13 was sequenced through the TAA stop codon only, as the exact end of this exon is unknown. Primers used to amplify each *PAX6* exon were described in a previous study (27). PCRs were run at 25ul reaction volume in triplicate, using *Taq* DNA polymerase (Invitrogen Corporation, Carlsbad, CA). PCR conditions were as follows: 2 min 94°C followed by 30 cycles of 60 sec 94°C, 60 sec 58°C, 60 sec 72°C, and a final extension of 7 min 72°C. However, an annealing temperature of 64° was used for exon 1 , and 56° for exons 4, 5a, 9, 12 and 13. PCRs were run on Amplitron II® Thermolyne (Barnstead Thermolyne Co., Dubuque, IA), and MJ Research Tetrad 2 (Global Medical Instrumentation Inc., Ramsey, MN) thermocyclers, and PCR products were separated by electrophoresis on 2% agarose gels (Invitrogen, Carlsbad, CA) with 1X TAE buffer

(0.04 M Tris-acetate buffer, pH 8, 100 mM ethylenediaminetetra-acetic acid) at 60V. Gels were stained with ethidium bromide, and visualized using an ultraviolet (UV) transilluminator (Spectronics Corporation, Westbury, NY). Digital images were recorded of each gel. PCR products were gel purified using the QIAquick® Gel Extraction kit (QIAGEN Inc., Valencia, CA) or the QIAquick® PCR purification kit (QIAGEN Inc., Valencia, CA). Purified PCR products were then sequenced on the Applied Biosystems Automated 3730 DNA Analyzer using Big Dye Terminator chemistry and Ampli Taq-FS DNA Polymerase.

Sequencher™ software (Gene Codes Corporation, Ann Arbor, MI) was used for sequence analysis. Nucleotide changes in *PAX6* identified in the study dogs were compared with sequences from normal beagle, 1.5X canine (poodle) genomic sequence (45) and 7.5X canine (boxer) genomic sequence (46). However, the 7.5X (boxer) sequence did not contain the *PAX6* exon 2 microsatellite, or the exon 7 SNP.

***Results***

*PAX6* sequences were analyzed in 6 dogs representing three breeds with inherited ocular diseases. These included; two Siberian huskies with cataracts, two Basenjis with PPM, and two SCWTs with PPM, sclero-cornea, and choroidal hypoplasia. Fourteen *PAX6* exons were examined for mutations, including untranslated exons 1-3, and part of exon 4, translated exons 4-13, and alternatively transcribed exon 5a. Exon 13 sequences were analyzed through the TAA stop codon (Figure 4.1).

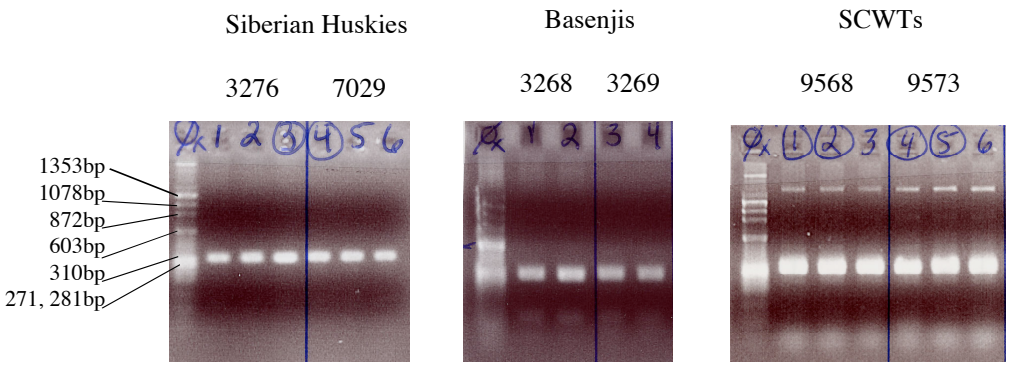


Figure 4.1. Representative 2% agarose gels showing PCR products amplified from genomic DNA using primers specific for *PAX6* exon 13 (318bp) in Siberian huskies with cataracts (gel #1), Basenjis with PPM (gel #2), and SCWTs with PPM, sclero-cornea, and choroidal hypoplasia (gel #3). Individual dog identification numbers are indicated above wells. Gels #1 and #3 show PCRs run in triplicate while gel #2 shows PCRs run in duplicate. The first column of each gel contains a PhiX174 DNA marker.

Intron/exon boundaries (splice sites) were also examined including at least 13 intronic nucleotides before each exon, and at least 16 intronic nucleotides after each exon. Introns 5a (94bp), 9 (234bp), and 10 (99bp) were examined in their entirety in all 6 dogs. Canine *PAX6*(5a) cDNA was 1766bp from exon 1 through the TAA stop codon in exon 13. The *PAX6*(5a) coding sequence was 1311bp and began at the ATG start codon in exon 4 (nucleotide 456), and ended at the TAA stop codon in exon 13 (nucleotide 1766). This sequence coded for a 436 amino acid protein (27).

The results of *PAX6* sequence analysis revealed 2 intronic SNPs, 2 exonic SNPs, and 2 microsatellite expansions (Table 4.1). At the 5' end of intron 2 there was a cytosine to guanine (C→ G) change at intronic nucleotide (+27), and a thymine to cytosine (T → C) change at intronic nucleotide (+51). The latter SNP (intron 2, +51), was located at the 3' end of a CTT microsatellite (5'-CTTCTTCTTCTT**T**TT-3') such that it expanded a microsatellite from four repeats (CTT)4, to five (CTT)5. Thus, dogs with a thymine (T) at this position had four microsatellite repeats (CTT)4, while dogs with a cytosine (C) had 5 repeats (CTT)5. Canine *PAX6* exon 2 was 224 bp and contained a 23bp poly-A region (nucleotides 229-251) followed by a (CCAA)7 microsatellite (nucleotides 259-286) which varied in repeat number in some subject dogs. This sequence was unavailable in the 7.5X canine (boxer) public genomic sequence (46), but was present in the 1.5X canine (poodle) public genomic sequence (45). Exonic SNPs included a previously reported cytosine to thymine (C→T) change in exon 7 at nucleotide 956 (codon 167; ACC, ACT = threonine) (27), and a novel guanine to adenine (G→A) change in exon 12, at nucleotide 1631 (codon 392; CAG, CAA = glutamine). Both exonic SNPs occurred at the third position of the codon and were synonymous changes which did not alter the amino acid coded.

Table 4.1. *PAX6* sequence changes identified in Siberian huskies (cataract), Basenjis (PPM), and Soft-coated wheaten terriers (SCWTs) with PPM, sclero-cornea, and choroidal hypoplasia. Changes were compared with normal controls taken from beagle, the 1.5X canine (poodle) genomic sequence, and the 7.5X (boxer) genomic sequence. The latter sequence did not contain *PAX6* exon 2 or exon 7; NA- not applicable.

| **AFFECTED DOGS** | | | | | | | **NORMAL CONTROLS** | | |
|---|---|---|---|---|---|---|---|---|---|
| | Siberian Husky cataract | | Basenji PPM | | SCWT PPM, sclero-cornea & choroidal hypoplasia | | | 1.5X Seq | 7.5X Seq. |
| PAX6 LOCA-TION | H-1 | H-2 | B-1 | B-2 | SCWT-1 | SCWT-2 | BEAGLE | POODLE | BOXER |
| EXON 2 (CCAA) repeat | (CCAA) x8 | (CCAA) x7 | (CCAA) x8 | (CCAA) x8 | (CCAA) x7 | (CCAA) x7 | (CCAA) x7 | (CCAA) x7 | NA |
| INTRON 2 (+27) | C/C | C/C | C/G | C/C | C/G | C/G | C/C | C/C | C/C |
| INTRON 2 (+51) | C/C (CTT)5 | T/C (CTT)4 (CTT)5 | T/C (CTT)4 (CTT)5 | C/C (CTT)5 | T/C (CTT)4 (CTT)5 | T/T (CTT)4 | T/C (CTT)4 (CTT)5 | T/T (CTT)4 | T/T (CTT)4 |
| EXON 7 (nt 956; codon 167) | C/T | C/C | C/C | C/C | C/T | T/T | C/C | C/C | NA |
| EXON 12 (nt 1631; codon 392) | G/G | G/G | G/G | G/G | A/G | G/G | G/G | G/G | G/G |

*Siberian Husky - cataract*

Within exon 2, H-1 was homozygous for eight microsatellite repeats (CCAA)8 while H-2 was homozygous for seven (CCAA)7 (Table 4.1). Both were homozygous C/C at intron 2 (+27). H-1 was also homozygous C/C at intron 2 (+51) resulting in five microsatellite repeats (CTT)5, while H-2 was heterozygous C/T resulting in both (CTT)4 and (CTT)5 alleles. At the exon 7 SNP, H-1 was heterozygous C/T while H-2 was homozygous C/C. Both were homozygous G/G at the exon 12 SNP.

*Basenji – persistent pupillary membrane*

Both dogs were homozygous for eight microsatellite repeats (CCAA)8 in exon 2 (Table 4.1). In intron 2 (+27), B-1 was heterozygous C/G while B-2 was homozygous C/C. At intron 2 (+51), B-1 was heterozygous T/C resulting in both four (CTT)4, and five (CTT)5 microsatellite repeats, while B-2 was homozygous C/C with five (CTT)5 repeats. Both were homozygous C/C and G/G for exon 7 and exon 12 SNPs, respectively.

*Soft-coated wheaten terriers – PPM, sclero-cornea, and choroidal hypoplasia*

Both dogs were homozygous for 7 microsatellite repeats (CCAA)7 in exon 2, and were heterozygous C/G at intron 2 (+27) (Table 4.1). SCWT-1 was heterozygous T/C at intron 2 (+51), resulting in both (CTT)4 and (CTT)5 alleles, while SCWT-2 was homozygous T/T with (CTT)4 repeats. SCWT-1 was heterozygous C/T at the exon 7 SNP and A/G at the exon 12 SNP while SCWT-2 was homozygous T/T, and G/G at the exon 7, and 12 SNPs, respectively.

*Discussion*

In an effort to identify missense mutations in *PAX6* which are associated with non-aniridia ocular phenotypes, exon scanning was used to evaluate *PAX6* in three dog

breeds with inherited ocular diseases. These included, Siberian huskies with cataract, Basenjis with PPM, and SCWTs with PPM, sclero-cornea, and choroidal hypoplasia. Assuming autosomal recessive inheritance for each disease analyzed, a pathological *PAX6* mutation must be homozygous, and present in both affected dogs of each breed. This criteria is only met for the exon 2, (CCAA)8 microsatellite which occurred in both Basenji dogs. All other sequence changes identified were either not present in both affected dogs, or were not present in a homozygous state (Table 4.1). Assuming autosomal dominant inheritance for each disease, a pathological *PAX6* mutation may be heterozygous, or homozygous, but must occur in both affected dogs of each breed. This criteria was fulfilled again in the exon 2, (CCAA)8 microsatellite in both Basenjis. In addition, both affected SCWTs had at least one "mutant" *PAX6* allele for the intron 2 (+21), and the exon 7 SNPs (Table 4.1).

However, none of the mutations identified in this study were expected to alter *PAX6* transcription or translation. The (CCAA)7-8 microsatellite was located within non-coding exon 2, and to date, there have been no pathological mutations identified in human non-coding exons 1 or 2. Nevertheless, pathological mutations have been identified in the human *PAX6* 5'UTR from intron 2 through exon 4, and also within introns 4-12 (The Human *PAX6* Allelic Variant Database:http://*PAX6*.hgu.mrc.ac.uk). Human *PAX6* exon 2 is 188 bp (NM001604) compared to 224bp in the dog (EF141017). The 36 bp difference is partly composed of a 23 bp poly-A sequence in the dog, from nucleotide 229-251 followed by the (CCAA)7 repeat from nucleotide 259-286. Human exon 2 contains a smaller poly-A sequence, consisting of 6 adenosine residues from nucleotide 242-247, followed by two CCAA repeats from nucleotide 250-257. The mouse *Pax6* sequence does not contain a poly-A, or a CCAA repeat. Microsatellite repeats are common in mammalian DNA, and are highly polymorphic among individuals.

Neither of the canine *PAX6* intron 2 SNPs identified in this study (intron 2(+27), and intron 2(+51)), were associated with splice donor or acceptor sites, and therefore should not affect post-transcriptional processing. However, the intron 2(+51) SNP was associated with a CTT microsatellite, and intronic microsatellites can be significant as in the case of Friedrich's ataxia which involves a GAA repeat expansion in intron 1 of the *FRDA* gene (47). Nevertheless, the occurrence of this SNP in a normal control (beagle) dog suggests that it is truly insignificant. The Human *PAX6* Allelic Variant Database (http://*PAX6*.hgu.mrc.ac.uk/) contains one unique mutation in intron 2 which involves a deletion of an invariant adenine (A) residue at the 3' end splice acceptor site (position –2) (48). The effect of this mutation on the corresponding RNA and amino acid products has not been determined, but it is expected to alter the splicing of exon 3, and in fact segregates with aniridia in two patients (48).

The exon 7 SNP located within the coding region was previously described in a family of Catalan sheepdogs with inherited aniridia (27). This SNP occured in the Linker region of *PAX6* between the paired and homeo domains, and created a synonymous change at codon 167 (C→T: ACC, ACT= threonine). The Human *PAX6* Allelic Variant database (http://*PAX6*.hgu.mrc.ac.uk/) contains 20 unique mutations in exon 7 which include insertions, deletions, missense, and nonsense changes. A cytosine to thymine (C→T) change in human exon 7, codon 140 creates a synonymous change (GAC, GAT = Aspartic acid) associated with a normal phenotype (49). This SNP also occurs in the Linker region.

The canine exon 12 SNP (G→A: CAG, CAA = glutamine) occurred at codon 392, in the proline-serine-threonine (PST) region, and represented the second synonymous change identified in this study. In man there are 17 unique mutations described in exon 12 including insertions, deletions, missense, and nonsense

mutations, but no synonymous changes (http://*PAX6*.hgu.mrc.ac.uk/), hence, this sequence change is considered non-pathogenic.

The four SNPs and 2 microsatellites identified here are not expected to alter the *PAX6* coding sequence or the corresponding amino acids. However, before *PAX6* can be definitively excluded as a candidate gene for cataracts in Siberian huskies, PPM in Basenjis, and PPM, sclero-cornea, and choroidal hypoplasia in SCWTs, additional pedigree information is needed from each breed for association testing of the disease phenotype with the *PAX6* locus. Tissue samples from normal and affected dogs should also be obtained for *PAX6* RNA and protein expression studies. The lack of pathological mutations in the 14 exons of the canine *PAX6* gene, including both coding, and non-coding exons, as well as intron/exon boundaries (splice sites), however, suggests that *PAX6* is not involved in the diseases examined.

# REFERENCES


1. Callaerts P, Halder G, Gehring WJ. PAX-6 in development and evolution. Annual Reviews in Neuroscience 1997;20:483-532.

2. Glaser T, Jepeal L, Edwards JG, Young SR, Favor J, Maas RL. PAX6 gene dosage effect in a family with congenital cataracts, aniridia, anophthalmia and central nervous system defects. Nature Genetics 1994;7(4):463-71.

3. Walther C, Gruss P. Pax-6, a murine paired box gene, is expressed in the developing CNS. Development 1991;113(4):1435-49.

4. Ton CC, Hirvonen H, Miwa H, Weil MM, Monaghan P, Jordan T, van Heyningen V, Hastie ND, Meijers-Heijboer H, Drechsler M, et al. Positional cloning and characterization of a paired box- and homeobox-containing gene from the aniridia region. Cell 1991;67(6):1059-74.

5. Ton CC, Miwa H, Saunders GF. Small eye (Sey): cloning and characterization of the murine homolog of the human aniridia gene. Genomics 1992;13(2):251-6.

6. Gerard M, Abitbol M, Delezoide AL, Dufier JL, Mallet J, Vekemans M. PAX-genes expression during human embryonic development, a preliminary report. Comptes rendus de l'Académie des sciences. Série III, Sciences de la vie 1995;318(1):57-66.

7. Grindley JC, Davidson DR, Hill RE. The role of Pax-6 in eye and nasal development. Development 1995;121(5):1433-42.

8. Koroma BM, Yang JM, Sundin OH. The Pax-6 homeobox gene is expressed throughout the corneal and conjunctival epithelia. Investigative Ophthalmology and Visual Science 1997;38(1):108-120.

9. Nishina S, Kohsaka S, Yamaguchi Y, Handa H, Kawakami A, Fujisawa H, Azuma N. PAX6 expression in the developing human eye. British Journal of Ophthalmology 1999;83(6):723-727.

10. Zhang W, Cveklova K, Oppermann B, Kantorow M, Cvekl A. Quantitation of PAX6 and PAX6(5a) transcript levels in adult human lens, cornea, and monkey retina. Molecular Vision 2001;7:1-5.

11. Azuma N, Tadokoro K, Asaka A, Yamada M, Yamaguchi Y, Handa H, Matsushima S, Watanabe T, Kohsaka S, Kida Y, Shiraishi T, Ogura T, Shimamura K, Nakafuku M. The Pax6 isoform bearing an alternative spliced exon promotes the development of the neural retinal structure. Hum Mol Genet. 2005;14(6):735-745.

12. Chow RL, Altmann CR, Lang RA, Hemmati-Brivanlou A. Pax6 induces ectopic eyes in a vertebrate. Development 1999;126(19):4213-22.

13. Halder G, Callaerts P, Gehring WJ. Induction of ectopic eyes by targeted expression of the eyeless gene in Drosophila. Science 1995;267(5205):1788-92.

14. Hill RE, Favor J, Hogan BL, Ton CC, Saunders GF, Hanson IM, Prosser J, Jordan T, Hastie ND, van Heyningen V. Mouse small eye results from mutations in a paired-like homeobox-containing gene. Nature 1991;354(6354):522-5.

15. Favor J, Peters H, Hermann T, Schmahl W, Chatterjee B, Neuhauser-Klaus A, Sandulache R. Molecular characterization of Pax6(2Neu) through Pax6(10Neu): an extension of the Pax6 allelic series and the identification of two possible hypomorph alleles in the mouse Mus musculus. Genetics 2001;159(4):1689-700.

16. Brown A, McKie M, van Heyningen V, Prosser J. The Human PAX6 Mutation Database. Nucleic Acids Research 1998;26(1):259-264.

17. Prosser J, van Heyningen V. PAX6 mutations reviewed. Human Mutation 1998;11(2):93-108.

18. Tzoulaki I, White IM, Hanson IM. PAX6 mutations: genotype-phenotype correlations. BMC Genetics 2005;6(1):27.

19. Hanson I, Churchill A, Love J, Axton R, Moore T, Clarke M, Meire F, van Heyningen V. Missense mutations in the most ancient residues of the PAX6 paired domain underlie a spectrum of human congenital eye malformations. Human Molecular Genetics 1999;8(2):165-172.

20. Hanson IM, Fletcher JM, Jordan T, Brown A, Taylor D, Adams RJ, Punnett HH, van Heyningen V. Mutations at the PAX6 locus are found in heterogeneous anterior segment malformations including Peters' anomaly. Nature Genetics 1994;6(2):168-173.

21. Mirzayans F, Pearce WG, MacDonald IM, Walter MA. Mutation of the PAX6 gene in patients with autosomal dominant keratitis. Am J Hum Genet. 1995;57(3):539-548.

22. Chao LY, Mishra R, Strong LC, Saunders GF. Missense mutations in the DNA-binding region and termination codon in PAX6. Human Mutation 2003;21(2):138-145.

23. Azuma N, Nishina S, Yanagisawa H, Okuyama T, Yamada M. PAX6 missense mutation in isolated foveal hypoplasia. nature genetics 1996;13(2):141-142.

24. Azuma N, Yamaguchi Y, Handa H, Hayakawa M, Kanai A, Yamada M. Missense mutation in the alternative splice region of the PAX6 gene in eye anomalies. American Journal of Human Genetics 1999;65(3):656-663.

25. Azuma N, Yamaguchi Y, Handa H, Tadokoro K, Asaka A, Kawase E, Yamada M. Mutations of the PAX6 gene detected in patients with a variety of optic-nerve malformations. am J Hum Genet. 2003;72(6):1565-1570.

26. Epstein JA, Glaser T, Cai J, Jepeal L, Walton DS, Maas RL. Two independent and interactive DNA-binding subdomains of the Pax6 paired domain are regulated by alternative splicing. Genes and Development 1994;8(17):2022-34.

27. Hunter LS, Sidjanin DJ, Hijar MV, Johnson JL, Kirkness E, Acland GM, Aguirre GD. Cloning and characterization of canine PAX6 and evaluation as a candidate gene in a canine model of aniridia. Molecular Vision 2007;13:431-442.

28. Guyon R, Lorentzen TD, Hitte C, Kim L, Cadieu E, Parker HG, Quignon P, Lowe JK, Renier C, Gelfenbeyn B, Vignaux F, DeFrance HB, Gloux S, Mahairas GG, Andre C, Galibert F, Ostrander EA. A 1-Mb resolution radiation hybrid map of the canine genome. Proceedings of the National Academy of Sciences of the U S A 2003;100(9):5296-5301.

29. Breen M, Hitte C, Lorentzen TD, Thomas R, Cadieu E, Sabacan L, Scott A, Evanno G, Parker HG, Kirkness EF, Hudson R, Guyon R, Mahairas GG, Gelfenbeyn B, Fraser CM, Andre C, Galibert F, Ostrander EA. An integrated 4249 marker FISH/RH map of the canine genome. BMC Genetics 2004;5(1):65.

30. Ostrander EA, Galibert F, Patterson DF. Canine genetics comes of age. Trends in Genetics 2000;16:117-124.

31. Starkey MP, Scase TJ, Mellersh CS, Murphy S. Dogs really are man's best friend--canine genomics has applications in veterinary and human medicine! Briefings in functional genomics and proteomics 2005;4(2):112-128.

32. Gelatt KN. Essentials of Veterinary Ophthalmology. 1 ed. Baltimore, Maryland: Lippincott Williams and Wilkins; 2000.

33. Gelatt KN, Mackay EO. Prevalence of primary breed-related cataracts in the dog in North America. Vet Ophthalmol 2005;8(2):101-11.

34. Roberts SR, Bistner SI. Persistent pupillary membrane in Basenji dogs. Journal of the American Veterinary Medical Association 1968;153(5):533-542.

35. Barnett KC, Knight GC. Persistent pupillary membrane and associated defects in the Basenji. Veterinary Research 1969;85(9):242-248.

36. Bistner SI, Rubin LF, Roberts SR. A review of persistent pupillary membranes in the Basenji dog. Journal of the American Animal Hospital Association 1971;7:143-157.

37. Mason TA. Persistent pupillary membrane in the Basenji. Australian Veterinary Journal 1976;52(8):343-344.

38. James RW. Persistent pupillart membrane in basenji dogs. Veterinary Research 1991;128(12):287-288.

39. Gronskov K, Rosenberg T, Sand A, Brondum-Nielsen K. Mutational analysis of PAX6: 16 novel mutations including 5 missense mutations with a mild aniridia phenotype. European Journal of Human Genetics 1999;7(3):274-286.

40. Willcock C, Grigg J, Wilson M, Tam P, Billson F, Jamieson R. Congenital iris ectropion as an indicator of variant aniridia. Br J Ophthalmol 2006;90(5):658-659.

41. Sonoda S, Isashiki Y, Tabata Y, Kimura K, Kakiuchi T, Ohba N. A novel PAX6 gene mutation (P118R) in a family with congenital nystagmus associated with a variant form of aniridia. Graefes Arch Clinical Experimental Ophthalmology 2000;238(7):552-558.

42. Vincent MC, Pujo AL, Olivier D, Calvas P. Screening for PAX6 gene mutations is consistent with haploinsufficiency as the main mechanism leading to various ocular defects. European Journal of Human Genetics 2003;11(2):163-169.

43. Neethirajan G, Krishnadas SR, Vijayalakshmi P, Shashikant S, Sundaresan P. PAX6 gene variations associated with aniridia in south India. BMC Medical Genetics 2004;5(9).

44. Sambrook J, Fritsch EF, Maniatis T. Molecular Cloning: A Laboratory Manual. Cold Spring Harbor, NY: Cold Spring Harbor Laboratory Press; 1989.

45. Kirkness EF, Bafna V, Halpern AL, Levy S, Remington K, Rusch DB, Delcher AL, Pop M, Wang W, Fraser CM, Venter JC. The dog genome: survey sequencing and comparative analysis. Science 2003;301(5641):1898-1903.

46. Lindblad-Toh K, Wade CM, Mikkelsen TS, Karlsson EK, Jaffe DB, Kamal M, Clamp M, Chang JL, Kulbokas EJ, 3rd, Zody MC, Mauceli E, Xie X, Breen M, Wayne RK, Ostrander EA, Ponting CP, Galibert F, Smith DR, DeJong PJ, Kirkness E, Alvarez P, Biagi T, Brockman W, Butler J, Chin CW, Cook A, Cuff J, Daly MJ, DeCaprio D, Gnerre S, Grabherr M, Kellis M, Kleber M, Bardeleben C, Goodstadt L, Heger A, Hitte C, Kim L, Koepfli KP, Parker HG, Pollinger JP, Searle SM, Sutter NB, Thomas R, Webber C, Baldwin J, Abebe A, Abouelleil A, Aftuck L, Ait-Zahra M, Aldredge T, Allen N, An P, Anderson S, Antoine C, Arachchi H, Aslam A, Ayotte L, Bachantsang P, Barry A, Bayul T, Benamara M, Berlin A, Bessette D, Blitshteyn B, Bloom T, Blye J, Boguslavskiy L, Bonnet C, Boukhgalter B, Brown A, Cahill P, Calixte N, Camarata J, Cheshatsang Y, Chu J, Citroen M, Collymore A, Cooke P, Dawoe T, Daza R, Decktor K, DeGray S, Dhargay N, Dooley K, Dorje P, Dorjee K, Dorris L, Duffey N, Dupes A, Egbiremolen O, Elong R, Falk J, Farina A, Faro S, Ferguson D, Ferreira P, Fisher S, FitzGerald M, Foley K, Foley C, Franke A, Friedrich D, Gage D, Garber M, Gearin G, Giannoukos G, Goode T, Goyette A, Graham J, Grandbois E, Gyaltsen K, Hafez N, Hagopian D, Hagos B, Hall J, Healy C, Hegarty R, Honan T, Horn A, Houde N, Hughes L, Hunnicutt L, Husby M, Jester B,

Jones C, Kamat A, Kanga B, Kells C, Khazanovich D, Kieu AC, Kisner P, Kumar M, Lance K, Landers T, Lara M, Lee W, Leger JP, Lennon N, Leuper L, LeVine S, Liu J, Liu X, Lokyitsang Y, Lokyitsang T, Lui A, Macdonald J, Major J, Marabella R, Maru K, Matthews C, McDonough S, Mehta T, Meldrim J, Melnikov A, Meneus L, Mihalev A, Mihova T, Miller K, Mittelman R, Mlenga V, Mulrain L, Munson G, Navidi A, Naylor J, Nguyen T, Nguyen N, Nguyen C, Nicol R, Norbu N, Norbu C, Novod N, Nyima T, Olandt P, O'Neill B, O'Neill K, Osman S, Oyono L, Patti C, Perrin D, Phunkhang P, Pierre F, Priest M, Rachupka A, Raghuraman S, Rameau R, Ray V, Raymond C, Rege F, Rise C, Rogers J, Rogov P, Sahalie J, Settipalli S, Sharpe T, Shea T, Sheehan M, Sherpa N, Shi J, Shih D, Sloan J, Smith C, Sparrow T, Stalker J, Stange-Thomann N, Stavropoulos S, Stone C, Stone S, Sykes S, Tchuinga P, Tenzing P, Tesfaye S, Thoulutsang D, Thoulutsang Y, Topham K, Topping I, Tsamla T, Vassiliev H, Venkataraman V, Vo A, Wangchuk T, Wangdi T, Weiand M, Wilkinson J, Wilson A, Yadav S, Yang S, Yang X, Young G, Yu Q, Zainoun J, Zembek L, Zimmer A, Lander ES. Genome sequence, comparative analysis and haplotype structure of the domestic dog. Nature 2005;438(7069):803-819.

47. Delatycki MB, Williamson R, Forrest SM. Friedreich ataxia: an overview. Journal of Medical Genetics 2000;37(1):1-8.

48. Axton RA, Hanson IM, Love J, Seawright A, Prosser J, van Heyningen V. Combined SSCP/heteroduplex analysis in the screening for PAX6 mutations. Molecular and Cellular Probes 1997;11:287-292.

49. Davis A, Cowell JK. Mutations in the PAX6 gene in patients with hereditary aniridia. Hum Mol Genet. 1993;2(12):2093-2097.

# CHAPTER 5

# CONCLUSION

Cataracts are the number one cause of blindness and low vision throughout the world. Over twenty-six million (22%) Americans greater than 40 years of age, have cataracts, or have undergone cataract surgery (1). Although cataracts can be successfully treated surgically, many people do not have access to health care that would provide this service. As a result, there is a need to understand how and why cataracts develop, with the hope of one day discovering a way to prevent, delay, or even medically cure cataracts. The study of congenital cataracts in man, as well as the study of cataracts in animal models, has helped to identify genes involved in cataractogenesis. As the functions of these genes are elucidated, we will increase our understanding of the mechanisms involved in cataract formation. The purpose of my thesis research was to facilitate the development of canine models of cataract, which could contribute to our understanding of the genes and mechanisms involved in cataract development.

When the Radiation Hybrid mapping project began (Chapter 2), the canine genome was not yet publicly available. The goal of the mapping project was to establish the locations of cataract gene homologues on canine chromosomes in relation to nearby markers. Polymorphic markers located near cataract genes can be used in association analysis to test for association of these genes with cataract phenotypes in canine pedigrees. This tool was created to facilitate association and linkage testing in canine pedigrees with inherited cataracts, and to support the use of canine models to study cataracts. Once association is established between a cataract phenotype and a candidate gene locus, the gene can be sequenced, and analyzed for the presence of disease-causing mutations.

Recently, mutations causing cataracts in three dog breeds were identified in *heat shock factor 4* (*HSF4*) (2), one of the candidate genes we mapped to canine chromosome 5. The markers on CFA5 , identified in the RH-mapping project may also be useful in linking *HSF4* to other cataract phenotypes in additional breeds. Furthermore, single nucleotide polymorphism (SNP) databases now exists that provide the locations of SNPs within the canine genome. The genomic locations determined for the cataract homologues in the RH-mapping project, can also be used to select nearby SNPs from these databases for association analysis. This is especially useful in cases where microsatellites are sparse or if the microsatellites identified are not polymorphic in the pedigree of interest.

Although the canine genomic sequence is now publicly available, many genes have not been annotated within the sequence. In addition, there are gaps throughout the genome where the sequence has not yet been determined, and these gaps may contain genes or parts of genes. For example, the cloning and characterization of the cataract candidate gene *PAX6* provided the annotated canine gene sequence, as well as sequences for two large gaps in the canine genome (Chapter 3). In addition, because *PAX6* is the primary aniridia gene in man, it was examined for mutations causing aniridia in dogs. However, no mutations were identified in the coding regions or splice sites examined. As a result, canine aniridia may be caused by a novel gene, and may even involve alternate mechanisms of pathogenesis compared with human aniridia. However, it is also possible that dogs affected with aniridia have a *PAX6* mutation in an area that was not examined, i.e. in an intron, a promoter, or other regulatory element. To rule out this possibility, additional pedigree information is needed to first, confirm the mode of inheritance of canine aniridia, and second, to definitively determine if an association exists between canine aniridia, and *PAX6*. If an association is established, then a search for mutations outside of the coding region

should be pursued. As well, ocular tissue samples are needed for both gene (mRNA), and protein expression analysis, to demonstrate potential differences in *PAX6* expression in normal versus affected dogs.

*PAX6* was also examined for mutations causing cataracts, PPM, sclero-cornea, and choroidal hypoplasia in three dog breeds (Chapter 4). Again, no pathological mutations were identified by direct sequencing within the *PAX6* coding regions, or splice sites. Unfortunately, sufficient pedigree information necessary to test for an association between the phenotypes examined and the *PAX6* locus, was not available for the dogs used in this study. However, by working with Siberian husky, Basenji, and SCWT breeders, we may obtain additional pedigree information and DNA samples from dogs which can be used to overcome this limitation. If markers at the *PAX6* locus co-segregate with the phenotypes of any of the breeds examined, then the non-coding regions of *PAX6* should be examined in those breeds. In addition, gene (mRNA), and protein expression should be analyzed.

Today many tools exist which support the development and use of canine models to study cataracts at the molecular level. These include the canine genomic sequence, gene maps, miscrosatellite and SNP markers, and Minimal Screening Sets (MSS) for genome wide scans. In addition, a large number of dog breeds are afflicted with naturally-occurring cataract phenotypes. Informative pedigrees from these breeds, can be used to determine the mode of inheritance of the observed cataract phenotypes. As well, DNA samples from selected members of these pedigrees can be used to test for linkage or association of the phenotype with cataract gene loci. This may be done using microsatellite or SNP markers from public databases, as well as SNPs independently discovered within the gene sequence. In addition, genome wide scans performed with the Minimal Screening Sets now available, may help to identify new cataract genes. Once the genes responsible for canine cataracts are identified, the

molecular mechanisms involved can be elucidated, creating new animal models which can be used to study non-surgical therapeutic interventions, including pharmaceutical and gene therapies. Finally, the dog can serve as an intermediate mammalian species model for assessing gene therapy interventions, after testing in rodents, and before implementing in human patients. The results of this research have taken initial steps to show that the dog is indeed a viable model for molecular studies of cataracts.

# REFERENCES

1. The Eye Diseases Prevalence Research Group: Congdon N, Vingerling JR, Klein BEK, West S, Friedman DS, Kempen, John, O'Colmain, Benita, Wu, Suh-Yuh Taylor, Hugh R., and Wang, Jie Jin. Prevalence of cataract and pseudophakia/aphakia among adults in the United States. Archives of Ophthalmology 2004;122(4):487-494.

2. Mellersh CS, Pettitt L, Forman OP, Vaudin M, Barnett KC. Identification of mutations in HSF4 in dogs of three different breeds with hereditary cataracts. Vet Ophthalmol 2006;9(5):369-378.